S
T
R
A
T
A

Travaux de Géologie sédimentaire et Paléontologie

Série 1 : communications

Editeurs :
Elise Nardin & Markus Aretz

PRE-CENOZOIC CLIMATES INTERNATIONAL WORKSHOP
When data and modeling meet

PROGRAMME & ABSTRACTS

June 17th - 19th 2013
Toulouse, France

ISSN 0761-2443

volume 14 - 2013

STRATA

Secrétaire de rédaction : Philippe Fauré

Editeur :
Association ASNAT,
http://strata.mp.free.fr

Dépôt légal : 2ème trimestre 2013
ISSN : 0761-2443

‘PRE-CENOZOIC CLIMATES’ INTERNATIONAL WORKSHOP

PROGRAMME & ABSTRACTS

June 17th – June 19th
Toulouse, France

Edited by

Elise NARDIN & Markus ARETZ

STRATA, série 2 : communications, volume 14, 2013, 99 p.

The organising committee gratefully acknowledges the support of

CNRS

INSU

ANR

Observatoire Midi-Pyrénées

Géosciences Environnement Toulouse (GET)

Université Paul Sabatier

Laboratoire des Sciences du Climat et de l'Environnement (LSCE)

Ville de Toulouse

SGF Jeune

Contents

Preface

We cordially welcome you, some seventy participants from twelve countries around the globe to the *'Pre-Cenozoic climates' International Workshop (PC^2IW)* in Toulouse, 17-19. June 2013.

'Pre-Cenozoic climates' is a multidisciplinary workshop that broadly addresses the pre-Cenozoic climatic phenomena and processes. The purpose of the workshop is to extend our understanding of the natural variations that take place within the earth's climate system in deep times by bringing together specialists from diverse fields including sedimentology, paleontology, geochemistry (data-community) and numerical modeling (model-community).

In recent years, the number of available data has grown exponentially. Two questions arise: (1) is there a unified picture of the pre-Cenozoic climates and environmental evolution emerging from this large amount of data, and (2) how can we promote dialogue between numerical models, which deliver large amounts of climatic and environmental parameters, and geological observations?

The workshop offers data- and model-workers an opportunity to discuss the strengths and weaknesses of the geological proxies and numerical models, to share their vision about the reconstruction of pre-Cenozoic climates, and to debate about emerging scientific questions.

PC^2IW is organised around 6 thematic sessions:

- S1: Isotopic records and past climate,
- S2: Modeling Past Climate,
- S3: Links between climate and biota,
- S4: Continental proxies in climate reconstruction,
- S5: Sediments as proxies in climate reconstruction,
- S6: Integrated approach in paleoclimate reconstruction.

In these sessions seven keynotes (C.J. Bjerrum, M.M. Joachimski, I.P. Montañez, C.J. Poulsen, B. von de Schootbrugge, R.J. Twitchett, and P. Valdes), 22 talks and 18 posters will be presented. Two Round Table Discussions are organised to encourage and initiate discussions around subjects and questions like:

- How to integrate sedimentological and geochemical data in paleoclimatic numerical models?
- What are the expectations and limitations of climatic models?
- How to solve problems of $\delta^{18}O$ interpretation in paleoclimatic studies?
- Are we able to produce reliable global temperature curves for the Pre-Cenozoic period?
- Shall we redefine 'Greenhouse' and 'Icehouse' terms?
- What is the reliability of current paleo-pCO_2 proxies?

We would also like to use this opportunity to acknowledge the support and help of the CNRS, INSU, ANR, Observatoire Midi-Pyrénées, Géosciences Environnement Toulouse (GET), Université Paul Sabatier, Laboratoire des Sciences du Climat et de l'Environnement (LSCE), Ville de Toulouse, SGF Jeune, and last but not least the members and students of Géosciences Environnement Toulouse helping on and behind the scenes.

We hope that the *'Pre-Cenozoic climates' International Workshop* becomes a successful and enjoyable meeting providing you with new insights, ideas and friends. We wish you a truly memorable and rewarding stay in the "Ville Rose"!

Yves GODDÉRIS, Bernard ANDREU, Markus ARETZ, Guillaume DERA, Yannick DONNADIEU, Vanessa LEBEDEL, Carine LÉZIN, Mélina MACOUIN, Elise NARDIN and Delphine ROUBY

Multiproxy Evidence of main Deccan Volcanic Pulse near the Cretaceous-Tertiary Boundary

Thierry Adatte[1], Alicia Fantasia[1], Bandana Samant[2], Gerta Keller[3], Hassan Khozyem[1] & Brian Gertsch[4]

[1]ISTE, Lausanne University, 1015 Lausanne, Switzerland; E-Mail: Thierry.adatte@unil.ch
[2]Department of Geology, Nagpur University, Nagpur 440 001, India; E-Mail: bandanabhu@gmail.com
[3]Department of Geosciences, Princeton University, Princeton NJ 08540, USA; E-Mail: Gkeller@princeton.edu
[4]Earth, Atmospheric and Planetary Science Department, MIT, Cambridge MA 02139, USA; E-Mail: bgertsch@mit.edu

Model results predict that Deccan Traps emplacement was responsible for a strong increase in atmospheric pCO_2 accompanied by rapid warming of 4°C (Dessert *et al.*, 2001, 2003) that was followed by global cooling. During the warming phase, increased continental weathering of silicates associated with consumption of atmospheric CO_2 likely resulted in the drawdown of greenhouse gases that reversed the warming trend leading to global cooling at the end of the Maastrichtian. Massive CO_2 input together with massive release of SO_2 may thus have triggered the mass extinctions in the marine realm as a result of ocean acidification leading to a carbon crisis and in the terrestrial realms due to acid rains (Fig. 1). Global stress conditions related to these climatic changes are well known and documented in planktic foraminifera by a diversity decrease, species dwarfing, dominance of opportunistic species and near disappearance of specialized species (review in Keller and Abramovich, 2009).

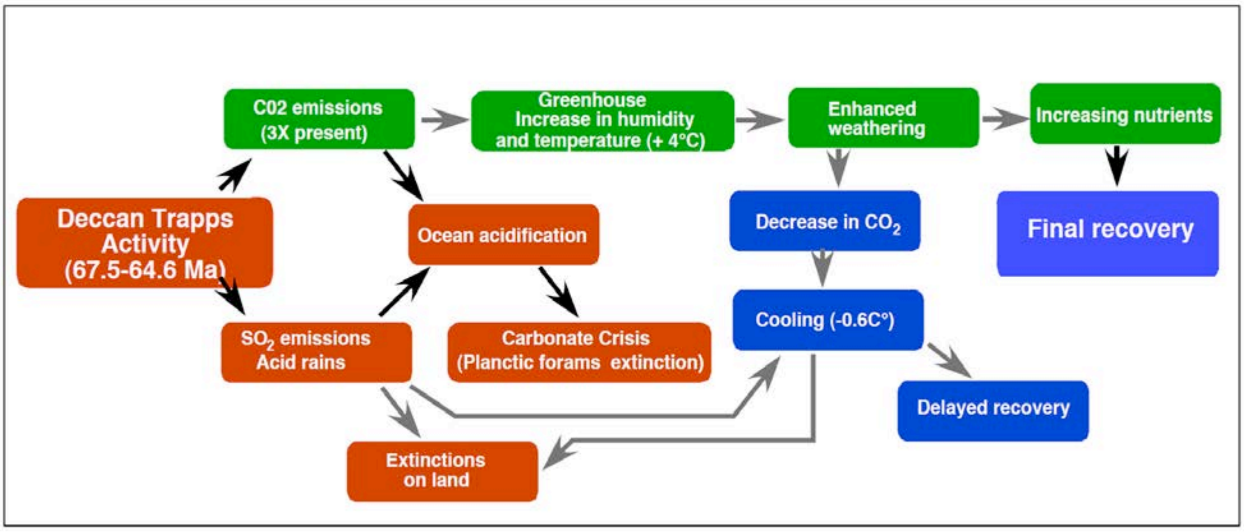

Fig. 1: **Flow chart for the model of massive Deccan volcanism as a main trigger of environmental changes leading to the KTB mass extinction.**

Recent studies indicate that the bulk (80%) of Deccan trap eruptions (phase-2) occurred over a relatively short time interval in magnetic polarity C29r (Chenet *et al.*, 2007). Multiproxy studies from central and southeastern India place the Cretaceous-Tertiary (KT) mass extinction near the end of this main phase of Deccan volcanism suggesting a cause-and effect relationship (Keller *et al.*, 2008, 2012).

In India a strong floral response is observed as a direct response to Deccan volcanic phase-2. In Lameta (infra-trapean) sediments preceding the volcanic eruptions, palynoflora are dominated by gymnosperms and angiosperms with a rich canopy of gymnosperms (Conifers and *Podocarpaceae*) and an understory of palms and herbs (Samant & Mohabey, 2005; Samant *et al.*, 2008). Immediately after the onset of Deccan phase-2, this floral association was decimated leading to dominance by angiosperms and pteridophytes at the expense of gymnosperms.

In subsequent intertrappean sediments a sharp decrease in pollen and spores coupled with the appearance of fungi mark increasing stress conditions apparently as a direct result of volcanic activity. The inter-trappean

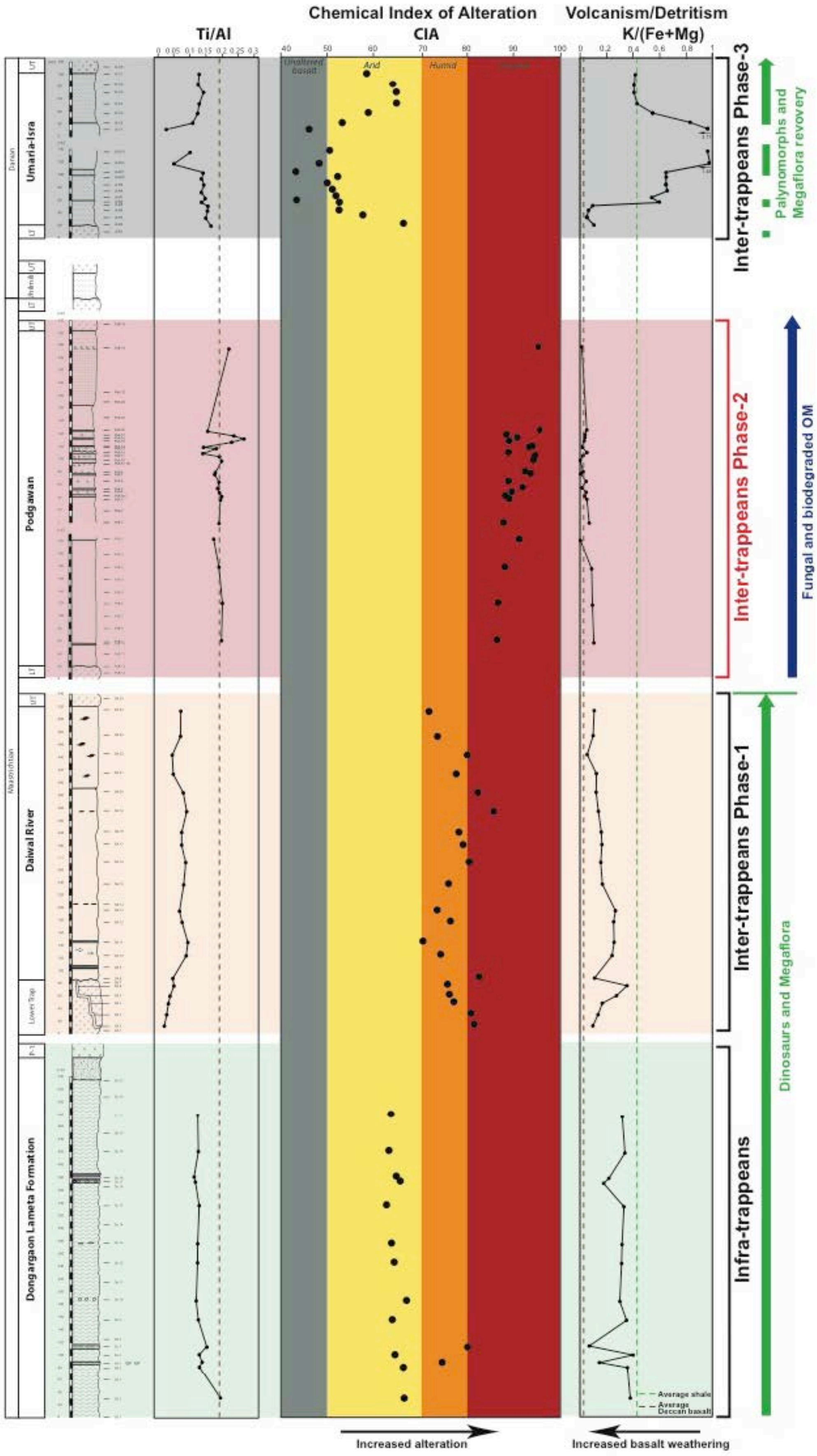

Fig. 2: **Ti/Al ratio, Chemical Index of Alteration (CIA), basalt weathering intensity (K/Fe+Mg) in infra and inter-trappean sediments, comparison with palynological data.**

sediments corresponding to Phase-2 (80% of Deccan basalt emissions, latest Maastrichtian) are characterized by the highest Chemical Index of Alteration (CIA) values (Fig.2). This can be explained by increased acid rains due to SO_2 emissions rather than a global climatic shift, because clay minerals from the corresponding sediments do not reflect a significant climate change. The increased weathering is coeval with the sharp decline in pollen and an increase in fungal spores observed by Samant & Mohabey (2009) and corresponds to the main phase-2 of Deccan activity. Values of K/(Fe+Mg) are very high in the final Deccan phase-3 of the early Danian suggesting ongoing alteration of huge amounts of basalt.

Beyond India, multiproxy studies also place the main Deccan phase in the uppermost Maastrichtian C29r below the KTB (planktic foraminiferal zones CF2-CF1 spanning 120ky and 160ky respectively), as indicated by a rapid shift in $^{187}Os/^{188}Os$ ratios in deep-sea sections from the Atlantic, Pacific and Indian Oceans (Robinson *et al*., 2009), coincident with rapid climate warming, coeval increase in weathering, a significant decrease in bulk carbonate indicative of acidification due to volcanic SO_2, and major biotic stress conditions expressed in species dwarfing and decreased abundance in calcareous microfossils (planktic foraminifera and nannofossils). These observations indicate that Deccan volcanism played a key role in increasing atmospheric CO_2 and SO_2 levels that resulted in global warming and acidified oceans, which led to increased biotic stress that predisposed faunas to eventual extinction at the KTB.

References

Chenet A-L., Quidelleur X., Fluteau F. & Courtillot V. (2007). 40K/40Ar dating of the main Deccan large igneous province: further evidence of KTB age and short duration. *Earth and Planetary Science Letters*, 263: 1-15.

Dessert C., Dupré B., François L.M., Schott J., Gaillardet J., Chakrapani G.J. & Bajpai S. (2001). Erosion of Deccan Traps determined by river geochemistry: impact on the global climate and the 87Sr/86Sr ratio of seawater. *Earth and Planetary Science Letters*, 188: 459– 474.

Keller G. & Abramovich S. (2009). Lilliput effect in late Maastrichtian planktic foraminifera: Response to environmental stress. *Palaeogeography, Palaeoclimatology, Palaeoecology*, 284: 47-62.

Keller G., Adatte T., Gardin S., Bartolini A. & Bajpai S. (2008). Main Deccan volcanism phase ends at K-T mass extinction: Evidence from the Krishna-Godavari Basin, SE India. *Earth and Planetary Science Letters*, 268: 29-311.

Keller G., Adatte T., Bhowmick P.K., Upadhyay H., Dave A., Reddy A.N. & Jaiprakash B.C. (2012). Nature and timing of extinctions in Cretaceous-Tertiary planktic foraminifera preserved in Deccan intertrappean sediments of the Krishna-Godavari Basin, India. *Earth and Planetary Science Letters*, 341: 211-221.

Robinson N., Ravizza G., Coccioni R., Peucker-Ehrenbrink B. & Norris R. (2009). A high-resolution marine 187Os/188Os record for the late Maastrichtian: Distinguishing the chemical fingerprints of Deccan volcanism and the KP impact event. *Earth and Planetary Science Letters*, 281: 159-168.

Samant B. & Mohabey D. M. (2005). Response of flora to Deccan volcanism: a case study from Nand-Dongargaon basin of Maharashtra, implications to environment and climate. *Gondwana Geological Magazin*, 8: 151–164.

Samant B., Mohabey D. & Kapgate D.K. (2008). Palynofloral record from Singpur intertrappean, Chhindwara district, Madhya Pradesh: implication for Late Cretaceous stratigraphic correlation and resolution. *Journal of the Geological Society of India*, 71: 851–858.

The spatial and temporal distribution of Mississippian rugose corals: contribution of modelled oceanic currents and temperature data to this problem

Markus Aretz[1], Guillaume Dera[1], Vincent Lefebvre[1], Yannick Donnadieu[2], Yves Godderis[1], Mélina Macouin[1], Elise Nardin[1]

[1]Géosciences Environnement Toulouse (GET), Observatoire Midi Pyrénées, Université de Toulouse, CNRS, IRD, 14 avenue E. Belin, F- 31400 Toulouse, France; E-mail: markus.aretz@get.obs-mip.fr
[2]Laboratoire des Sciences du Climat et de l'Environnement (LSCE), UMR 8212 - CNRS-CEA-UVSQ, CEA Saclay/ Orme des Merisiers/ Bat. 701, 91191 Gif/Yvette, France

Everybody will agree that distribution patterns of biota are controlled by a variety of biological and non-biological factors, but those will be assessed very differently, especially when adding the uncertainties of deep time perspectives.

Non-biological factors as temperature, salinity, turbidity, ocean currents, oxygenation and geography play important roles in the distribution and dispersion of recent corals. They are often integrated in the interpretations of the distribution patterns of corals in the fossil record, but the availability of data to support the influence of these factors is often limited.

Herein global distribution data of Mississippian (Carboniferous) corals are compared to two maps of current patterns resulting from numerical modelling approaches. These new simulations were done using the Fast Ocean Atmosphere Model (FOAM), which describes the dynamics of atmospheric and oceanic parameters under different constraints. For each simulation, the pCO_2 was fixed to two times pre-industrial levels, allowing a direct appraisal of the importance of palaeogeographic constraints on current direction and intensity.

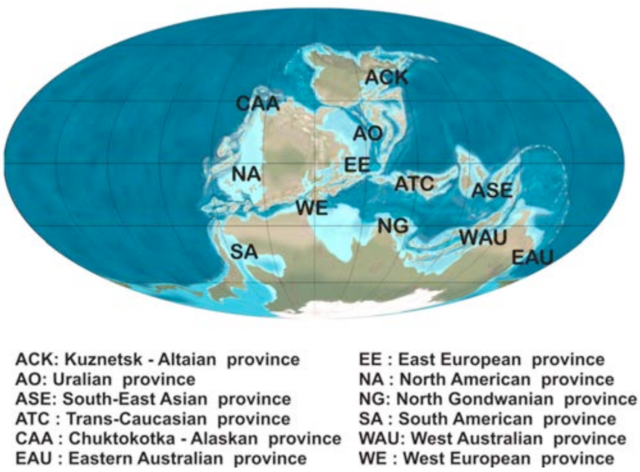

Fig. 1: **Main Mississippian coral provinces, modified from Fedorowski (1977) and Dubatolov & Vassiljuk (1980). on the palaeogeographic reconstruction for the 340 Ma time slice of Blakey.**

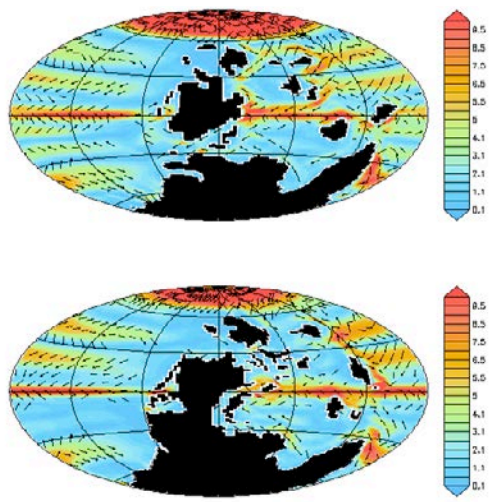

Fig. 2: **Numerical simulations showing the intensity ($cm.s^{-1}$) and directions of ocean surface currents for Tournaisian-Viséan (above) and Serpukhovian palaeogeographies (below)**

Starting with the work of Fedorowski (1977) and Dubatolov & Vassiljuk (1980) a significant number of provinces (Fig. 1), often divided into subprovinces, have been defined based on the absence and presence of taxa, sometimes explained by the above mentioned factors. The degree of faunal exchange between these palaeobiogeographic entities varies. Some of these coral provinces in tropical latitudes like the Eastern Australian and the North American provinces contain high ratios of endemic taxa, which seem to be the result of geographical isolation along continental margins (Webb, 1990). High endemism of the provinces in South America and in NE Siberia (ACK) are most likely the response of temperate to cold water conditions. Tropical provinces around the Palaeotethyan Ocean (WE, EE, ATC, ASE, WAU, NG) show diverse assemblages with relatively low degrees of endemism. Communication between these provinces has been explained with anti-clockwise migrations along the ocean borders, and in this respect SE Asia, especially China, has often be considered as the diversity hotspot and origination centre of many taxa However, if we add a temporal dimension, taxa common to Western Europe and China, always appear earlier in Western Europe (Poty *et al.*, 2011). This challenges the anti-clockwise migration.

It has to be recalled that dispersion of corals is due to a short-living larvae, and thus spatial displacement is limited and the influence of fast ocean currents can be critical. The modelled ocean current data can partly explain and support the above described distribution of coral provinces and migrations.

In the case of Eastern Australia, the modelled ocean currents for a Tournaisian-Viséan palaeogeography, coming directly from the Panthalassan Ocean and bypassing pole wards the eastern continental margin of Gondwana, effectively block faunal exchange with the Palaeotethyan provinces. This circulation pattern brakes down during the Variscan Orogeny and from the Serpukhovian on Eastern Australia could be connected to the Palaeotethyan provinces. However at the time the rotation of Gondwana has brought Eastern Australia into a more temperate southern position unsuitable for corals. This movement is also seen in the gradual disappearance of Mississippian corals and reefs in the Viséan of Eastern Australia, which starts earlier in the south (N.S.W.) than in the North (Queensland) (Webb 2000).

The modelled current pattern in the Palaeothethyan Ocean can partly explain the observed delayed appearance of Western European taxa in China. Both simulations show the presence of currents from the West to the East, which could enable migration in this direction if geographical features like islands or seamounts would have been present along the potential migration route. However the simulations also show the consistent presence of strong equatorial East-West currents. So far it is not clear why these currents did not result in the migration of Chinese taxa towards Western Europe. The data on coral distribution show Chinese coral taxa in the western ATC, but not in the western Palaeotethyan Ocean. However, the modelled current directions are in agreement with migrations from Eastern Europe into Western Europe (including North Africa) during upper Viséan and Serpukhovian times, but migration further to the East along the northern margin of Gondwana seems to be less common. Thus this pathway seems to be excluded for migration of Western European taxa into China.

The high endemism of the North American fauna is also a result of geographic isolation along the western margin of Laurussia. The exchange with the Western European province via the southern margin of the continent is blocked by a strong East-West current. Migrations from the Palaeotethyan provinces to the western margin of Laurussia via its northern margin are not well supported by the current patterns and also may have been difficult in respect to distance and water temperatures. However, the North American coral faunas with the most Palaeotethyan aspects are known from Alaska.

In conclusion, the modelled current and temperature data can help to interpret the distribution of Mississippian corals. However in further steps more palaeoecological limitations have to be incorporated in this analysis.

References

Dubatolov V.N. & Vassiljuk N.P. (1980). Coral Paleozoogeography in the Devonian and Carboniferous of Eurasia. *Acta Palaeontologica Polonica*, 25 (3-4): 519-529.

Fedorowski J. (1977). Development and distribution of Carboniferous corals. Mémoires du Bureau de Recherches Géologiques et minières (BRGM), 89: 234-248.

Poty E., Aretz M. & Xu S. (2011). A comparison of Mississippian colonial rugose corals from Western Europe and South China. In Aretz M., Delculée S., Denayer J. & Poty E. (Eds). XIth International Symposium on Fossil Cnidaria and Porifera, Liège, Belgium. *Kölner Forum für Geologie und Paläontologie*, 19: 135-136.

Webb G.E. (1990). Lower Carboniferous coral fauna of the Rockhampton Group, East-Central Queensland. *Memoirs of the Association of Australian Palaeontologists*, 10: 1-167.

Webb G.E. (2000). The palaeobiogeography of Eastern Australian Lower Carboniferous corals. *Historical Biology*, 15: 91-119.

Ocean oxygenation and nutrification in relation Phanerozoic climate evolution

Christian J. Bjerrum

Nordic Center for Earth Evolution, and Department of Geosciences and Natural Resource Management, University of Copenhagen, Øster Voldgade 10, DK-1350 Kbh. K, Denmark; E-Mail: cjb@geo.ku.dk

The geobiological co-evolution of life and surface chemistry on Earth is a fundamental premise that we are only just beginning to understand. Paleo-biogeography, -biodiversity and -ecosystem evolution variably depend on the physical and chemical oceanography through time. Yet, the ocean-atmosphere chemistry is influenced by biological changes. Great progress has been made in understanding and reconstructing the spatial and temporal evolution of paleoclimate. In contrast we have limited understanding of the evolution of ocean chemistry through time. Of particular importance to marine ecosystems are ocean oxygenation and nutrient levels. Here a model of the long term mean nutrient and oxygen levels of the world ocean through the Phanerozoic is presented and accompanied by a review available proxies and implications.

The mean oxygen concentration of the world ocean, and thereby the oceans susceptibility de-oxygenation, is at any point in time dependent on multiple factors. Nutrient levels (dissolved inorganic phosphate (DIP) and/or nitrate etc.) set the marine productivity, ecosystem structure and particle flux to the ocean interior, and thereby the ocean interior oxygen demand. Seeking to understand oxygenation-anoxia in the world ocean it is therefore pertinent to ask what processes control the nutrient inventory and how much it could have changed through the Phanerozoic?

In quantification of nutrient changes through time it is of primary importance to model how sea-level change and shelf-area extent influence the DIP inventory, marine productivity and burial of organic carbon (Bjerrum *et al*., 2006). The model of Bjerrum *et al*. (2006) is update to include explicit resolution of a two layer shelf system. The biogeochemical model explicitly considers the seafloor – surface area distribution of Earth as a function of elevation and the burial efficiency now as a function of siliciclastic sedimentation rate. Based on the model results we find that sea-level rise, on time scales longer than ~100 kyr, results in a significant decreased nutrient inventory of the ocean because of the greater burial efficiency in expanded shelf areas (Fig. 1). The reduced nutrient inventory results in decreased productivity which eventually causes oxygenation of the global ocean.

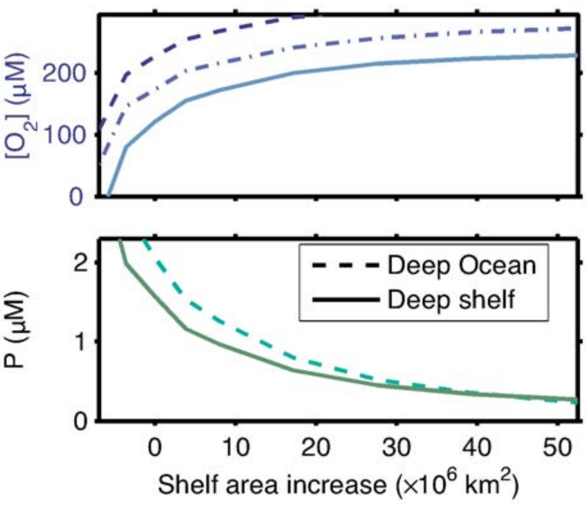

Fig. 1: **Model phosphate and oxygen concentrations as function of shelf area increase relative to present. The Cretaceous shelf area (~30 to 50 $\times 10^6$ km^2 larger than today) would imply the deep ocean had <0.5 μM PO4, if shelf area was the only thing that was different.**

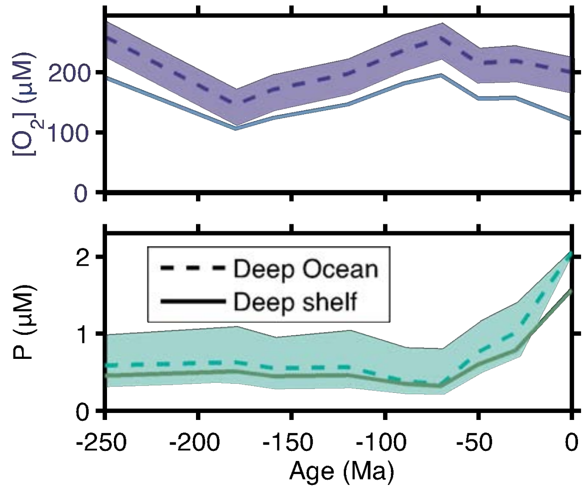

Fig. 2: **Model phosphate and oxygen concentrations over the last 250 Ma. Note how the long term mean Mesozoic deep ocean perhaps had a significantly reduced phosphate concentration and variably oxygen replete conditions.**

Additional processes can result in changes in the nutrient inventory and thereby the oceans susceptibility to be oxygenated or de-oxygenated. In particular we find that the temperature dependent decay of organic matter in the ocean is quite significant. We evaluate changes such at atmospheric O_2; ocean sulfate concentration; high latitude preformed phosphate and trace nutrient fertilization of other regions with high-nutrient, low-chlorophyll; ocean meridional circulation; and phosphate scavenging associated with sea-floor spreading.

How the DIP inventory may have changed through the Phanerozoic is modeled building on the sensitivity experiments. The phosphate model is coupled to a carbon-sulfur cycle model derived from the family of simple silicate weathering models (Berner, 2006; Wallmann, 2004). The nutrient inventory of the world ocean and its base state oxygen concentration is thereby a function of the model derived weathering and temperature changes as well as global sedimentation rates. Even though the model derived oceanic nutrient change has a large uncertainty, a picture emerges of low mean DIP in the Mesozoic in contrast to the increasing levels during the Cenozoic (Fig. 2). The modeled very oligotrophic ocean is associated with low productivity of marine organic matter and has a long term mean well oxygenated ocean interior.

References

Berner R.A. (2006). GEOCARBSULF: A combined model for Phanerozoic atmospheric O-2 and CO_2. *Geochimica et Cosmochimica Acta*, 70(23): 5653-5664.

Bjerrum C.J., Bendtsen J. & Legarth J.J.F. (2006). Modeling organic carbon burial during sea level rise with reference to the Cretaceous. *Geochemistry Geophysics Geosystems*, 7(Q05008), doi:10.1029/2005GC001032.

Wallmann K. (2004). Impact of atmospheric CO_2 and galactic cosmic radiation on Phanerozoic climate change and the marine d18O record. *Geochemistry Geophysics Geosystems*, 5, doi:10.1029/2003GC000683.

Behavior of phosphorus during the Cenomanian-Turonian anoxic event

Brahimsamba Bomou[1,4], Thierry Adatte[1], Haydon Mort[2], Brian Gertsch[3], Karl B. Föllmi[1]

[1]Institut des Sciences de la Terre, Université de Lausanne, Unil-Mouline, Geopolis, 1015 Lausanne, Suisse
[2]Department of Geology, Federal University of Pernambuco, Cidade Universitária, 50.740-530, Recife – PE, Brazil
[3]Earth, Atmospheric and Planetary Science Department, MIT, Cambridge, MA 02139, USA
[4]present address: UMR-CNRS 6249 Chrono-environnement, Université de Franche-Comté, 16 route de Gray, 25030 Besançon Cedex, France; E-Mail: bbomou@univ-fcomte.fr

Oceanic Anoxic Events represent ones of the most important global environmental changes throughout the Phanerozoic and the identification of the precise triggers have been subject of much debate, in particular for the Cenomanian-Turonian oceanic anoxic event (OAE2). Recent reconstructions of the phosphorus (P) accumulation have provided new perspectives in this regard. Dependent on the oxygen concentration in the depositional environment, this element can be incorporated into organic matter as well as various mineral phases.

Previous works have shown that P accumulation peaking globally at the onset of OAE 2, a period of time that saw a rapid increase in primary productivity. In Tethyan sediments, this peak in P was occurring independently of detrital fluctuations. It was concluded that the peak in P burial was a result of the increase production of organic matter, followed by a shutdown in P burial, brought on by increased anoxic conditions.

However, this explanation does not work in sediments deposited in oxic conditions, as observed in more eastern parts of the Tethys (e.g. Tibet, Sinai). We present data suggesting that P distribution patterns were driven by fluctuation in detrital input. The correspondence of detrital flux proxies with the rapid late Cenomanian sea-level transgression, points to the increased distance of continental P sources as the main cause of the decline in P accumulation. Using mineralogy, we also note a significant climatic shift from humid to more arid conditions, which may have also decreased the chemical erosion of phosphate minerals, further dampening the P signature in offshore settings.

The evidence of detrital-P being the likely cause of P fluctuations in the Eastern Tethys does not negate the idea that anoxia was the principal driver of these fluctuations in the organic-rich Western Tethys. However, this requires an explanation as to why the P accumulation signal is mirrored in both oxic and anoxic sedimentary successions. 'Eustatic/climatic' and 'productivity/anoxic' models may have both operated simultaneously in different parts of the world depending on local conditions, both producing similar trends in P accumulation.

Carbonate clumped isotopes thermometry for reconstructing paleoenvironments: principles, applications and challenges

Magali Bonifacie, Damien Calmels

Institut de Physique du Globe de Paris. Equipe de Géochimie des Isotopes Stables, 1 rue Jussieu, 75238 Paris Cedex 05, France; E-Mail: bonifaci@ipgp.fr, calmels@ipgp.fr

One of the most critical parameter for determining past environmental conditions at the Earth's surface is the temperature of the oceans that are necessary for constraining the feedbacks between climate, biogeochemical cycling, ocean circulation, and tectonics, and understanding the controls on mass extinctions, evolutionary radiations, and other ups and downs in the biodiversity. For decades, the most quantitative approach for reconstructing paleotemperature has been the use of oxygen isotope ratios in carbonate minerals, based on the thermodynamic fractionation between ^{16}O and ^{18}O during carbonate precipitation (Urey, 1947, Equation 1).

$$Ca^{2+} + 2\ HCO_3^- \rightleftarrows CaCO_3 + CO_2 + H_2O \text{ [Eq. 1]}$$

This approach is still debated because the $\delta^{18}O$ of marine carbonate depends on both the temperature (through the thermodynamic isotopic fractionation) and the $\delta^{18}O$ of seawater from which the mineral has precipitated. The $\delta^{18}O$ of seawater is impacted by various local or global factors such as the amount and geographic distribution of ice, the sea level, the ocean circulation, the evaporation–precipitation balance or water-rock interaction with seafloor. All these possible effects cast considerable uncertainty on the use of oxygen isotopic ratios as a robust paleothermometer. Moreover, additional problems appear when studying deep time sediments, namely the preservation of the initial carbonate composition. Indeed, once crystallized, carbonate minerals can interact with fluids during diagenesis, metamorphism or weathering, and this process can significantly alter the original composition of carbonate minerals (e.g., Knauth & Kennedy, 2009). Many alternative paleothermometers have been proposed to overcome the problem inherent to the carbonate-water oxygen isotope paleothermometry such as thermometers based on organic biomarkers (e.g., alkenones) or on the partitioning of elements (e.g., Mg/Ca ratios) between seawater and biogenic carbonates. However these approaches rely on empirical calibrations of complex non-equilibrium phenomena and can hardly be extrapolated to organisms or conditions beyond their calibrations (mainly pre-Cenozoic times). Furthermore, trace-metal thermometers generally suffer from vital effects and are sensitive to the composition of the water from which minerals grew. Carbonate clumped isotope thermometry shows unprecedented promises to remove uncertainties arising from traditional paleothermometers since it is based on principles that differ in many aspects. In brief, the carbonate clumped isotope paleothermometry (Δ_{47}) is based on the temperature-dependent formation of $^{13}C^{18}O^{16}O_2^{2-}$ ion groups within solid carbonate minerals: at low temperatures ^{13}C - ^{18}O bonds are thermodynamically favored and at really high temperature (>1000°C) the abundance of ^{13}C -^{18}O bonds is stochastic, ie., random. This method is particularly interesting as it is based on internal equilibrium (Equation 2) and thus rigorously provides crystallization temperature by measuring the isotopic composition of a single phase: the carbonate.

$$X^{12}C^{18}O^{16}O_2 + X^{13}C^{16}O_3 \rightleftarrows X^{13}C^{18}O^{16}O_2 + X^{12}C^{16}O_3 \text{ [Eq. 2]}$$

For this reason the carbonate clumped isotope thermometer is particularly useful for reconstructing past temperature as it does not require the knowledge of the isotopic composition of the water in which the carbonate has grown. Moreover carbonate clumped isotope analysis is always accompanied by measurement of $\delta^{18}O$, giving access to the $\delta^{18}O$ of the water from which carbonate grew. Another attractive feature of the Δ_{47} thermometer, as compared with the $\delta^{18}O$ thermometer, is that it is based on a thermodynamically controlled process that apparently differs little among various kinds of inorganic and biogenic carbonates (i.e., there is no vital effects, and therefore can be used on a large variety of carbonate minerals). Here we will describe some key applications of Δ_{47} that helped to better constrain pre-Cenozoic environments (Came *et al.*, 2007; Finnegan *et al.*, 2011; Bristow *et al.*, 2011) as well as current methodological and interpretational challenges of this proxy that are currently studied at IPGP.

References

Bristow T.F., Bonifacie M., Derkowski A., Eiler J.M. & Grotzinger J.P. (2011). A hydrothermal origin for isotopically anomalous cap dolostone cements from south China. *Nature*, 474: 68-71.

Came R., Eiler J. M., Veizer J., Azmy K., Brand U. & Weidman C. R. (2007). Coupling of surface temperatures and atmospheric CO_2 concentrations during the Palaeozoic era. *Nature***,** 449: 198 – 201.

Knauth L.P. & Kennedy M.J. (2009). The late Precambrian greening of the Earth. *Nature*, 460: 728–732.

Finnegan S., Bergmann K., Eiler J.M., Jones D.S., Fike D.A., Eisenman I., Hughes N.C., Tripati A.K. & Fischer W.W. (2011). The magnitude and duration of Late Ordovician-Early Silurian glaciation. *Science*, 331(6019): 903-906.

Urey H. C. (1947). The Thermodynamic Properties of Isotopic Substances. *Journal of the Chemical Society*, 562–581.

Paleoclimatic maps, new element to discuss evolution and radiation of major clades, exemple of angiosperms radiation

Anne-Claire Chaboureau[1], Yannick Donnadieu[1], Pierre Sepulchre[1], Alain Franc[2]

[1]Laboratoire des Sciences du Climat et de l'Environnement (LSCE) UMR 8212 - CNRS-CEA-UVSQ, CEA Saclay/ Orme des Merisiers/ Bat. 701, 91191 Gif/Yvette, France; E-Mail: anne-claire.chaboureau@lsce.ipsl.fr; yannick.donnadieu@lsce.ipsl.fr; pierre.sepulchre@lsce.ipsl.fr
[2]UMR Biodiversité Gènes et Communautés, INRA, 69 route d'Arcachon, 33612 CESTAS Cedex, France; E-Mail: alain.franc@pierroton.inra.fr

The « sudden » appearance of Angiosperms during the Cretaceous, also called « abominable mystery » by Darwin currently remains a major discussion point. The origin of Angiosperms, leading to the replacement of gymnosperms, is still debated, especially the nature of primitive flowers and the evolution of major lineages.

The first indices of angiosperms are lower Cretaceous ages and are mainly localized in the northern hemisphere. They are dated around the Barremian-Aptian boundary, in eastern North America (e.g., Hickey and Doyle, 1977) and eastern China (Li, 2003), and in Portugal. The first distinctive angiosperm fossil is found in strata of the Yixian Fm of northeastern China and is also dated around the Barremian–Aptian boundary. Except some pollen types that have been reported from the Hauterivian in Europe (Hughes and McDougall, 1990; Hughes *et al.*, 1991) there are currently no other fossils from pre-Barramian age that can be assigned to the angiosperms with certainty (Friis *et al.*, 2006).

A few millions years later, during Aptian and Albian times, a dramatic increase in abundance and diversity of pollen types, leaf floras and fossil assemblages is described in many localities. Fossils of angiosperms are described in Europe (Friis *et al.*, 2000, 2001; Schönenberg and Friis, 2001), North America (Gandolfo *et al.*, 2002), Asia (Sun *et al.*, 2002; Leng and Friis, 2003), South America (Mohr and Friis, 2000), New Zealand (Kennedy *et al.*, 2003) and even Antarctica (Eklund, 2003), covering the lower-middle Cretaceous (Barremian-Aptian boundary) to the Upper Cretaceous (Maastrichtian). This diversification marks the beginning of a transition in the Mesozoic floras from a dominance of ferns, conifers and cycads to ecosystems dominated by angiosperms (Crane *et al.*, 1995).

This sudden appearance and diversity is a major question, as many authors attempted to explain the origin and radiation of this clade. Recently, Coiffard *et al.* (2012) have explained this "sudden" appearance by a diversification of their habitats in three steps, by benefiting from any opportunities offered by climatic changes. Here we are particularly interested by the latter, and by the relation between global climate and evolution of major clades. Is the apparition of Angiosperms, and of other certain floras due to concomitant evolution of climate? According to climate and paleogeographic constraints, what were the migration routes possible?

We discuss the evolution of Angiosperms with paleoclimatic maps from the Jurassic, lower middle and late Cretaceous, Eocene to Miocene. Climate modeling has been performed with the global climate model FOAM to obtain monthly precipitations and temperatures. These climatic variables have been translated to climatic regions (polar, cold, temperate warn and cold, arid, and tropical climates) according to the classification of Köppen. Combined paleogeography and climatic regions provide new elements of discussion about the dispersal paths for the species.

The first results show that with a CO_2 value fixed to 560 ppm for each paleogeography, the Cenomanian is characterized by higher global mean surface temperatures and precipitations. Futhermore, from the lower to the middle Cretaceous, the percentage of climate temperate zones has doubled, reaching the highest value and involving more extensive temperate regions, ultimately opening more migration routes at this period.

An interesting point is the location of various Angiosperms fossils (Central Europe, North America, Asia) dated from the middle-late Cretaceous in temperate zones of Köppen. The location of the fossils-rich regions under a temperate climate raises the hypothesis that the development of temperate humid conditions could trigger explosion and expansion of Angiosperms clades. The successful invasion of Angiosperms in restrained environments and their expansion into others within 45 My (Coiffard *et al.*, 2012) could be caused and enhanced by the temperate climatic optimum regions, in a world of dispersed continents.

References

Coiffard C., Gomez B., Daviero-Gomez V. & Dildcher D.L. (2012). Rise to dominance of angiosperm pioneers in European Cretaceous environments. *PNAS*, 109 (51): 20955–20959.

Crane P.R., Friis E.M. & Pedersen K.R. (1995). The origin and early diversification of angiosperms. *Nature*, 374: 27–33.

Eklund H. (2003). First Cretaceous flowers from Antarctica. *Review of Palaeobotany and Palynology*. 127: 187-217.

Friis E.M., Pedersen K.R. & Crane P.R. (2000). Fossil floral structures of a basal angiosperm with monocolpate, reticulate-acolumellate pollen from the Early Cretaceous of Portugal. *Grana*, 3: 226-245.

Friis E.M., Pedersen K.R. & Crane P.R. (2001). Fossil evidence of water lilies (Nymphaeales) in the Early Cretaceous. *Nature*, 410: 357-360.

Friis E.M., Pedersen K.R. & Crane P.R. (2006). Cretaceous angiosperm flowers: Innovation and evolution in plant reproduction. *Palaeogeography, Palaeoclimatology, Palaeoecology*, 232: 251-293.

Gandolfo M.A., Nixon K.C. & Crepet W.L. (2002). Triuridaceae fossil flowers from the Upper Cretaceous of New Jersey. *American Journal of Botany*, 89: 1940-1957.

Hickey L.J. & Doyle J.A. (1977). Early Cretaceous fossil evidence for angiosperm evolution. *The Botanical Review*, 43: 2-104.

Hughes N.F. Mcdougall A.B. (1990). Barremian–Aptian angiospermid pollen records from southern England. *Review of Palaeobotany and Palynology*, 65: 145–151.

Hughes N.F., Mcdougall A.B. & Chapman J.L. (1991). Exceptional new record of Cretaceous Hauterivian angiospermid pollen from southern England. *Journal of Micropalaeontology*, 10: 75– 82.

Li H. (2003). Lower Cretaceous angiosperm leaf from Wuhe in Anhui, China. *Chinese Science Bulletin*, 48: 611– 614.

Kennedy E.M., Lovis J.D. & Daniel J.L. (2003). Discovery of a Cretaceous angiosperm reproductive structure from New Zealand. *New Zealand Journal of Geology and Geophysics*, 46: 519-522.

Leng Q. & Friis E.M. (2003). *Sinocarpus decussatus* gen. et sp. nov, a new angiosperm with syncarpous fruits from the Yixian Formation of Northeast China. *Plant Systematics and Evolution*, 241: 77-88.

Mohr B. & Friis E.M. (2000). Early angiosperms from the Aptian Crato Formation (Brazil), a preliminary report. *International Journal of Plant Sciences*, 161(6 Suppl.): S155-S167.

Schönenberger J. & Friis E.M. (2001). Fossil flowers of ericalean affinity from the Late Cretaceous of Southern Sweden. *American Journal of Botany*, 88: 467-480.

Sun G., Ji Q., Dilcher D.L., Zheng S., Nixon K.C. & Wang X. (2002). Archaefructaceae, a new basal angiosperm family. *Science*, 296: 899-904.

Rhythms and blues: Flood basalt volcanism and environmental change

Vincent Courtillot, Frédéric Fluteau

Institut de Physique du Globe and Université Paris-Diderot, Sorbonne Paris Cité, 1 rue Jussieu, Paris, France

Although correlation of the dates of emplacement of large igneous provinces (LIP) and mass extinctions do suggest a causal relationship, details of the mechanism are not still well understood. Many factors can play a key role in the destructive consequences of their emplacement: among these, we have chosen to concentrate on eruptive rhythms. There has been further recent work on the detailed timing of volcanic sequences showing that flood basalts may differ in latitude, strength, chemistry, intruded crust, but that the main parameter controlling the features and intensity of mass extinctions could be the exact time sequence and volumes of extruded lava and gases injected by these flows into the atmosphere (actually stratosphere). We have been able to determine the sequence of volcanic pulses in the Deccan traps (Chenet *et al.*, 2007, 2008, 2009) and subsequently in the Karoo traps (Moulin *et al.*, 2011, 2012, in prep).

In the Deccan case, there appear to have been three main periods of volcanism spanning some 2.5 Myr, but with each sequence having lasted on the order of 100 kyr or less. On a much smaller time scale (<1 ka), detailed analysis of secular variation has allowed us to show that the Deccan traps were built as a succession of volcanic pulses that could have exceeded 10^4 km^3 in volume extruded in less than a century, possibly only a decade (using geomagnetic and paleomagnetic secular variation as a relative dating tool). For the Main Province (80% of the total volume of Deccan traps), the duration of Deccan volcanism did not exceed 600 kyr but the duration of volcanic activity (*stricto sensu*, corresponding to the total duration of flow emplacement but excluding quiescence periods between flows) probably did not exceed 10 kyr. Observations from paleontology and physical volcanology have been blended with our own work to produce a more complete picture. So volcanism appears as a fractal time sequence (somewhat like Cantor dust), with several embedded time scales from a million years down to a decade. In the end, it appears that some individual major pulses could have had durations and consequences rather similar to the Chicxulub impact. An impact alone is not likely to cause a mass extinction, but in the KT case an impact occurred after volcanism had started and added a major blow to the sequence of events.

The Karoo traps are often associated with the environmental perturbations and (second order) biotic crises near the Pliensbachian-Toarcian boundary. Applying the procedure used in the Deccan traps, we find two rather brief paroxysmal phases, separated by a few million years. The duration of the first phase, amounting about 10% of the total lava volume, did not exceed ~100 kyr and the duration of the main volcanic phase (some 90% of the volume) did not exceed 900 kyr, and possibly much less. Detailed analysis of secular variation recorded in three sampled sections in South Africa and Lesotho reveals a succession of volcanic pulses, each lasting less than a century. For each one of them, total volcanic activity probably did not exceed a few centuries for phase 1 and a few millennia for phase 2. Using magnetic directions, several volcanic pulses could be correlated over distances up to 200 km. Combined analysis of available geochronologic, geochemical and paleomagnetic data from the entire Karoo-Farrar traps leads us to suggest that they were emplaced as a small number (3 or 4) of paroxysmal phases, whose duration probably did not exceed a million years. This emplacement chronology is in good agreement with the discontinuous rhythm of environmental and biotic perturbations near the Pliensbachian-Toarcian boundary.

We are also pursuing climate modelling to quantitatively analyse the consequences of massive CO_2 and SO_2 injection into the environment (see Mussard *et al.*, this volume).

References

Chenet A.L., Quidelleur X, Fluteau F. & Courtillot V. (2007). 40K-40Ar dating of the main Deccan large igneous province: Further evidence of KTB age and short duration. *Earth and Planetary Science Letters*, 263: 1-15, doi:10.1016/j.epsl.2007.07.011.

Chenet A.L., Fluteau F., Courtillot V., Gérard M. & Subbarao K.V. (2008). Determination of rapid Deccan eruptions across the Cretaceous-Tertiary boundary using paleomagnetic secular variation: Results from a 1200-m-thick section in the Mahabaleshwar escarpment. *Journal of Geophysical Research*, 113: B04101, doi:10.1029/2006JB004635.

Chenet A. L., Courtillot V., Fluteau F., Gérard M., Quidelleur X., Khadri S.F.R., Subbarao K.V. & Thodarson T. (2009). Determination of rapid Deccan eruptions across the Cretaceous-Tertiary boundary using paleomagnetic secular variation: 2. Constraints from analysis of eight new sections and synthesis for a 3500-m-thick composite section. *Journal of Geophysical Research*, 114: B06103, doi:10.1029/2008JB005644.

Courtillot V. & Fluteau F. (2010). Cretaceous Extinctions: The Volcanic Hypothesis. *Science*, 328: 973-974.

Moulin M., Fluteau F., Courtillot V., Marsh J., Delpech G., Gérard M. & Jay E.A. (2011). An Attempt to Constrain the Age, Duration and Eruptive History of the Karoo Flood Basalt: the Naude's Nek Section (South Africa). *Journal of Geophysical Research*, 116: B07403, 27pp., doi:10.1029/2011JB008210.

Moulin M., Courtillot V., Fluteau F. & Valet J.P. (2012). The "van Zijl" Jurassic geomagnetic reversal revisited. *Geochemistry, Geophysics, Geosystems*, 13, doi:10.1029/2011GC003910.

Fifty years of $\delta^{18}O$ data accumulation on the Jurassic system: But what paleoclimatic patterns arise in time and space?

Guillaume Dera

Géosciences Environnement Toulouse (GET), Observatoire Midi Pyrénées, Université de Toulouse, CNRS, IRD, 14 avenue E. Belin, F- 31400 Toulouse, France; E-mail: guillaume.dera@get.obs-mip.fr

Since the pioneering works of Urey *et al.* (1951), the use of the oxygen isotope composition of marine fossils as paleothermometer has been widely democratized in the geological community. Rapidly, numerous Earth scientists adopted this geochemical approach, leading to regular international publications on the evolution of seawater temperatures during geological periods. For the Jurassic, the first studies using $\delta^{18}O$ values of fossil shells as paleoclimatic indicators go back to the sixties with the works of Bowen (1961), Berlin *et al.* (1964), Fritz (1964) and Stahl & Jordan (1969). These initial results obtained from European, American, and Russian basins showed that the Jurassic climate was probably warmer and more equable than today but marked by important variations through time.

Owing to the continuous influx of well-dated $\delta^{18}O$ data both from different regions of the world and different marine fossils (calcitic, aragonitic or phosphated), our knowledge of Jurassic paleoclimatic changes has been considerably improved. Nevertheless, rare are studies embracing and comparing all Jurassic data. This large-scale approach is though necessary to decipher global vs. regional trends through time as well as potential latitudinal gradients in seawater temperatures. In this study, we tackle this issue by exhaustively compiling data from eighty papers published from 1961 to 2013, representing more than 5800 data from all continents. The comparison of data measured on organisms inhabiting different parts of the water column (belemnites, ammonites, bivalves, brachiopods, fishes, ostracods, crocodylians) allows the variations in deep and surface seawater temperatures to be discussed. Importantly, the main temporal changes are observed independently of organisms used. For instance, the Toarcian and Kimmeridgian periods appear warmer in most cases. However, Jurassic $\delta^{18}O$ trends may be very divergent according to studied areas. The most obvious example concerns the beginning of the Late Jurassic when SST seems to increase in northern Tethyan areas (Europe) whereas it decreases in southern Tethyan areas (India, Australia). These regional divergences lead therefore to discuss the paleoclimatic vs. paleoceanographic origin of trends in $\delta^{18}O$ data. Also, an emerging question is the choice of seawater $\delta^{18}O$ values used to calculate temperatures. Arbitrarily, most paleoclimatologists use constant and spatially homogeneous values of -1‰ for an ice-free world or 0‰ if geochemical data relate to subtropical environments with higher evaporation rates. Compared to modern spatial patterns showing strong drops in oceanic $\delta^{18}O$ values from equator to poles (up to 2‰ of difference), this straightforward approach tends to artificially increase polar temperatures and it gives an erroneous idea of an equable Jurassic climate. Here, we show that by assuming more realistic seawater $\delta^{18}O$ values (taken from present patterns or GCM simulations), latitudinal thermal gradients are more pronounced and it is likely that near-freezing water conditions sporadically occurred in polar areas. These results question therefore the dogmatic "greenhouse" definition for the Jurassic paleoclimate.

References

Berlin T.S., Naydin D.P., Saks V.N., Teis R.V. & Khabokov A.V. (1967). Jurassic and Cretaceous climate in northern USSR, from paleotemperature determinations. *International Geology Review*, 9(8): 1080-1092.

Bowen R. (1961). Paleotemperature analyses of Belemnoidea and Jurassic Paleoclimatology. *Journal of Geology*, 69(3): 309-320.

Fritz P. (1964). O^{18}/O^{16} Isotopeanalysen und Paleotemperaturbestimmungen an Belemniten aus dem Schäbischen Jura. *Geologische Rundschau*, 54: 261-269.

Stahl W. & Jordan R. (1969). General considerations on isotopic paleotemperature determinations and analyses on Jurassic ammonites. *Earth and Planetary Science Letters*, 6: 173-178.

Urey H.C., Lowenstam H.A., Epstein S., & McKinney C.R. (1951). Measurements of paleotemperatures and temperatures of the Upper Cretaceous of England, Denmark, and the southern United States. *Bulletin Geological Society of America*, 62: 399-416.

Continental drainage and oceanic circulation during the Jurassic inferred from the Nd isotope composition of biogenic phosphates and sediments

Guillaume Dera[1], Jonathan Prunier[1], Paul Smith[2], Jim Haggart[2,3], Evgeny Popov[4], Alexander Guzhov[5], Mikhail Rogov[6], Dominique Delsate[7], Detlev Thies[8], Gilles Cuny[9], Emmanuelle Pucéat[10], Guillaume Charbonnier[11], Germain Bayon[12]

[1]Géosciences Environnement Toulouse (GET), Observatoire Midi Pyrénées, Université de Toulouse, CNRS, IRD, 14 avenue E. Belin, F- 31400 Toulouse, France; E-mail: guillaume.dera@get.obs-mip.fr
[2]Department of Earth, Ocean and Atmospheric Sciences, University of British Columbia, 2207 Main Mall, Vancouver, British Columbia V6T 1Z4, Canada
[3]Geological Survey of Canada, 1500-605 Robson Street, Vancouver, British Columbia V6B 5J3, Canada
[4]Department of Palaeontology, Geological Faculty, Saratov State University, 83 Astrakhanskaya Str., 40012 Saratov, Russia
[5]Paleontological Institute, Russian Academy of Sciences, 123 Profsoyuznaya ul., 117997 Moscow, Russia
[6]Geological Institute, Russian Academy of Sciences, 7 Pyzhevsky lane, 119017 Moscow, Russia
[7]Muséum National d'Histoire Naturelle, 25 rue Munster, 2160 Luxembourg, Luxemburg
[8]Institut für Geologie, Leibniz Universität Hannover, Callinstr. 30, D-30167 Hannover, Germany
[9]The Natural History Museum of Denmark, Øster Voldgade 5-7, 1350 Copenhagen, Denmark
[10]Laboratoire Biogéosciences, Université de Bourgogne, 6 Bd Gabriel, 21000 Dijon, France
[11]Laboratoire IDES, Université Paris Sud XI, Bâtiment 504, 91405 Orsay, France
[12]Ifremer, Unité de Recherche Géosciences Marines, 29280 Plouzané, France

The Jurassic Period marked the onset of Pangean dislocation that led to our modern geography. The initiation of this major continental reorganisation involved numerous geodynamic processes whose timing, interaction and feedback had important paleoclimatic and geochemical consequences. Among them, the opening of the northern Atlantic Ocean and the development of transcontinental seaways across the Laurasian and Gondwanan cratons caused major modifications to global oceanic circulation which significantly affected heat and moisture transport (Donnadieu *et al*., 2006). At the same time, the incipient growth of the Pacific plate triggered increases in plate subduction rates, terrane accretion, and volcanism all around the Panthalassan ocean (Bartolini & Larson, 2001). Similarly, many subduction and accretion events occurred in other domains, leading to progressive closures of the Paleotethyan and Mongol-Okhotsk oceans. This global reorganisation of both continental masses and oceanic circulation patterns likely affected the Jurassic climate by shifting the climatic belts, changing albedo, and modulating atmospheric pCO_2 through volcanic degassing or changes in silicate weathering rates (Dera *et al*., 2011).

In this study, we attempt to better constrain oceanic connections as well as the modifications in continental drainage that resulted from the Jurassic paleogeographical reorganisation. For this purpose, we present 53 new neodymium isotope values (noted $\varepsilon Nd_{(t)}$) measured on fossil fish teeth, ichthyosaur bones, phosphate ooids, and sediments from Europe, European Russia, and North America. Application of this geochemical proxy is based on the principle that rocks weathered on continents have different Nd isotope compositions according to their origin (volcanic vs. cratonic) and age (Precambrian to recent). Through fluvial discharge, seawater acquires its εNd signal (recorded by phosphate during early diagenesis) reflecting all potential sources in the drainage area (Tachikawa *et al*., 2003). As the Nd residence time is relatively short compared with the global oceanic mixing rate, this geochemical proxy is deemed conservative and very suitable for tracking exchanges of water masses with different isotopic signatures (Martin & Scher, 2004). For example, Stille *et al*. (1996) showed that during the Triassic Period, Panthalassan and Tethyan ocean waters were very radiogenic owing to extensive volcanic sources. During the Pangean dislocation, climate changes caused stronger weathering of the cratons, leading to less radiogenic Tethyan seawaters. Recently, Dera *et al*. (2009) also reported that tropical and boreal waters of the Tethyan Ocean could sporadically have been mixed during the Early Jurassic. Here we reappraise the evolution of circulation patterns at high stratigraphical resolution (ammonite biozone) by specifying both the potential sources and the drainage pathways that influenced seawater signatures throughout the Jurassic Period.

Combined with an exhaustive compilation of worldwide εNd data from the literature, our new results show that the sources of Nd were very different according to oceanic domains (Fig. 1). In contrast to current patterns showing that all circum-Pacific volcanic areas of the Ring of Fire contribute to the radiogenic signal of the Pacific Ocean (Jeandel *et al*., 2007), the radiogenic signature of Panthalassan waters (≈ -3.9) was mainly dependant on North-American and southern Gondwanan volcanic arc inputs. Indeed, the sediments of Asian Panthalassan margins show very low $\varepsilon Nd_{(t)}$ values presumably resulting from the dilution of local volcanic sources by massive Precambrian cratonic input from rising Amurian relief. In the Tethyan domain, the tropical seawater $\varepsilon Nd_{(t)}$ values are comparatively less radiogenic (≈ -6.3). This probably reflects a mixing of radiogenic sources such as Panthalassan waters or volcanic Cimmerian inputs and unradiogenic influxes from former Laurasian and Gondwanan crust. Toward higher latitudes, the Nd isotope composition of Tethyan waters strongly decreases in the Euro-boreal domain (-8.6) but remains higher in the Russian seaway (-7.4). This difference could result from the respective influences of unradiogenic Precambrian Fenno-Scandian sources to the north and radiogenic Cimmerian volcanic inputs to the east. Finally, we note that the $\varepsilon Nd_{(t)}$ values of Euro-boreal and Russian seawaters strongly fluctuate through time and reflect short-term changes in water mass circulation patterns and/or sporadic modifications of drainage areas during the Jurassic.

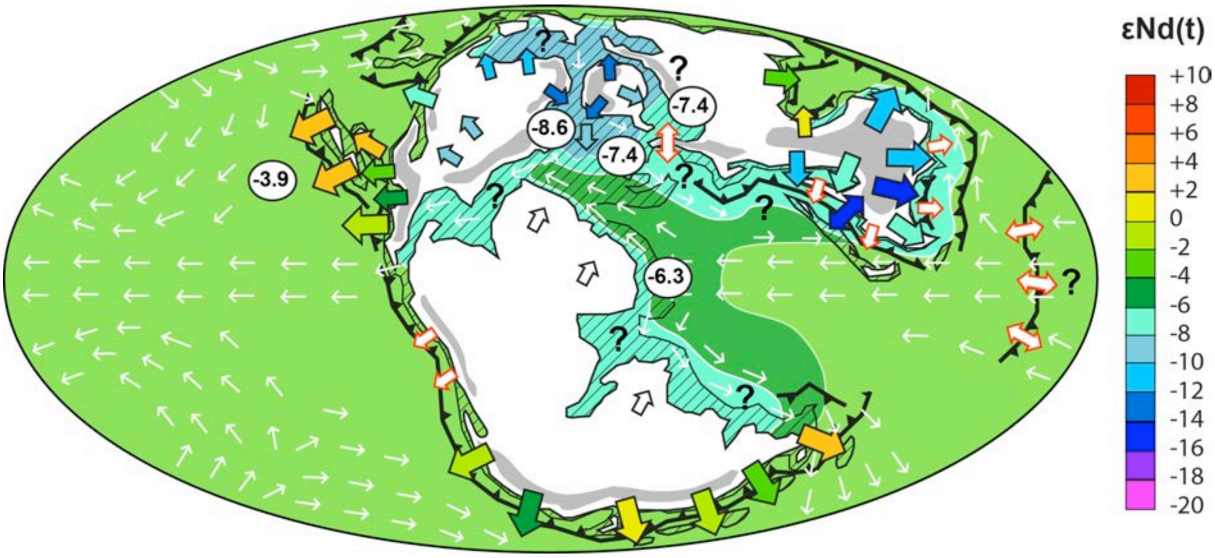

Fig. 1: **Schematic map of the Nd isotope composition of Jurassic seawaters and sedimentary inputs. Numerical values indicate the median values of regional seawater. Fine white arrows represent the main surface oceanic currents (based on numerical simulations of Dera & Donnadieu 2012). Dashed areas correspond to epicontinental seas and grey areas represent high reliefs. Blank arrows with black and red contours respectively show potential unradiogenic and radiogenic inputs. Question marks represent areas with extrapolated or unknown $\varepsilon Nd_{(t)}$ signatures.**

References

Bartolini A. & Larson R. (2001). Pacific microplate and the Pangea supercontinent in the Early to Middle Jurassic. *Geology*, 29(8): 735-738.

Dera G. & Donnadieu Y. (2012). Modeling evidences for global warming, Arctic seawater freshening, and sluggish oceanic circulation during the Early Toarcian anoxic event. *Paleoceanography*, 27: PA2211, doi:10.1029/2012PA002283.

Dera G., Brigaud B., Monna F., Laffont R., Pucéat E., Deconinck J.-F., Pellenard P., Joachimski M. & Durlet C. (2011). Climatic ups and downs in a disturbed Jurassic world. *Geology*, 39(3): 215-218.

Dera G., Pucéat E., Pellenard P., Neige P., Delsate D., Joachimski M.M., Reisberg L. & Martinez M. (2009). Water mass exchange and variations in seawater temperature in the NW Tethys during the Early Jurassic: Evidence from neodymium and oxygen isotopes of fish teeth and belemnites. *Earth and Planetary Science Letters*, 286: 198–207.

Donnadieu Y., Goddéris Y., Pierrehumbert R., Dromart G., Fluteau F. & Jacob R. (2006). A GEOCLIM simulation of climatic and biogeochemical consequences of Pangea breakup. *Geochemistry, Geophysics, Geosystems*, 7(11): Q11019, doi:10.1029/2006GC001278.

Jeandel C., Arsouze T., Lacan F., Téchiné P. & Dutay J.-C. (2007). Isotopic Nd compositions and concentrations of the lithogenic inputs into the ocean: A compilation, with an emphasis on the margins. *Chemical Geology*, 239: 156-164.

Martin E.E. & Scher H.D. (2004). Preservation of seawater Sr and Nd isotopes in fossil fish teeth: bad news and good news. *Earth and Planetary Science Letters*, 220: 25–39.

Stille P., Steinmann M. & Riggs S.R. (1996). Nd isotope evidence for the evolution of the paleocurrents in the Atlantic and Tethys oceans during the past 180 Ma. *Earth and Planetary Science Letters*, 144: 9–19.

Tachikawa K., Athias V. & Jeandel C. (2003). Neodymium budget in the modern ocean and paleo-oceanographic implications. *Journal of Geophysical Research* 108, 10/1–10/3.

What can be inferred on the late Ordovician cooling using a climate model

Yannick Donnadieu[1], Alexandre Pohl[1], Guillaume Le Hir[2], Jean-François Buoncristiani[3]

[1] Laboratoire des Sciences du Climat et de l'Environnement (LSCE),, CNRS, CE Saclay, Orme des Merisiers, 91191 Gif/Yvette, France; E-Mail: yannick.donnadieu@lsce.ipsl.fr
[2]IPGP, Paris, France; E-Mail: lehir@ipgp.fr
[3]Biogéoscience, Université de Bourgogne, Dijon, France; E-Mail: jfbuon@u-bourgogne.fr

The Ordovician is an exciting period for climate modelers as this is a completely different Earth characterized by an asymmetric distribution of the continents with a northern hemisphere covered by ocean from the North pole to 50°N. In addition, recent studies point to a cooling slowly beginning in the Katian and with an acceleration during the Hirnantian. Here we use the fully coupled ocean atmosphere model "FOAM" to test the impact of the land-sea distribution on the global climate and on the oceanic surface currents. Despite glacial conditions, atmospheric CO_2 levels during this period were thought to be elevated with estimated ranges from as high as 16x, to low values such as 4x pre-industrial levels (i.e. 280 ppm). We apply FOAM to test climate state for atmospheric CO_2 levels ranging from 16x to 4x. Preliminary results show a tipping point between 8x and 6x with a mean global temperature fall of 8°C. We will show the consequences of this non-linear instability on the tropical surface currents, on the equatorial temperatures and, on the geometry and on the volume of the ice-sheets (using the GRISLI ice-sheet model).

A Phanerozoic CO_2 history driven by tectonics

Yannick Donnadieu[1], Yves Goddéris[2], Guillaume Le Hir[3], Vincent Lefebvre[1,2], Elise Nardin[2]

[1] Laboratoire des Sciences du Climat et de l'Environnement (LSCE),, CNRS, CE Saclay, Orme des Merisiers, 91191 Gif/Yvette, France; E-Mail: yannick.donnadieu@lsce.ipsl.fr
[2]Géosciences Environnement Toulouse (GET), Observatoire Midi Pyrénées, Université de Toulouse, CNRS, IRD, 14 avenue E. Belin, F- 31400 Toulouse, France; E-mail: yves.godderis@get.obs-mip.fr
[3]IPGP, Paris, France; E-Mail: lehir@ipgp.fr

Our understanding of the geological regulation of the carbon cycle has been deeply influenced by the contribution of Bob Berner with his well-known model GEOCARB. Here, we will present a fundamentally different carbon cycle model that explicitly accounts for the effect of the paleogeography using physically based climate simulations and using 22 continental configurations spanning the whole Phanerozoic. We will show that several key features of the Phanerozoic climate can be simply explained by the modulation of the carbon cycle by continental drift. In particular, the continental drift may have strongly impacted the runoff intensity as well as the weathering flux during the transition from the hot Early Cambrian world to the colder Ordovician world. Another fascinating example is the large atmospheric CO_2 decrease simulated during the Triassic owing to the northward drift of Pangea exposing large continental area to humid sub-tropics and boosting continental weathering. Conversely, our model fails to reproduce the climatic trend of the last 100 Ma. This is due to the highly dispersed continental configurations of the last 100 Ma that optimize the consumption of CO_2 through continental weathering. This discrepancy may be reduced if we account for a larger influence of the Earth degassing flux on the atmospheric CO_2 evolution, which could come from the increase contribution of the pelagic component on the oceanic crust on the global carbonate flux and from the many sub-marine LIPs occurring during the Late Cretaceous.

Magnetite dissolution by acid rains due to volcanogenic atmospheric halogen input: an "experimental" approach

Sébastien Fabre[1], Anne Nédélec[2], Eric Font[3]

[1]IRAP, OMP, Université de Toulouse, France; E-Mail: sebastien.fabre@irap.omp.eu
[2]Géosciences Environnement Toulouse (GET), Observatoire Midi Pyrénées, Université de Toulouse, CNRS, IRD, 14 avenue E. Belin; F- 31400 Toulouse, France
[3]IDL-UL, Instituto Dom Luís, Universidade de Lisboa, Portugal

The origin of the Cretaceous-Palaeogene crisis is still disputed, notably because the duration of the two causal phenomena -Deccan volcanism and Chixculub impact- can hardly be separated in the sedimentary record. Below the Iridium-rich layer of the Bidart (France) section, there is a low magnetic susceptibility interval hypothesized to result from Deccan Phase-2 (Appelo *et al.*, 1999). This interval shows a drastic diminution of detrital magnetite content regarded as a consequence of enhanced magnetite dissolution on the continent. This hypothesis is supported by the recent recognition of basaltic trap volcanism as a major contributor to the halogen budget of the atmosphere (Chenet *et al.*, 2007).

We constructed a geochemical weathering model with the code PHREEQC (Font *et al.*, 2011), in order to constrain the time required to reach nearly complete magnetite dissolution inland. Results show that such process is possible in ca 33,000 yrs when considering acid rain (pH=4.3) waters resulting from the Deccan volcanism and a runoff typical of intertropical conditions. This time interval matches duration of the Deccan phase-2 (Self *et al.*, 2008). Finally, we propose a sedimentary model linked to environmental changes induced by Deccan volcanism.

References

Appelo C.A.J. & Parkhurst D.L. (1999). *User's guide to PHREEQC version 2 - A computer program for speciation, batch-reaction, one-dimensional transport, and inverse calculations*. Water-Ressources Investigations Rep. 99-4259, U.S. Geological Survey, Denver, Colorado.

Chenet A.L., Quidelleur X., Fluteau F., Courtillot V. & Bajpai S. (2007). K-40-Ar-40 dating of the Main Deccan large igneous province: Further evidence of KTB age and short duration. *Earth and Planetary Science Letters*, 263: 1-15, doi:DOI 10.1016/j.epsl.2007.07.011.

Font E., Nedelec A., Ellwood B.B., Mirao J. & Silva P.F. (2011). A new sedimentary benchmark for the Deccan Traps volcanism? *Geophysical Research Letters*, 38, doi:10.1029/2011gl049824.

Self S., Blake S., Sharma K., Widdowson M. & Sephton, S. (2008). Sulfur and chlorine in Late Cretaceous Deccan magmas and eruptive gas release. *Science*, 319: 1654-1657.

Understanding mid-Cretaceous carbon cycling: an integrated approach from the non-marine sediments of West Greenland

Corinne Fay[1], Stuart Robinson[2], Jennifer McElwain[3], Stephen Hesselbo[4], Gunver Pedersen[5], Richard Barclay[6], Ken Amor[7], Paul Bown[8]

[1]Department of Earth Sciences, University College London, United Kingdom; E-Mail: corinne.fay.10@ucl.ac.uk
[2]Department of Earth Sciences, University College London, United Kingdom; E-Mail: stuart.robinson@ucl.ac.uk
[3]School of Biology and Environmental Science, University College Dublin, Ireland; E-Mail: jennifer.mcelwain@ucd.ie
[4]Department of Earth Sciences, University of Oxford, United Kingdom; E-Mail: Stephen.Hesselbo@earth.ox.ac.uk
[5]Department of Geography and Geology, University of Copenhagen, Danmark; E-Mail: Gunver@geo.ku.dk
[6]National Museum of Natural History, Smithsonian Institution, U.S.A.; E-Mail: barclayrs@si.edu
[7]Department of Earth Sciences, University of Oxford, United Kingdom; E-Mail: kena@earth.ox.ac.uk
[8]Department of Earth Sciences, University College London United Kingdom; E-Mail: p.bown@ucl.ac.uk

It is widely accepted that the climate for the majority of the Cretaceous was in a greenhouse state, caused primarily by high atmospheric carbon dioxide (CO_2) concentrations. However, CO_2 levels were likely not constant through time and many studies have shown the Cretaceous carbon cycle and climate were dynamic. One of the most striking manifestations of carbon cycle disturbance in the Cretaceous geological record is the occurrence of widespread marine black shales (Jenkyns, 2003 and references therein). These shales represent up to 1 million year durations of marine anoxia, whereby biological demand for oxygen exceeded supply from ocean ventilation, and are called oceanic anoxic events or OAEs (Schlanger & Jenkyns, 1976). Such anoxic events have been identified at other times in Earth's history (e.g. the Toarcian OAE – Jenkyns, 1988), but the mid-Cretaceous ocean appears to have been particularly sensitive to factors promoting anoxia (Fig. 1). The exact trigger mechanisms of OAEs are still debated, and each event may be unique to a certain extent. However, suggested causes include factors that affect ocean circulation (promoting stagnation) and nutrient balance (driving productivity demand). Cretaceous ocean circulation is likely to have been more sluggish due to high temperatures and probably operated differently to present-day thermohaline circulation (Hay, 2008). Large igneous province emplacement probably had a key role in the initiation of marine anoxia, and geological and geochemical records of these extrusive phases closely coincide with those of OAEs. For example, the Selli Event (OAE 1a, 124 Ma) occurred during the emplacement of the Ontong Java Plateau (126-119 Ma), which rapidly released large pulses of CO_2 into the atmosphere (Tejada *et al.*, 2009). Other tectonic changes also contributed CO_2 to the atmospheric budget, evidenced by strontium-isotope ratios of marine carbonates (Jones & Jenkyns, 2001). During the Selli Event the strontium-isotope ratios suggest increased hydrothermal activity, which could be interpreted as an increase in sea-floor spreading rates (Jones & Jenkyns, 2001). This too would have contributed large amounts of mantle-derived CO_2 to the atmosphere. Increased CO_2 is thought to have accelerated the hydrological cycle, increasing surface run-off and nutrient flux to the oceans, enhancing productivity (Bailey *et al.*, 2003). In addition, increased hydrothermal activity may have fertilised low productivity areas through iron release (micronutrient), enhancing productivity and driving the region towards anoxia (Larson & Erba, 1999). The tectonic and temperature-driven sea level changes may also have affected the nutrient balance by changing the marine shelf area exposed, affecting productivity and carbon burial (Bjerrum *et al.*, 2006). Despite the variety of hypothesised impacts on the carbon cycle and atmospheric pCO_2 levels, there are only a few high-resolution pCO_2 records across OAEs (Barclay *et al.*, 2010; McElwain *et al.*, 2005a).

Significant changes occurred on land during the Cretaceous; higher temperatures compared to present-day allowed life to thrive at high latitudes. Vertebrate fossil records from the Canadian Arctic of champsosaurs, turtles and fish, indicate a mean annual temperature of 14 °C (Tarduno *et al.*, 1998; Friedman *et al.*, 2003). On the Antarctic Peninsula, fossil tree ring analyses suggest temperatures of 13-27 °C (Francis & Poole, 2002 and references therein), but it is the change in the floral assemblages through the Cretaceous that is of interest to this study. The exact time of origin of the angiosperms (flowering plants) is still debated, but there is definitive evidence in the Barremian and Aptian from fossil flowers, fruits and seeds. Once established, the angiosperms rapidly diversified and radiated through the Albian and Campanian, and it has been suggested that diversity changes and the rise of angiosperms to ecological dominance occurred in phases to the detriment of other floral groups (McElwain *et al.*, 2005b and references therein).

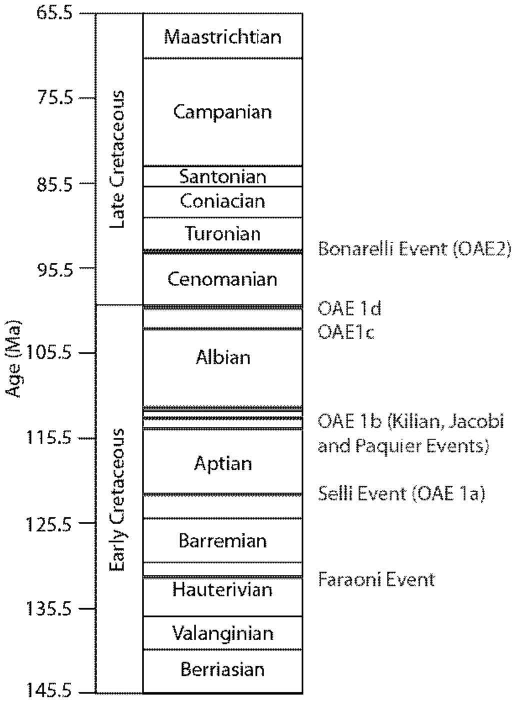

Fig. 1: **Generalised Cretaceous Stratigraphy with presently recognised oceanic anoxic events, adapted from Gradstein *et al.* (2004).**

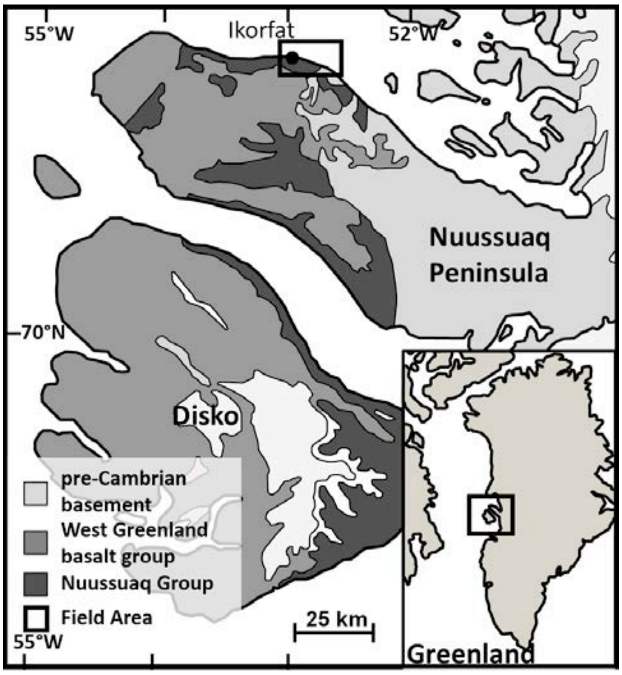

Fig. 2**: Summary geological map of field area adapted from Dam *et al.* (2009), showing the location of the Nuussuaq Peninsula (inset) and the distribution of the Nuussuaq Group (Cretaceous sediments) in the Baffin Bay area.**

This study seeks to explore the relationship between the disturbances to the carbon cycle during OAEs and the radiation of the angiosperms, by investigating the applicability of the CO_2 starvation hypothesis to this interval of time. The CO_2 starvation hypothesis (Teslenko, 1967; Robinson, 1994; McElwain *et al.*, 2005b) proposes periods of decreased atmospheric CO_2 concentrations may have been a forcing factor in plant evolution, selecting for angiosperous traits that would maximize photosynthesis and transpiration under a declining atmospheric CO_2 regime. The possession of traits such as high vein density and finely controllable stomata would confer a competitive advantage to angiosperms over other incumbent plant groups such as gymnosperms and pteridophytes, attaining ecological dominance as a result. Currently, the timing of acquisition of biological traits that would confer an advantage in a low CO_2 world are relatively well constrained (Feild *et al.*, 2011) but our understanding of coeval changes in atmospheric CO_2 concentration is less well established. We propose relative decreases in pCO_2 (partial pressure of CO_2) occurred during OAEs, whereby massive burial of carbon in black shales during marine anoxia resulted in an oceanic carbon deficit, buffered by CO_2 down-draw from the atmosphere into the ocean (Kump & Arthur, 1999). This has been evidenced using the stomatal index technique of atmospheric pCO_2 reconstruction by Barclay *et al.* (2010) for the Cenomanian-Turonian boundary OAE (OAE 2), but trends in pCO_2 during other OAEs remain unknown, or are simply inferred from trends in carbon-isotope ratios ($\delta^{13}C$). In order to test the hypothesis, we aim to generate pCO_2 records that span mid-Cretaceous OAEs. To reconstruct pCO_2, we use the stomatal density and index of fossil leaf cuticle because this method allows high-resolution stratigraphic records to be generated, and is relatively precise compared to other proxy methods that are applicable to the Cretaceous, such as soil carbonates (Royer *et al.*, 2001 and references therein). Plants optimise their stomatal characters to maximise photosynthetic gain against water loss in response to pCO_2, such that during intervals of relatively high pCO_2, plants reduce the number of stomata on the leaf surface (Salisbury, 1927; Woodward, 1987). By measuring the stomatal density of leaves through an interval of time, the relative changes in pCO_2 can be determined. Environmental stresses such as drought reduces the volume of all cells, generating an apparent increase in stomatal density. This is resolved by using the stomatal index: an expression of stomatal density relative to the number of epidermal cells (Salisbury, 1927). On long timescales, reconstructions of pCO_2 derived from fossil leaf material tend to agree with predictions based on carbon cycle modelling (Royer *et al.*, 2001).

Well-preserved fossil leaves are generally found in marginal and non-marine palaeoenviroments. The Albian-Cenomanian sediments of the Nuussuaq Group found across the Nuussuaq Peninsula of West Greenland (Fig. 2), have long been known to contain well-preserved fossil floras dating back toexpeditions and collections curated by Oswald Heer (1874-1883). More recent work on the north coast of the Nuussuaq Peninsula by Austin Boyd (1998a, b, c, 2000) documented the location and content of florules (plant-rich horizons) and forms the basis of our field sampling strategy. The field team revisited Boyd's localities in 2009, in order to sample stratigraphy covering the radiation of angiosperms recorded in Boyd's work. The lithologies encountered were dominantly fluvio-deltaic and lacustrine deposits containing abundant fossil leaf cuticle and fossil wood pieces (Dam *et al.*, 2009).

The age estimates for our studied sections are based on the fossil flora and a few dinoflagellate cysts that occur during brackish incursions in the otherwise freshwater palaeoenvironment (Dam *et al.*, 2009 and references therein). We use carbon-isotope chemostratigraphy of fossil wood and bulk organic matter to correlate the field sections to published hemipelagic and pelagic carbon-isotope records of OAEs. If OAEs are global carbon cycle perturbations, they should disturb the carbon-isotopic budget of surficial carbon reservoirs (Gröcke *et al.*, 1999 and references therein), and would be expressed in most carbon-isotopic profiles, including those from terrestrially derived organic material, which reflects changes in the atmospheric carbon-isotopic budget. The carbon-isotope stratigraphy generated by this study allows, for the first time, a more refined age estimate of the sediments along the north coast of the Nuussuaq Peninsula, in addition to covering two carbon cycle disturbances that are likely attributable to OAE1b and OAE1d. We also provide the preliminary findings of the stomatal density investigation, and highlight the excellent level of preservation of the fossil leaf cuticle (chemically macerated from the sediment) through a demonstration of initial morphotypes identified. We believe the integrated approach of this study is of particular importance in understanding past climate systems and we plan to explore the complex impact and feedbacks that atmospheric CO_2 can have on the terrestrial biosphere, to provide some insight into future climate change related to elevated CO_2 conditions.

References

Bailey T.R., Rosentha, Y., Mcarthu, J.M., Van De Schootbrugge, B. & Thirlwal, M.F. (2003). Paleoceanographic changes of the Late Pliensbachian-Early Toarcian interval: a possible link to the genesis of an Oceanic Anoxic Event. *Earth and Planetary Science Letters*, 212: 307-320.

Barclay R.S., McElwai, J.C. & Sagema, B.B. (2010). Carbon sequestration activated by a volcanic CO_2 pulse during Ocean Anoxic Event 2. *Nature Geoscience*, 3: 205-208.

Bjerrum C.J., Bendtsen J. & Legarth J.J.F. (2006). Modeling organic carbon burial during sea level rise with reference to the Cretaceous. *Geochemistry, Geophysics, Geosystems*, 7: 1-24.

Boyd A. (1998a). Macroleaf biostratigraphy of the Early Cretaceous beds in West Greenland. *Zentralblatt für Geologie und Paläontologie*, 1996: 1455-1468.

Boyd A. (1998b). The Bennettitales of the Early Cretaceous floras from West Greenland: *Pseudocycas. Palaeontographica Abteilung B*, 247: 123-155.

Boyd A. (1998c). Cuticular and impressional angiosperm leaf remains from the Early Cretaceous floras of West Greenland. *Palaeontographica Abteilung B*, 247: 1-53.

Boyd A. (2000). Bennettitales from the Early Cretaceous floras of West Greenland: *Pterophyllum* and *Nilssoniopteras*. *Palaeontographica Abteilung B*, 255: 47-77.

Dam G., Pedersen G.K., Sønderholm M., Midtgaard H.H., Larsen L.M., Nøhr-Hansen H. & Pedersen A.K. (2009). Lithostratigraphy of the Cretaceous-Paleocene Nuussuaq Group, Nuussuaq Basin, West Greenland. *Geological Survey of Denmark and Greenland Bulletin*, 19: 171 pp.

Feild T.S., Brodribb T.J., Iglesias A., Chatelet D.S., Baresch A., Upchurch G.R., Gomez B., Mohr B.A.R., Coiffard C., Kvacek J. & Jaramillo C. (2011). Fossil evidence for Cretaceous escalation in angiosperm leaf vein evolution. *PNAS*, 108, 8363-8366.

Francis J.E. & Poole I. (2002). Cretaceous and early Tertiary climates of Antarctica: evidence from fossil wood. *Palaeogeography, Palaeoclimatology, Palaeoecology*, 182: 47-64.

Friedman M., Tarduno J.A. & Brinkman D.B. (2003). Fossil fishes from the high Canadian Arctic: further palaeobiological evidence for extreme climatic warmth during the Late Cretaceous (Turonian-Coniacian). *Cretaceous Research*, 24: 615-632.

Gradstein F.M., Ogg J.G. & Smith A.G. (Eds) (2004). *A Geologic Time Scale 2004*. Cambridge University Press, Cambridge.

Gröcke D.R., Hesselbo S.P. & Jenkyns H.C. (1999). Carbon-isotope composition of Lower Cretaceous fossil wood: Ocean-atmosphere chemistry and relation to sea-level change. *Geology*, 27: 155-158.

Hay W.W. (2008). Evolving ideas about the Cretaceous climate and ocean circulation. *Cretaceous Research*, 29: 725-753.

Heer O. (1874). Nachträge zur miocenen Flora Grönlands. *Kungliga Svenska Vetenskaps-Akademiens Handlingar*, 13: 29 pp.
Heer, O. (1880). Nachträge zur fossilen Flora Grönlands. *Kungliga Svenska Vetenskaps-Akademiens Handlingar*, 18: 17 pp.
Heer O. (1882). Flora fossilis Grönlandica. Die fossile Flora Grönlands. Erster Theil, *Verlag von J. Wurster & Comp*., Zïrich. 112 pp.
Heer O. (1883a). Flora fossilis Grönlandica. Die fossile Flora Grönlands. Zweiter Theil, *Verlag von J. Wurster & Comp*., Zïrich. 275 pp.
Heer O. (1883b). Oversigt over Grønlands fossile flora. *Meddelelser om Grønland*, 5: 79–202.
Jenkyns H.C. (2003). Evidence for rapid climate change in the Mesozoic-Palaeogene greenhouse world. *Philosophical Transactions of the Royal Society of London A*, 361: 1885-1916.
Jones C.E. & Jenkyns H.C. (2001). Seawater strontium isotopes, oceanic anoxic events and seafloor hydrothermal activity in the Jurassic and Cretaceous. *American Journal of Science*, 301: 112-149.
Kump L.R. & Arthur M.A. (1999). Interpreting carbon-isotope excursions; carbonates and organic matter. *Chemical Geology*, 161: 181-198.
Larson R.L. & Erba E. (1999). Onset of the mid-Cretaceous greenhouse in the Barremian-Aptian: Igneous events and the biological, sedimentary and geochemical responses. *Paleoceanography*, 14: 663-678.
McElwain J.C., Wade-Murphy J., & Hesselbo S.P., (2005a). Changes in carbon dioxide during an oceanic anoxic event linked to intrusion into Gondwana coals. *Nature*, 435: 479-482.
McElwain J.C., Willis K.J. & Lupia R. (2005b). Cretaceous CO_2 decline and the radiation and diversification of angiosperms. In: Ehleringer, J.R., Cerling, T.E. & Dearing, M.D. (Eds), *A history of atmospheric CO_2 and its effect on plants, animals and ecosystems*. Springer, New York. pp. 133-165.
Robinson J.M. (1994). Speculations on carbon dioxide starvation, Late Tertiary evolution of stomatal regulation and floristic modernization. *Plant, Cell & Environment*, 17: 345-354.
Royer D.L., Berner R.A. & Beerling D.J. (2001). Phanerozoic atmospheric CO_2 change: evaluating geochemical and paleobiological approaches. *Earth-Science Reviews*, 54: 349-392.
Salisbury E.J. (1927). On the causes and ecological significance of stomatal frequency, with special reference to the woodland flora. *Philosophical Transactions of the Royal Society of London, Series B*, 216: 1-65.
Schlanger S.O. & Jenkyns H.C. (1976). Cretaceous Oceanic Anoxic Events: Causes and Consequences. *Geologie en Mijnbouw*, 55: 179-184.
Tarduno J.A., Brinkman D.B., Renne P.R., Cottrell R.D., Scher H. & Castillo P. (1998). Evidence for Extreme Climatic Warmth from Late Cretaceous Arctic Vertebrates. *Science*, 282: 2241-2244.
Tejada M.L.G., Suzuki K., Kuroda J., Coccioni R., Mahoney J.J., Ohkouchi N., Sakamoto T. & Tatsumi Y. (2009). Ontong Java Plateau eruption as a trigger for the early Aptian oceanic anoxic event. *Geology*, 37: 855-858.
Teslenko Y.V. (1967). Some aspects of evolution of terrestrial plants. *Geologia I Geofizica (Novosibirsk)*, 11: 58-64.
Woodward F.I. (1987). Stomatal numbers are sensitive to increases in CO_2 from pre-industrial levels. *Nature*, 327: 617-618.

Atmospheric halogen and acid rains during the major Deccan episode: magnetic and mineral evidences

Eric Font[1], Sébastien Fabre[2], Anne Nédélec[3], Thierry Adatte[4], Gerta Keller[5], Jorge Ponte[1]

[1]IDL-UL, Instituto Dom Luís, Universidade de Lisboa, Portugal
[2]IRAP, Université de Toulouse, France
[3]Géosciences Environnement Toulouse (GET), Observatoire Midi Pyrénées, Université de Toulouse, CNRS, IRD, 14 avenue E. Belin; F- 31400 Toulouse, France
[4]ISTE, Geopolis, CH-1015 Lausanne, Switzerland
[5]Geosciences Department, Princeton University, Princeton, NJ 08544, USA

Environmental and climatic changes linked to Deccan volcanism are still poorly known. A major limitation resides in the paucity of direct Deccan volcanism markers and in the geologically short interval where both impact and volcanism occurred, making it hard to evaluate their contributions to the mass extinction. We investigated the low magnetic susceptibility interval just below the Iridium-rich layer of the Bidart (France) section, which was recently hypothesized to be the result of palaeoenvironmental perturbations linked to paroxysmal Deccan phase-2. Results show a drastic decrease of detrital magnetite and presence of fine specular akaganeite, a hypothesized reaction product between $FeCl_2$ from the volcanic plume with water and oxygen in the high atmosphere. A weathering model of the consequences of acidic rains on a continental regolith reveals nearly complete magnetite dissolution after about 33,000 years, which is consistent with our magnetic data and the duration of the Deccan phase-2. This discovery represents an unprecedented piece of evidence of the nature and importance of the Deccan-related environmental changes.

The Jurassic world: from stable isotopes to numerical simulations of the climate and carbon cycle

Yves Goddéris[1], Guillaume Dera[1], Yannick Donnadieu[2]

[1]Géosciences Environnement Toulouse (GET), Observatoire Midi Pyrénées, Université de Toulouse, CNRS, IRD, 14 avenue E. Belin, F- 31400 Toulouse, France; E-mail: yves.godderis@get.obs-mip.fr
[2]Laboratoire des Sciences du Climat et de l'Environnement, CNRS-CEA, Gif sur Yvette, France

Oxygen isotope data acquired on belemnites are used to constrain the sea surface temperature in the European basins of the Tethys ocean (Dera *et al.*, 2011). From these subtropical temperature data we infer the corresponding global climate and atmospheric CO_2 levels using simulations of a coupled general circulation model covering the whole Jurassic (Donnadieu *et al.*, 2006). Coupling these climatic and CO_2 output to the belemnite $\delta^{13}C$ evolution, we reconstruct the major carbon flux over the Jurassic, including the solid Earth CO_2 degassing and the weathering fluxes. We found that the Toarcian and Kimmeridgian are characterized by intense solid Earth degassing fluxes. The high CO_2 degassing flux in the Toarcian can be correlated with the onset of the Karoo-Ferrar igneous province. However, the calculated degassing exceeds by a factor of 2 to 3 the maximum degassing rate capability estimated from independent inventory. To solve this paradox, we hypothesize that, during warm events, continental silicate weathering cannot indefinitely rise, being ultimately limited by the development of thick soils shielding the fresh bedrock from percolating waters in warm and humid areas, and by the expansion of arid areas (Goddéris *et al.*, 2008). Accounting for these two effects, we predict that the Toarcian volcanic degassing rate required to balance the CO_2 consumption by buffered silicate weathering falls within acceptable limits (within the present day range of uncertainty, Gerlach, 2011). This modeling study suggests that extreme warmth in the Phanerozoic may have been linked to the buffering of silicate weathering by the development of thick soils in humid areas and by the coeval expansion of deserts, rather than by extreme volcanic degassing.

References

Dera G., Brigaud B., Monna F., Laffont R., Pucéat E., Deconinck J.-F., Pellenard P., Joachimski M.M. & Durlet C. (2011). Climatic ups and downs in a disturbed Jurassic world. *Geology*, 39: 215-218.

Donnadieu Y., Goddéris Y., Pierrehumbert R., Dromart G., Fluteau F. & Jacob R. (2006). A GEOCLIM simulation of climatic and biogeochemical consequences of Pangea breakup. *Geochemistry, Geophysics, Geosystems*, 7(11): Q11019, doi:10.1029/2006GC001278.

Donnadieu Y., Dromart G., Goddéris Y., Pucéat E., Brigaud, B., Dera G., Dumas C. & Olivier N. (2011). A mechanism for brief glacial episodes in the Mesozoic greenhouse. *Paleoceanography*, 26, doi: 10.1029/2010PA002100.

Gerlach T. (2011). Volcanic versus anthropogenic carbon dioxide. *EOS*, 92: 201-202.

Godderis Y., Donnadieu Y., Tombozafy M. & Dessert C. (2008). Shield effect on continental weathering: implication for climatic evolution of the Earth at the geological timescale. *Geoderma*, 145: 439-448.

Deep time palaeoclimate: insights from oxygen isotopes in biogenic apatite

Michael M. Joachimski

GeoZentrum Nordbayern, University of Erlangen-Nuremberg, Germany; E-Mail: michael.joachimski@fau.de

Oxygen isotopes of calcitic fossil hardparts have been successfully applied to studies on climate and ice volume history in the younger geological history of the Earth (Zachos *et al.*, 2001). The use of oxygen isotopes in older geological time periods is hampered by potential diagenetic resetting of the oxygen isotope signals. In comparison to biogenic calcite, conodont apatite represent an alternative mineralogical phase for oxygen isotope analysis since apatite is considered to be relatively resistant to diagenetic exchange of phosphate-bound oxygen. Conodonts are phosphatic microfossils composed of carbonate-fluorapatite which vary in size from less than 0.5 mm up to approximately 2 mm. The tooth-like elements represent the only skeletal remains of the marine conodont animal, which is assumed to have been one of the earliest jawless vertebrates and which became extinct at 200 Ma. Short-term as well as long-term changes in the oxygen isotope ratios of Ordovician to Early Triassic (488 to 245 Ma) apatite are interpreted to reflect climatic changes as well the waning and waxing of high-latitude continental ice sheets. Devonian conodonts were studied from several sections in Europe, USA and Australia spanning the time interval of latest Silurian (Pridoli) to Late Devonian (Famennian). Reconstructed Late Silurian to Lochkovian sea surface temperatures (SST) were relatively high and start to decrease in the early Pragian with minimum and about 8° C cooler SSTs registered in the late Emsian to Givetian. Temperatures reconstructed for the middle to late Frasnian and early Famennian were again significantly warmer indicating considerable warming of low latitudes during the Frasnian. During the middle to late Famennian a moderate cooling trend is apparent culminating in the short-term glaciation at the Devonian–Carboniferous boundary, documented by a positive δ_{18}O excursion in conodont apatite (Kaiser *et al.*, 2006; Buggisch *et al.*, 2008). The Devonian palaeotemperature record contradicts earlier views that the Middle Devonian represented a supergreenhouse. The climax of coral–stromatoporoid reef development was during the Middle Devonian, an interval characterized by cool to intermediate tropical SSTs. Coral–stromatoporoid reefs were rare in the Early Devonian, finally becoming extinct in the latest Frasnian. Microbial reefs were abundant in the Early and Late Devonian suggesting that warm to very warm SSTs in the Early and Late Devonian were unfavourable for the development of coral–stromatoporoid reefs, but promoted growth of autotrophic reefs. Our data suggest that SST exerted a control on Devonian reef development and that climatic warming in the Late Frasnian in conjunction with short-term cooling pulses may have contributed to the extinction of coral–stromatoporoid reef ecosystems during the Frasnian–Famennian life crisis (Joachimski *et al.*, 2009).

Oxygen isotope ratios measured on Permian conodonts from South China exhibits relatively high values for the glaciated Early Permian, translating into warm low-latitudinal seawater temperature between 26 and 30 °C (assuming that Early Permian ice volume was comparable to the Pleistocene glacial maxima). In contrast to the earlier views that the Late Palaeozoic Ice Age terminated in the late Sakmarian, the conodont apatite oxygen isotope record suggests waning of the ice sheets in the Kungurian (Chen *et al.*, 2013). Ice melting is indicated by a pronounced decrease in δ_{18}O, which is interpreted as reflecting the combined effect of climatic warming and glacial ice melting. Significant temperature fluctuations (4 °C warming succeeded by 6 to 8 °C cooling) are observed during the Guadalupian–Lopingian transition, interpreted as combined climate changes induced by Emeishan volcanism and changes in habitat depth of analysed gondolellid conodonts. Oxygen isotope values increase in the Changhsingian suggesting climate cooling and potentially moving of studied conodont taxa *Clarkina* to deeper waters because of the Changhsingian sea level rise. Across the Permian–Triassic boundary, δ_{18}O values decrease parallel to the globally observed negative carbon isotope excursion suggesting significant climatic warming (Joachimski *et al.*, 2012). The latter is pointing to a cause–effect relationship between massive release of volcanic greenhouse gases derived from the Siberian Trap volcanism and related processes, climatic warming and the most dramatic extinction event in Earth history. In addition, very warm climate conditions in the Early Triassic played an important role in the timing and pattern of the slow recovery of marine and terrestrial ecosystems in the aftermath of the Permian-Triassic crisis (Sun *et al.*, 2012; Romano *et al.*, 2012).

References

Buggisch W., Joachimski M.M., Sevastopulo G. & Morrow J. (2008). Mississippian $\delta^{13}C_{carb}$ and conodont apatite $\delta^{18}O$ records: Their relation to the Late Palaeozoic glaciation. *Palaeogeography, Palaeoclimatology, Palaeoecology*, 268: 273-292.

Chen B., Joachimski M.M., Shen S.-Z., Lambert L., Lai X.L., Wang X.D. & Yuan D.X. (2013). Conodont apatite oxygen isotope record of the Permian: ice volume and palaeotemperature evolution. *Gondwana Research* (in press). http://dx.doi.org/10.1016/j.gr.2012.07.007.

Joachimski M.M., Breisig S., Buggisch W., Talent J.A., Mawson R., Gereke M., Morrow J.M., Day J. & Weddige K. (2009). Devonian climate and reef evolution: insights from oxygen isotopes in apatite. *Earth and Planetary Science Letters*, 284: 599-609.

Joachimski M.M., Lai X., Shen S., Jiang H., Luo G., Chen B. & Sun Y. (2012). Climatic warming in the latest Permian and the Permian-Triassic mass extinction. *Geology*, 40: 195-198.

Kaiser S.I., Steuber T., Becker R.T. & Joachimski M.M. (2006). Geochemical evidence for major environmental change at the Devonian-Carboniferous boundary mass-extinction. *Palaeogeography, Palaeoclimatology, Palaeoecology*, 240: 146-160.

Romano C., Goudemand N., Vennemann T.W., Ware D., Schneebeli-Hermann E., Hochuli P.Q., Brühwiler T., Brinkmann W. & Bucher W. (2012). Climatic upheavals following the end-Permian mass-extinction. *Nature Geoscience*, 6: 57-60.

Sun Y., Joachimski M.M., Wignall P.B., Yan C., Jiang H., Wang L. & Lai X. (2012). Lethally hot temperatures during the Early Triassic. *Science*, 338: 366-370.

Zachos J., Pagani M., Sloan L. & Thomas E.K. (2001). Trends, rhythms, and aberrations in global climate. *Science*, 292: 686-693.

Biotic Effects of Climate change the Chicxulub Impact and Deccan Volcanism during the Maastrichtian

Gerta Keller

Department of Geosciences, Princeton University, Princeton NJ 08540, U.S.A.; E-Mail: gkeller@princeton.edu

Climate changes during the late Cretaceous mark episodes of long-term cooling and short-term rapid warming from the late Campanian through the Maastrichtian. But the most rapid climate changes immediately followed the maximum cooling at the C30n/C29r transition. Shortly thereafter rapid greenhouse warming followed and ended by similarly rapid cooling prior to the end-Cretaceous mass extinction. These extreme rapid climate changes coincide with Deccan volcanism and the Chicxulub impact.

How these climate changes affected marine biota can be glimpsed from planktic foraminiferal species assemblages, the quantitative abundances of individual species their geographic and latitudinal distributions, affinity to changes in oxygen and carbon isotopes, and species depth habitats based on stable isotope ranking Abramovich *et al*. (2003, 2010). Through the Maastrichtian the climatic changes are strongly associated with variations in species diversity, morphologic and intraspecies size reductions, and commonly blooms of the disaster opportunist *Guembelitria cretacea* (Keller & Abramovich, 2009; Pardo & Keller, 2008). The biologic response varies depending on the nature of the environmental stress (climate cooling or warming), and the cause for the climate change (long-term climate change, or short-term volcanism, impacts).

This can be seen in blooms of the disaster opportunist *Guembelitria cretacea* from India through the eastern Tethys, North Atlantic to Texas (Fig. 1). The biotic response to greenhouse warming in C29r, as well as C29n appears universal in mesotrophic or restricted basins, shallow marginal or open marine settings and volcanically active regions – decreased species diversity through selective extinctions and elimination of large specialized species (k-strategists), decreased species population abundances, species dwarfing and/or gigantism. Both these climatic events coincide with Deccan volcanism phase-2 (C29r) and phase-3 (C29n) (Keller *et al*., 2012). A smaller initial phase-1 marks the onset of Deccan volcanism near the base of C30n and coincides with reduced biotic effects.

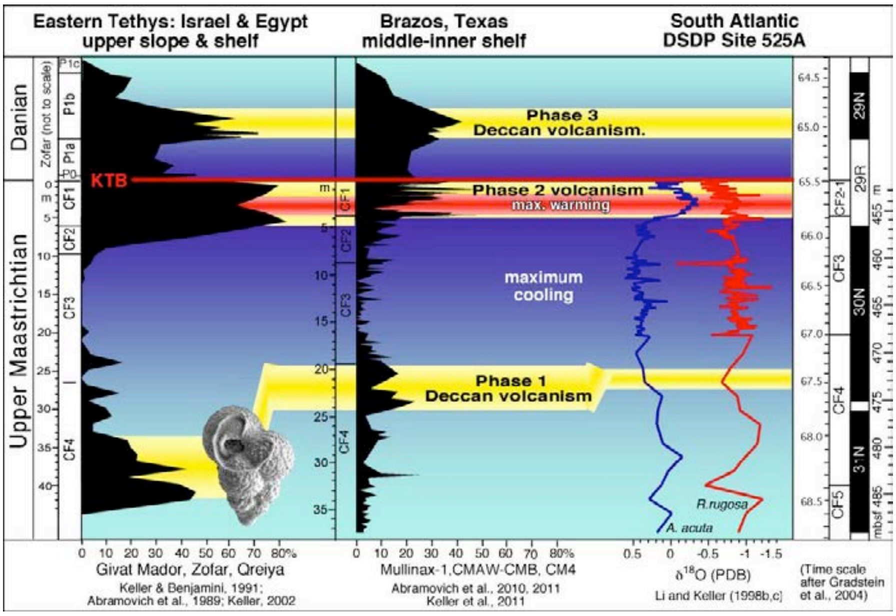

Fig. 1: **Stratigraphic correlation of Guembelitria bloom events in the upper Maastrichtian of the eastern Tethys (Israel) and Western Interior Seaway (Brazos, Texas) correlated with the climate record of South Atlantic DSDP Site 525A and Deccan volcanism phase-1, phase-2 and phase-3. Three Guembelitria blooms in zones CF4, CF2-CF1, and P1b mark major environmental stress conditions correlative with the three major phases of Deccan volcanism (From Keller *et al*., 2012).**

Thus, at the extreme end of the biotic response are volcanically influenced environments, which experienced the same detrimental environmental effects as observed in the aftermath of the KTB mass extinction, including the disappearance of most species and blooms of the disaster opportunist *Guembelitria cretacea*. No species extinctions or any other significant biotic effects could be observed at the level of the Chicxulub impact spherule deposition in zone CF1 about 130ky prior to the KTB (based on the KTB at 65.5Ma) (Keller *et al*., 2009). This indicates that the biotic effects of the Chicxulub impact have been vastly overrated and that the environmental effects were relatively short lived and not detectable at the 500-1000 year time scale. In contrast, the biotic effects of Deccan volcanism were extreme and leading up to the KTB mass extinction (Keller *et al*., 2012).

In contrast to climate warming, the biotic response to climate cooling is variable and can lead to dramatically reduced species abundances and diversity such as in the early and latest Maastrichtian. But the transition from cool to warm climate in early late Maastrichtian C31r lead to rapidly increased evolutionary activity and planktic foraminiferal diversity reached its maximum ever. Association with dramatically increased primary productivity suggests upwelling and increased water-mass stratification.

The biotic response to climate change is thus variable and depends on what caused the climate change in the first place. At the extreme ends are volcanically induced rapid climate and environmental changes that tend to be catastrophic for marine carbonate secreting critters. Longer-term climate cooling may result in changes of bottom water circulation and upwelling regime that may lead to dramatically increased evolutionary activity.

References

Abramovich S., Keller G., Stueben D. & Berner Z. (2003). Characterization of late Campanian and Maastrichtian planktic foraminiferal depth habitats and vital activities based on stable isotopes. *Palaeogeography, Palaeoclimatology, Palaeoecology*, 202: 1-29.

Abramovich S., Yovel-Corem S., Almogi-Labin A. & Benjamini C. (2010). Global climate change and planktic foraminiferal response in the Maastrichtian. *Paleoceanography*, 25: PA2201.

Keller G. & Abramovich S. (2009). Lilliput Effect in late Maastrichtian planktic Foraminifera: Response to Environmental Stress. *Palaeogeography, Palaeoclimatology, Palaeoecology*, 271: 52-68.

Keller G., Adatte T., Berner Z., Pardo A. & Lopez-Oliva L. (2009). New Evidence concerning the Age and Biotoc Effects of the Chicxulub impact in Mexico. *Journal Geological Society, London*, 166: 393-411.

Keller G., Adatte T., Bhowmick P.K., Upadhyay H., Dave A., Reddy A.N. & Jaiprakash B.C. (2012). Nature and timing of extinctions in Cretaceous-Tertiary planktic foraminifera preserved in Deccan intertrappean sediments of the Krishna-Godavari Basin, India. *Earth and Planetary Science Letter*, 341: 211-221.

Pardo A. & Keller G. (2008). Biotic Effects of Environmental Catastrophes at the end of the Cretaceous: *Guembelitria* and *Heterohelix* Blooms. *Cretaceous Research*, 29 (5/6): 1058-1073.

Eifelian – Givetian crisis: Evidence from lithological, geochemical and geophysical records of the Carnic Alps

Erika Kido[1], Thomas J. Suttner[1], Monica Pondrelli[2], Carlo Corradini[3], Maria G. Corriga[3], Luca Simonetto[4], Stanislava Vodrážková[5], Michael M. Joachimski[6], Leona Koptíková[7]

[1]University of Graz, Institute for Earth Sciences (Geology & Paleontology), Heinrichstrasse 26, A-8010 Graz, Austria; E-Mail: erika.kido@uni-graz.at, thomas.suttner@uni-graz.at
[2]International Research School of Planetary Sciences, Dipartimento di Scienze, Università d'Annunzio, viale Pindaro 42, I-65127 Pescara, Italy; E-Mail: monica@irsps.unich.it
[3]Dipartimento di Scienze Chimiche e Geologiche, Università di Cagliari, via Trentino 51, I-09127 Cagliari (Italy); E-Mail: corradin@unica.it, maria.corriga@unica.it
[4]Museo Friulano di Storia Naturale, via Marangoni 39-41, I-33100 Udine, Italy; E-Mail: luca.simonetto@comune.udine.it
[5]Czech Geological Survey, P.O.B. 85, 118 21 Praha 1, Czech Republic /GeoZentrum Nordbayern, Fachgruppe Paläoumwelt, University of Erlangen-Nürnberg, Loewenichstrasse 28, Erlangen, D-91054, Germany; E-Mail: stana.vodrazkova@seznam.cz
[6]GeoZentrum Nordbayern, University of Erlangen-Nürnberg, Schlossgarten 5,Erlangen, 91054, Germany; E-Mail: michael.joachimski@fau.de
[7]Institute of Geology AS CR, v.v.i., Rozvojova 269, 16500 Prague 6, Czech Republic; E-Mail: koptikova@gli.cas.cz

The Early to Middle Devonian is known as an interval dominated by global greenhouse conditions with an acme in diversity of marine fauna, and widely distributed reef-growth during the Middle Devonian (Copper, 2002). Nonetheless, persistent climate perturbations that resulted in faunal extinction and faunal turnover have been reported through the Eifelian to Givetian (Middle Devonian), which are represented by Basal Choteč, Bakoven, Stony Hollow, Kačák, Pumilio, Taghanic and Geneseo events (House, 2002; Ogg *et al*., 2008; DeSantis & Brett, 2011). In our study we focus on the identification of Middle Devonian biotic events of different depositional settings in the Carnic Alps (Austria-Italy) by using microfacies analysis, conodont biostratigraphy and the application of geochemistry (carbon and oxygen isotopes, TOC and sulfur content, major and trace elements) and geophysics (magnetic susceptibility and gamma-ray spectrometry).

Basically two different paleoenvironmental settings are investigated: the Hoher Trieb Formation (Eifelian - Frasnian) of Zuc di Malaseit Basso section in Lanza (Italy) which accumulated at the distal slope and the Valentin Limestone (Emsian - Famennian) in Wolayer Glacier section near Valentintörl (Austria) which conforms to pelagic deposits. The first mentioned formation is composed of gray to dark gray platy limestone beds which are intercalated by black shale and chert beds (sampling interval: ca. 4.5 m). The limestone beds show fine grained peloidal- or bioclastic grainstone to packstone, mudstone and wackestone. Within the *kockelianus – hemiansatus* conodont zones we observed three remarkable depressions of $\delta^{13}C_{carb}$ between beds ZMB30 to ZMB26, beds ZMB23 to ZMB20 and beds ZMB13 to ZMB6 in ascending order, which correspond with increasing values of TOC and sulfur. The second depression of $\delta^{13}C_{carb}$ starts with the largest negative shift of carbon isotope values in the section, ranging from 2.2 to 0.1 ‰. Within the beds ZMB23 to ZMB20, a positive spike of MS value is observed just after a minor negative shift. Such a minor negative shift is also found in the Th/U values (GRS) of the same interval. We considered that the shifts observed in the carbon isotope, TOC and sulfur content, MS and GRS in beds ZMB23 to ZMB20 in the HoherTrieb Formation are related to paleoenvironmental changes which were associated with the late Eifelian Kačák Event. Other two shifts which are recorded between beds ZMB30 to ZMB26 and beds ZMB13 to ZMB6 could be associated with other Middle Devonian events known from western Laurussia (DeSantis& Brett, 2011) and peri-Gondwana (Aboussalam, 2003).

Oxygen isotope-values of conodont apatite were measured by using multi-generic conodont assemblages from 11 samples (sampling distance: 15 – 80 cm). The color alteration index (CAI) of conodont elements is 4, 4-5. The range of $\delta^{18}O_{apatite}$ values is 18.2 to 19.1 ‰ (V-SMOW) with the lowest value observed in sample ZMB20.

The Valentin Limestone(late Eifelian and Givetian interval: about 25 cm) in the Wolayer Glacier section is characterized by highly condensed but rhythmically deposited sediments. Except for one thin layer (70a middle) below the E/G boundary (Schönlaub, 1985), which shows fine grained peloidal packstone with rare tentaculites the dominant facies is composed of tentaculitid wackestone. Additionally, between beds 70a base and 70 top across the layer 70a middle a pronounced negative excursion is observed in the MS-plot. TOC and sulphur content show increased values within the bed 70a. Although $\delta^{13}C_{carb}$ values show only a slight negative shift across the layer 70a middle, it is suggested that the layer 70a middle might be associated with the Kačák Event.

The Middle Devonian of the Carnic Alps preserved not only slope and pelagic deposits but also deposits of the carbonate platform (Lambertenghi, Spinotti and Kellergrat Reef Limestones). In order to clarify whether the shallow water deposits in the Carnic Alps were also affected by Middle Devonian events which we recorded from the corresponding pelagic sequence, we carried out geochemical- and geophysical analysis of more than 580 samples through the carbonate platform deposits.

Acknowledgements: Research is funded by FWF P23775-B17 and Project no. P210/12/2018 of the Czech Science Foundation. This is a contribution to IGCP 580 and IGCP 596.

References

Aboussalam Z.S. (2003). Das "Taghanic-Event" im höheren Mitteldevon von West-Europa und Marokko. *Münstersche Forschungen zur Geologie und Paläontologie*, 97: 1-332.

Copper P. (2002). Silurian and Devonian reefs: 80 million years of global greenhouse between two ice ages; In Kiessling W., Flügel E. & Golonka J. (Eds.), *Phanerozoic Reef Patterns*. Society of Economic Paleontologists and Mineralogists Special Publication, 72: 181-238.

House M.R. (2002). Strength, timing, setting and cause of mid-Palaeozoic extinctions. *Palaeogeography, Palaeoclimatology, Palaeoecology*, 181, 5-25.

Ogg J.G., Ogg G. & Gradstein F.M. (2008). The concise geologic time scale. *Cambridge University Press*. pp. 177.

Desantis M.K. & Bret, C.E. (2011). Late Eifelian (Middle Devonian) biocrises: Timing and signature of the pre-Kačák Bakoven and Stony Hollow events in eastern North America. *Palaeogeography, Palaeoclimatology, Palaeoecology*, 304(1–2): 113–135.

Schönlaub H.P. (1985). Das Paläozoikum der Karnischen Alpen. *Arbeitstagung der Geologischen Bundesanstalt 1985*, pp. 34-52.

Geochemical and palaeoecological record of the Cenomanian–Turonian Anoxic Event in the carbonate platform of the Preafrican Trough, Morocco

Vanessa Lebedel[1], Carine Lézin[1], Bernard Andreu[1], Marie-José Wallez[1], El Mostafa Ettachfini[2], Laurent Riquier[3]

[1]Géosciences Environnement Toulouse (GET), Observatoire Midi Pyrénées, Université de Toulouse, CNRS, IRD, 14 avenue E. Belin, F- 31400 Toulouse, France; E-mail: vanessa.lebedel@get.obs-mip.fr
[2]Université Chouaïb Doukkali, Faculté des Sciences, Géologie, Laboratoire Géosciences & Techniques de l'Environnement, B.P. 20, 24 000, El Jadida, Morocco
[3]Institut des Sciences de la Terre de Paris (UMR CNRS 7193), Université Pierre et Marie Curie, Paris 6, 4 place Jussieu, 75252 Paris cedex 05, France

In the upper Cenomanian–lower Turonian carbonate platform of the Preafrican Trough (Morocco), on the western part of the Saharan platform, and subjected to Tethyan and Atlantic marine influences, palaeontological and sedimentological studies were carried out from rock samples and thin sections collected from twelve outcrop sections, and geochemical analyses (major and trace elements), based on bulk samples, were carried out from three outcrop sections (Goulmima, Ziz and Tazzouguert), in order to 1/ reconstruct the geometry of the platform, 2/ determine if oxygen-depleted conditions affected the platform, 3/ highlight the possible impact of oxygen variation on carbonate production, particularly during the Oceanic Anoxic Event 2 (OAE2) which took place in the late Cenomanian and 4/ propose possible mechanisms for the installation of the dysoxia.

The upper Cenomanian–lower Turonian deposits of the Preafrican Trough, Morocco, are composed by fossil-rich limestones accumulated in environments ranging from the peritidal zone to the outer ramp. The OAE2 is well recorded, in the upper Cenomanian, by $\delta_{13}C$ excursions, in all the depositional environments, even in shallow water.

In the late Cenomanian, two distinct domains appeared on the platform. In the east and south-east, a shallow water sedimentation predominated in a peritidal zone/inner ramp, while, in the west and north-west, a deeper sedimentation developed on a mid/outer ramp (Lezin *et al.*, 2012; Andreu *et al.*, 2013). Three 3_{rd}-order depositional sequences are recorded; two of these before the OAE2, and one during the event.

The shallow-water environment developed in the east (Ziz and Tazzouguert sections) is characterized by a high diversity and abundance of benthic organisms, and in some cases, by a high diversity of planktonic organisms, associated with low concentrations of authigenic markers (U, Mo, V and Cr: redox proxies), indicating oxic conditions. In the deep environment of the west (Goulmima section), the redox proxies record a high enrichment, an indicator of reducing conditions, associated with a low diversity and abundance of organisms and the presence of Buliminidae. Bottom waters were dysoxic and the palaeoproductivity was low at the sea surface. Thus, during the late Cenomanian, oxygenation conditions were relatively good on the eastern domain of the platform, even during the OAE2, but, in the western domain, in the deeper environments, bottom waters were depleted in oxygen (Lebedel *et al*., 2013).

During the OAE2, the dysoxia was linked to the influx of poorly-oxygenated waters coming from the deeper anoxic basins of the Atlantic and/or the Tethys oceans. This transgression led also to the supply of additional nutrients to the platform, due to the leaching of continental soils.

In the Lower Turonian (post-OAE2), one 3rd-order depositional sequence is recorded, including the maximum flooding and deepening phase (drowning) of the Cenomanian–Turonian, associated with outer ramp sedimentation over the whole area. Geochemical, palaeontological and sedimentological disturbances are recorded everywhere on the platform. Palaeontological proxies show a huge decrease in group diversity, with the disappearance of benthic foraminifera - except for the Buliminidae which proliferated - and only shallow-water planktonic foraminifera survive. Geochemical proxies of redox and palaeoproductivity conditions show a marked enrichment in all three outcrop sections, with higher values in the west. The dysoxia occurred in response to a climatic change, from warm with contrasting seasons to hot and wet, increasing the chemical weathering in the Anti-Atlas in the southwest of the platform. This substantial input of nutrients increased the palaeoproductivity, which finally enhanced the consumption of O_2 owing to the decay of organic matter. The contribution of the Atlantic nutrients, from the Agadir Basin, reinforced this palaeoproductivity.

References

Andreu B., Lebedel V., Wallez M.-J, Lezin C. & Ettachfini El M. (2013). The upper Cenomanian-lower Turonian carbonate platform of the Preafrican Trough, Morocco: biostratigraphic, palaeoecological and palaeobiogeographical distribution of ostracods. *Cretaceous Research* (in press).

Lebedel V., Lezin C., Andreu B., Wallez M.-J., Ettachfini El M. & Riquier L. (2013). Geochemical and palaeoecological record of the Cenomanian–Turonian Anoxic Event in the carbonate platform of the Preafrican Trough, Morocco. *Palaeogeography, Palaeoclimatology, Palaeoecology* 369: 79–98.

Lezin C., Andreu B., Ettachfini El M., Wallez M.-J., Lebedel V. & Meister C. (2012). The upper Cenomanian–lower Turonian of the Preafrican Trough, Morocco. *Sedimentary Geology* 245–246: 1–16.

Impact of the Hercynian range evolution on the Late Paleozoic climate: a modelling approach

Vincent Lefebvre[1], Yannick Donnadieu[2], Yves Goddéris[1], Pierre Sepulchre[2], Mélina Macouin[1], Markus Aretz[1], Guillaume Dera[1]

[1]Géosciences Environnement Toulouse (GET), Observatoire Midi Pyrénées, Université de Toulouse, CNRS, IRD, 14 avenue E. Belin, F- 31400 Toulouse, France; E-mail: vincent.lefebvre@lsce.ipsl.fr.
[2] Laboratoire des Sciences du Climat et de l'Environnement (LSCE),, CNRS, CE Saclay, Orme des Merisiers, 91191 Gif/Yvette, France; E-Mail: yannick.donnadieu@lsce.ipsl.fr

The collision of the Gondwana and Laurussia paleocontinents throughout the Late Paleozoic (370-250Ma) and the related Hercynian range uplift might have lead to drastic climatic perturbations during this time slice. This equatorial mountain range is considered as the strongest erosional system of the Phanerozoic, as suggested by the strontium isotope dataset (Veizer *et al*., 1999). The debate is still open but chemical weathering and organic carbon burial intensifications related to the uplift of this mountain range (Tribovillard *et al*., 2004; Averbuch *et al*., 2005) are considered as important drivers of the Late Paleozoic glaciation. By analogy, this mountain range is often compared to the Himalayan one, described as an important forcing of the Cenozoic glaciation. Up to now, climate modelling studies only focused on the climatic impact of the elevation of the mountain range (Fluteau *et al*., 2001), or on the CO_2 threshold allowing ice accumulation on Gondwana during the Sakmarian (290Ma, see Horton *et al*., 2007). Here we used five paleogeographic reconstructions from Golonka (2002) (365Ma, 330Ma, 310Ma, 290Ma and 265Ma) to depict the impact of plate tectonic and mountain uplift on the global atmospheric circulation. The Hercynian range history considered in these geographic reconstructions is consistent with the paleo-elevation estimations (Fluteau *et al*., 2001 and references therein). In practice, we forced the LMDZ climate model (high atmospheric resolution) with the SST calculated by FOAM (coarse ocean atmosphere model). Such a method allows a better consideration of the oceanic circulation, often put aside in previous modeling studies due to complexity of using ocean atmosphere models in deep times. Our results show an intensification of the precipitation regime over the Hercynian range during the Serpukhovian (330Ma) and Moscovian (310Ma) with a maximum during the Moscovian. The resulting intensification of runoff during this time slice might have lead to an intense weathering as suggested by the strontium isotopes (McArthur *et al*., 2001).

References

Averbuch O., Tribovillard N., Devleeschouwer X., Riquier L., Mistiaen B. & Van Vliet-Lanoe B. (2005). Mountain building-enhanced continental weathering and organic carbon burial as major causes for climatic cooling at the Frasnian-Famennian boundary (c. 376 Ma)? *Terra Nova*, 17: 25-34.

Fluteau F., Besse J., Broutin J. & Ramstein G. (2001). The Late Permian climate. What can be inferred from climate modelling concerning Pangea scenarios and Hercynian range altitude? *Palaeogeography, Palaeoclimatology, Palaeoecology*, 167: 39-71.

Golonka J. (2002). Plate-tectonic maps of the Phanerozoic. In: Kiessling W., Flügel E. & Golonka J. (eds), *Phanerozoic reef patterns.* SEPM Special Publication, 72: 21–75.

Horton D.E., Poulsen C.J. & Pollard D. (2007). Orbital and CO_2 forcing of late Paleozoic continental ice sheets. *Geophysical Research Letters*, 34, doi:10.1029/2007GL031188.

Mcarthur J.M., Howarth R.J.N & Bailey T.R. (2001). Strontium Isotope Stratigraphy: LOWESS Version 3: Best Fit to the Marine Sr-Isotope Curve for 0–509 Ma and Accompanying Look-up Table for Deriving Numerical Age. *The Journal of Geology*, 109: 155–170.

Tribovillard N.P., Averbuch O., Devleeschouwer X., Racki G. & Riboulleau A. (2004). Deep-water anoxia over the Frasnian-Famennian boundary (La Serre, France): a tectonically induced oceanic anoxic event ? *Terra Nova*, 16: 288-295.

Veizer J., Ala D., Azmy K., Bruckschen P., Buhl D., Bruhn F., Carden G.A.F., Diener A., Ebneth S. & Goddéris Y. (1999). $^{87}Sr/^{86}Sr$, $\delta^{13}C$ and $\delta^{18}O$ evolution of Phanerozoic seawater. *Chemical Geology*, 161(1-3): 59-88.

Sedimentological, paleontological, geochemical records of the climate variability during the Upper Hauterivian in lagoonal environment

Carine Lézin[1], Paulo S. Caetano[2], Paula Gonçalves[3], Jacques Rey[1], Fernando Rocha[3], Rogério B. Rocha[2]

[1]Géosciences Environnement Toulouse (GET), Observatoire Midi Pyrénées, Université de Toulouse, CNRS, IRD, 14 avenue E. Belin, F- 31400 Toulouse, France; E-mail: lezin.carine@get.obs-mip.fr
[2]Universidade Nova de Lisboa, Faculdade de Ciências e Tecnologia, CICEGe, Campus de Caparica, 2829-516 Caparica, Portugal
[3]Universidade de Aveiro, Departamento de Geociências, GEOBIOTEC, Campus de Santiago, 3810-193 Aveiro, Portugal

An integrated analysis of the Hauterivian shallow-marine carbonates from the western margin of the Lusitanian Basin (Portugal) allows us to assess the paleoenvironmental significance of variations of biological, mineralogical, chemical and magnetic markers in a lagoonal environment.

From a paleontological point of view, this study is focused on the benthic foraminifera. For each, studied bed, we estimate the microfaunal density (total concentration per unit area), the contribution of the various biological groups (morphogroups, genera or species) and, finally, we classify them into different microhabitats according to their morphology. The infaunal/epifaunal ratio is calculated on the basis of the attributed microhabitats. The intensity of organic activity has been estimated from a quantification of the micritized grains. The lithological variations are defined by the measure of the carbonate and clay content (Caetano *et al*. (2005) and Gonçalves *et al.* (2007)). Sr, Mn, Fe, K and stable isotope (δ_{18}O and δ_{13}C) are used to analyze platform carbonate facies in terms of paleoenvironment. Finally, we demonstrate that the magnetic susceptibility can be used as an indicator of detrital influx, especially clay (Lézin *et al*., 2012).

The studied Guincho section (West of Lisbon) is characterized by nine facies included in different environments ranging from terrestrial and restricted lagoon to high-energy open platform (Lézin *et al*., 2012). The variations of the different markers show a clear cyclic pattern. Certain curves are relatively well correlated, thus exhibiting a parallel trend, while others are anti-correlated.

In this shallow water context, there is relation between the habitat and concentration of benthic foraminifera, the presence and activity of boring and micritizing organisms, the detrital input expressed by magnetic susceptibility (MS) as well as the chemical and isotopic composition of the carbonate fraction (especially K content and δ_{13}C).

In this lagoonal environment, the increasing detrital input appears to reduce the relative density of infaunal benthic foraminifera in favor of epifaunal benthic foraminifera. These conditions lead to the development and prevalence of large benthic foraminifera with agglutinated tests, more particularly *Choffatella decipiens*. At the same time, there is a reduced activity of organisms, such as endolithic algae and cyanobacteria, which cause micritization of the grains; as a result, the δ_{13}C decreases while the magnetic susceptibility (MS) and K content increase. When the detrital input decreases, a reverse tendency is recorded and there is an enhanced contribution of Miliolidae and small Textulariidae.

Thus, the silicilastic input in the lagoon modifies the water turbidity and the light intensity, decreasing photosynthetic activity and also the microbial calcification. In the studied area, the positive δ_{13}C excursion is associated with enhanced carbonate accumulation and production, while a negative shift in δ_{13}C is recorded during episodes of increased clay input. This relationship can be explained by carbonate precipitation by whitings.

High detrital input cause a decrease of primary productivity, which leads to a reduction of boring and micritizing organisms (microplants, fungi and bacteria), as well as deep infaunal species, and benthic foraminifera. The siliciclastic input modifies the biological content and promotes the dominance of larger agglutinated benthic foraminifera such as *Choffatella decipiens*.

In the Guincho section, the increasing carbonate production and deposition could be related to changes from humid to dry climatic conditions which also control the decrease in siliciclastic input in the marine realm, and which may also drive salinity variations. Climatic control on quantitative and qualitative carbonate production is confirmed by the close relation between the bed thickness variations, the insolation variability and the variation of micritized grains concentrations (Lézin *et al*., 2010).

References

Caetano P.S., Goncalves P., Lézin C., Rocha F., Rey J. & Bonnet L. (2005). Clay mineral stratigraphy of a 3rd order depositional sequence: paleoenvironmental reconstruction and relations to orbital cycles. *Clay Science*, *Morioka* 12 (2): 11–14.

Gonçalves P., Caetano P.S., Rocha F., Lézin C. & Rey J. (2007). Caracterização mineralógica da sequência sedimentar Ha7 do Cretácico Inferior do Guincho (Bacia Lusitaniana). *Ciências da Terra* (UNL) 16: 143–150.

Lézin C., Bonnet L., Rey J., Caetano P.S., Gonçalves P., Rocha F.T. & Rocha R.B. (2010). Orbital forcing of stratal patterns in an inner platform carbonate succession: an example from an Upper Hauterivian series of the Lusitanian Basin, Portugal. *Ciências da Terra* (UNL), 17: 29-44.

Lézin C., Caetano P.S., Goncalves P., Rey J., Rocha F. & Rocha R.B. (2012). Biosedimentary disturbances in shallow-water carbonate environments: An example from the Upper Hauterivian in the Lusitanian Basin. *Palaeogeography, Palaeoclimatology, Palaeoecology* 315-316: 24–37.

Exploring Ediacaran environmental conditions with rock magnetism

Mélina Macouin[1], Magali Ader[2], Ganqing Jiang[3], Ricardo I.F. Trindade[4], Charles Poitou[5], Anne Nedelec[1], Zhenyu Yang[6], Zhimming Sun[6], Marie- Gabrielle Moreau[5]

[1]Géosciences Environnement Toulouse (GET), Observatoire Midi Pyrénées, Université de Toulouse, CNRS, IRD, 14 avenue E. Belin, F- 31400 Toulouse, France; E-mail: melina.macouin@get.obs-mip.fr

[2] Équipe de géochimie des isotopes stables, Institut de Physique du Globe de Paris, Sorbonne Paris Cité, Univ Paris Diderot, UMR 7154 CNRS, F-75005 Paris, France

[3] Departamento de Geofisica, Instituto de Astronomia, Geofisica e Ciencias Atmosfericas, Universidade de Sao Paulo, Sao Paulo, Brazil

[4] Department of Geoscience, University of Nevada, Las Vegas, NV 89154-4010, USA

[5] Équipe de Paléomagnétisme, Institut de Physique du Globe de Paris, Sorbonne Paris Cité, Univ Paris Diderot, UMR 7154 CNRS, F-75005 Paris, France

[6] Institut of Geomechanics, CAGS, Beijing, China

Severe glaciations referred to as "snowball Earth" occurred at least twice during the Neoproterozoic, namely the Sturtian (ca. 710 Ma) and the Marinoan (ca. 635 Ma) glaciation. The evidence for those glaciations are derived from paleomagnetic data that indicate that sea-ice was present in the equatorial zone (see a review in Hoffman & Li, 2009). These glaciations came with large negative $\delta^{13}C$ excursions that are generally thought to reflect a global change in dissolved inorganic carbon (DIC) isotope composition in the ocean. However, recently this has been questioned (Knauth & Kennedy, 2009; Derry, 2010, Swanson-Hysell *et al*., 2010; Johnston *et al*., 2012). Whether the absolute value and secular changes in C-isotopic signatures are accurate indicator of global biogeochemical processes or reflect diagenetic processes are still debated and are crucial for climatic simulations.

Magnetic minerals are strongly sensitive to environmental conditions. Considering this, acquisition of rock magnetic properties becomes a potential tool to unravel the environmental changes held in the sedimentary archives and for tracing old climate dynamics. Moreover, measurements allowing magnetic mineralogy characterization (as opposed to paleodirections determination) are low cost, time efficient and non-destructive, and thus ideal screening tools to use.

Here we use the magnetic signal to investigate environmental conditions prevailing in the aftermath of the Neoproterozoic glacial events. For that, we have acquired several rock magnetic parameters in Ediacaran carbonates from South China and from Ghana (Volta basin). These parameters are derived from classical magnetic measurements (ARM, IRM, hysteresis, susceptibility) and from MEB observations. Some samples have been studied additionally by low-temperature magnetic techniques (including high-field and low-field magnetometry).

Cap carbonates in the Volta basin (Ghana) display fine magnetic grains. Hematite and goethite are the main carriers with various relative abundance. (Titano-)magnetite is also present in small content (less than 10% of the magnetic grains content).

A detailed analysis was performed in three Ediacaran sections from South China (described in Jiang *et al*., 2010). In all samples, low temperature measurements indicate the presence of goethite, while magnetite and hematite are present in various amounts and various grain sizes. Strongly negative $\delta^{13}C$ values found at the intermediate sector of the Yangjiaping and more generally in all the South China's Ediacaran sections, are associated with a loss of remanence intensity, which probably results from the dissolution of magnetite to pyrite by H_2S produced by methane oxidation (Fig. 1). Thus, the negative $\delta^{13}C$ excursion of the Yangjiaping section is largely due to diagenesis (Macouin *et al*., 2012).

In the cap carbonates of the Yangjiaping section (South China), secondary magnetite dominates the signal and indicates the dissolution of primary oxide. In all sections, $\delta^{13}C$ values from carbonates decrease upward in the cap dolostones, while both susceptibilities and IRM values increase. A synthesis of the magnetic properties found at the different sections worldwide and their relation to the C-isotope signal will be shown that helps constrain the environmental significance. The influence of diagenesis on the magnetic and isotopic records will be discussed.

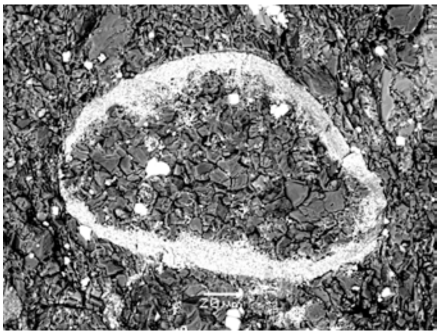

Fig. 1: **Back scattered electron images of the Upper Doushantuo beds samples. Spherical microfossil (Animal embryo or acritarch?) in the dolomitic matrix. Pyrite (white) are visible inside the fossil.**

References

Derry L.A. (2010). On the significance of delta(13)C correlations in ancient sediments. *Earth and Planetary Science Letters*, 296: 497-501

Halverson G.P., Wade B.P., Hurtgen M.T. & Barovich K.M. (2010). Neoproterozoic chemostratigraphy. *Precambrian Research*, 182: 337-350.

Hoffman P.F., Li Z.X. (2009). A palaeogeographic context for Neoproterozoic glaciation. *Palaeogeography Palaeoclimatology Palaeoecology*, 277: 158-172.

Jiang G.Q., Wang X.Q., Shi X.Y., Zhan S.H., Xiao S.H. & Dong J. (2010). Organic carbon isotope constraints on the dissolved organic carbon (DOC) reservoir at the Cryogenian-Ediacaran transition. *Earth and Planetary Science Letters*, 299: 159-168.

Johnston D.T., Macdonald F.A., Gill B.C., Hoffman P.F. & Schrag D.P. (2012). Uncovering the Neoproterozoic carbon cycle. *Nature*, 483: 320-U110.

Knauth L.P. & Kennedy M.J. (2009). The late Precambrian greening of the Earth. *Nature*, 460: 728-732.

Macouin M., Ader M., Moreau M.-G., Poitou C., Yang Z. & Sun Z. (2012). Deciphering the impact of diagenesis overprint on negative δ13C excursions using rock magnetism: Case study of Ediacaran carbonates, Yangjiaping section, South China. *Earth and Planetary Science Letters*, 351–352: 281-294.

Swanson-Hysell N.L., Rose C.V., Calmet C.C., Halverson G.P., Hurtgen M.T. & Maloof A.C. (2010). Cryogenian Glaciation and the Onset of Carbon-Isotope Decoupling. *Science*, 328: 608-611.

A Late Devonian terrestrial palaeoclimate record: ground-truthing the modellers

John Marshall[1], Olga Tel'nova[2], Tim Astin[3]

[1]School of Ocean and Earth Science, University of Southampton, National Oceanography Centre, European Way, Southampton, SO14 3ZH, United Kingdom; E-Mail: jeam@noc.soton.ac.uk
[2]Institute of Geology, Komi Science Centre, Russian Academy of Sciences (Ural Division), Pervomaiskay st., 54, Syktyvkar, Komi Republic, Russia
[3]School of Human and Environmental Science, The University of Reading, Whiteknights, PO Box 217, Reading, RG6 6AH, UK

The Mid and Late Devonian interval sees the establishment of the second carbon cycle within the terrestrial environment. This clearly has an impact on global biogeochemical cycles and has been both factored into models for the Devonian Earth System and frequently invoked as an explanation for Mid Palaeozoic extinction events. For example, the spread of the first forests and the increasing stature of the therein trees is commonly hypothesized to substantially increase the release of nutrients from the soils in which they were growing. This then destabilised both the marine environment through input of excess nutrients and the terrestrial climate through drawdown of CO_2 and the descent into an icehouse. The presence of two mass extinction events in the Devonian (the Frasnian/Famennian and the End Devonian Mass Extinction at the Devonian-Carboniferous boundary) has very much encouraged modellers to link all these events. The Devonian has a well developed terrestrial facies that is present within extensional basins on the Old Red Sandstone continent. This contains a direct record of climatic change within the Late Devonian that can be integrated with the palynological record. This can then be used to show how land plants might be interacting with the environment through these extinction events. The key question being; are they driving these events or responding to them?

The Frasnian/Famennian terrestrial section from East Greenland is characterized by extremes in palaeoclimate. There are two paired events, each with a lower interval of fluvial sandstones deposited in a warm wet climate followed by a very cool arid climate with a distinctive sequence of palaeosols. Spores show that the humid climates correspond to the Lower and Upper Kellwasser black shales whereas the arid events represent the regressive intervals that follow each of the transgressions. The plant extinctions are progressive and represent a series of down steps in diversity. The plants, as represented by the spores, are not increasing in diversity or abundance and are responding to progressive palaeoenvironmental events rather than driving them.

The integrated spore and palaeoclimate record from the D-C boundary of East Greenland shows that the plants survived the cool arid time of the Strunian glaciation to then provide, initially high diversity palynofloras as the climate changed to warm and wet conditions. But as the sedimentary system flooded to form a megalake, with coincident margins, the plants suffered significant habitat loss, ultimately becoming extinct and never returning to the system as the lake dried out. This is quite surprising as the Strunian palynofloras contain a number of very persistent and abundant elements (as exemplified by *Retispora lepidophyta)* which achieved a global distribution and were clearly highly successful and able to survive in many different climate zones.

The fossil record of trees across the D-C boundary is not well understood but it is becoming clear (Decombeix *et al*., 2011) that major groups such as *Archaeopteris* did not survive to cross the boundary. This collapse of the forest environment is show here by a quantitative count of fossil plant stems across the D-C boundary from Celsius Bjerg. Substantial sized plant stems are abundant up to the boundary and then immediately disappear at the boundary. Large trees only reappear, and then as a different plant group- the lycopsids, with the appearance of warm wet conditions in the Viséan. The spore floras show associated changes and particularly the demise of spores that were produced by the *Rhacophyton* dominated understorey vegetation to these Famennian forests.

The style of sedimentation also changes immediately above the D-C boundary. A system that was river channels with significant overbank deposits then becomes replaced by a stack of river channels with little preserved overbank. These channels are significantly thicker, faster flowing with higher discharges and contain substantial bedload but now without any visible plant debris. The discharge can be high enough to form small Gilbert-type deltas and ephemeral lakes. However, there is an arid season as shown by the ubiquitous presence of calcrete clasts. This change is regarded as representing a time of ecosystem collapse with the removal of both the forest trees and understorey vegetation with the fluvial system reverting to a more arid and ephemeral character typical of the early Devonian.

The earliest Carboniferous palynofloras are striking in being very impoverished and contain only a few common taxa that are generally simple spores. Higher up section the palynological floras recover in this wetter early Tournaisian interval and includes the appearance of lycopod megaspores. However, the character of the sediment then changes to a sustained interval of aridity. This interval contains multiple evidences for arid conditions including the presence of thick vertisol palaeosols that represent a low seasonal contrast within an arid climate. There are no palynomorphs preserved through this interval. Following this arid interval the climate becomes wetter with the appearance of immature sandstones followed by thin coals and black shales. These sediments contain abundant *Lycospora* and are accompanied by tree-sized lycopod trunks and are Viséan in age. The interval is now more typically of Coal Measures character and on Backlund Ridge continues (Vigran *et al*., 1999) into the Namurian.

References

Decombeix A.-L., Meyer-Berthaud B. & Galtier J. (2011). Transitional changes in arborescent lignophytes at the Devonian-Carboniferous boundary. *Journal of the Geological Society*, 168: 547-557.

Vigran J.O., Stemmerik L. & Piasecki S. (1999). Stratigraphy and depositional evolution of the uppermost Devonian-Carboniferous (Tournaisian-Westphalian) non-marine deposits in North-East Greenland. *Palynology*, 23: 115-152.

Orbital calibration of the Valanginian Stage: new insight on the palaeoceanographic changes during the $\delta^{13}C$ Mid-Valanginian Event

Mathieu Martinez[1], Jean-François Deconinck[1], Pierre Pellenard[1], Stéphane Reboulet[2], Laurent Riquier[1,3]

[1]UMR/CNRS 6282 Biogeosciences, Université de Bourgogne, 6 boulevard Gabriel, 21000 Dijon, France; E-Mail: mathieu.martinez@u-bourgogne.fr (M. Martinez)
[2]UMR/CNRS 5276 Laboratoire de Géologie de Lyon: Terre, Planètes, Environnement, Observatoire des Sciences de l'Univers de Lyon, Université Claude Bernard Lyon 1, Bâtiment Géode, 2 rue Raphaël Dubois, 69622 Villeurbanne, Cedex, France
[3]UMR/CNRS 7193 ISTeP: Institut des Sciences de la Terre – Paris, Université Paris VI, 4 place Jussieu, 75255 Paris cedex 05, France

The Valanginian Stage (Early Cretaceous) experienced a major disturbance of the carbon cycle, mirrored by a $\delta^{13}C$ positive excursion (namely the „Weissert Event"). This shift is concomitant with fluctuations of atmospheric pCO_2 (Gröcke *et al*., 2005), faunal turnovers (Kemper *et al*., 1981; Reboulet & Atrops, 1995), a major carbonate platform drowning (Föllmi *et al*., 1994), hiatus or condensed intervals throughout Western Europe and Tethys (Hoedemaeker & Herngreen, 2003; Bonin *et al*., 2012), decreasing in kaolinite contents (Fesneau, 2008; Duchamp-Alphonse *et al*., 2011) and a pause in the $^{87}Sr/^{86}Sr$ increasing trend (McArthur *et al*., 2007). In the absence of reliable radioisotopic ages biostratigraphically well-constrained, the causes and consequences of the Weissert episode remain poorly understood. As an example, a cooling trend is suggested in the Late Valanginian after the shift in $\delta^{13}C$, maybe leading to the development of polar ice caps (McArthur *et al*., 2007; Price & Nunn, 2010), but sea-surface temperatures seem to indicate equable greenhouse conditions (Littler *et al*., 2011). In addition, the onset of the $\delta^{13}C$ excursion is attributed either to the activity of the Paraná-Etendeka Large Igneous Province (LIP; Erba *et al*., 2004), either to the massive storage of continental organic carbon (Westermann *et al*., 2010). In order to refine the Valanginian time scale, and to better constrain such palaeoclimatic events, we provide here an astronomical tuning of the Valanginian Stage, performed on biostratigraphically well-dated sections. Five reference sections of the Vocontian Basin (SE France) were selected for this study. These include Vergol (GSSP candidate, Berriasian-Valanginian boundary), Reynier, Morénas, Angles (Hypostratotype, Valanginian) and La Charce (GSSP candidate, Valanginian-Hauterivian boundary). The sections are composed of regular marl-limestone hemipelagic rhythmits accompanied by chemical, clay mineralogical and faunal fluctuations that reflect orbitally-forced climatic and sea-level changes (e.g., Cotillon, 1987). The series encompass the whole Valanginian Stage without any synsedimentary disturbance (e.g. slumps). The sections can be accurately correlated using limestone bundles (Cotillon, 1971), a bentonite layer (Fesneau *et al*., 2009) and a detailed ammonite zone scheme (Bulot *et al*., 1992; Blanc, 1995; Reboulet & Atrops, 1999). The standard zonation established by the IUGS Lower Cretaceous Working Group was used in this work (Reboulet *et al*., 2011). Gamma-ray spectrometry measurements (GRS) were performed every 20 cm. As expected, at a marl-limestone alternation scale, GRS values are higher in marls than in limestone beds. The series show the same long-term trends that were removed using the LOWESS regression (Cleveland, 1979). Spectral analyses were performed to recover the sedimentary cycles, using the multi-taper method (Thomson, 1982, 1990). Significant cycles were recognized by fitting a red-noise model on the spectra (e.g., Mann & Lees, 1996; Martinez *et al*., 2012; Moiroud *et al*., 2012).

All series display sedimentary periods at ~1 m and ~20 m that were attributed to precession (~20 kyr) and 405-kyr eccentricity, respectively. The amplitude of the 405-kyr eccentricity has a modulation covering six of its repetition, probably due to the 2.4-myr eccentricity (Laskar *et al*., 2011). Transient obliquity controls on the marl-limestone appear during the 405-kyr eccentricity minima, and in the Late Valanginian between the *O. (O.) nicklesi* and *C. furcillata* subzones. The Valanginian Stage spans twelve to thirteen repetitions of the 405-kyr eccentricity, leading to a total duration of 5.08 myr. The duration assessed here refines previous durations proposed for the Valanginian Stage, ranging from 4.8 myr to 6.4 myr, based on directly counted alternations on the field (Huang *et al*., 1993; Giraud *et al*., 1995; Gréselle & Pittet, 2010). In addition, this duration is in good agreement with the duration of 5.2 myr proposed in the Maiolica Fm (Central Italy),

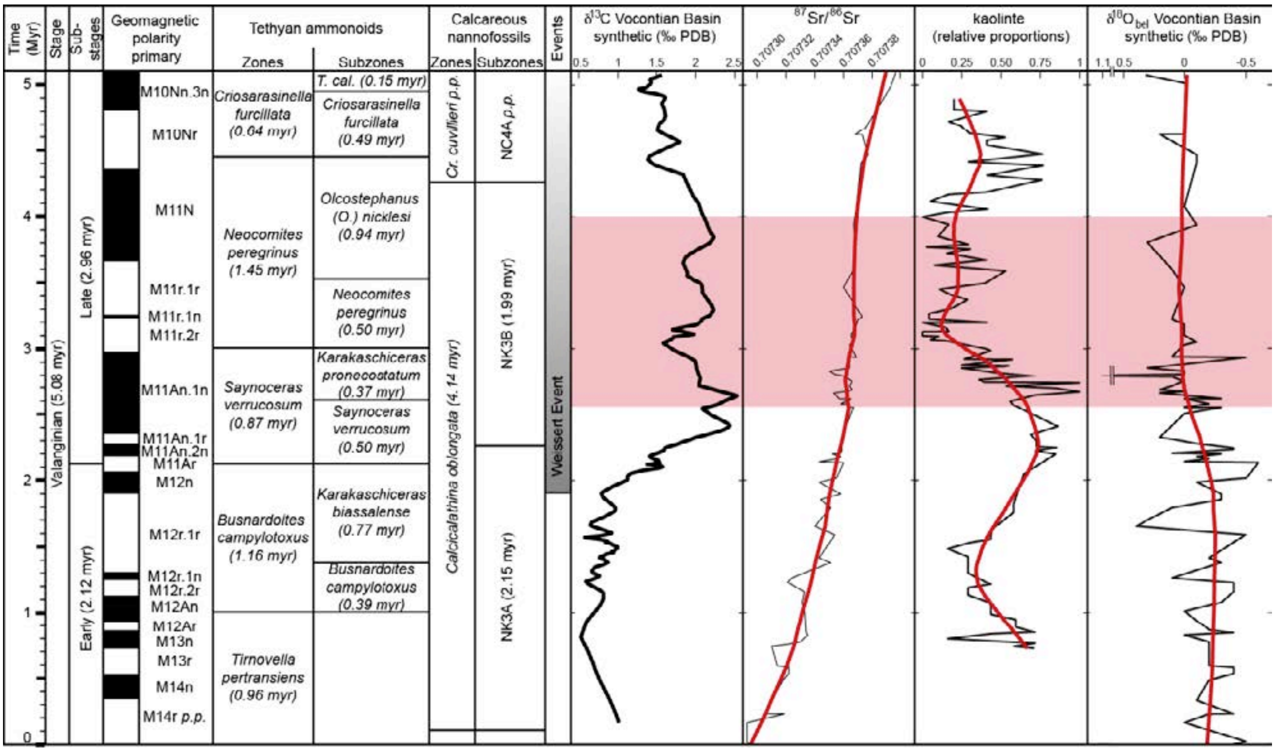

Fig. 1: **Valanginian time scale and proposed durations for substages, magnetochrons, ammonite (sub)zones (Standard Ammonite Zonation; Reboulet *et al.*, 2011), calcareous nannofossil (sub)zones and rising $\delta^{13}C$ Weissert, strontium isotope stratigraphy, clay minerals (Fesneau, 2008), oxygen isotopes (van de Schootbrugge *et al.*, 2000; McArthur *et al.*, 2007), in the Vocontian Basin. $\delta^{13}C$ data are smoothed with clay minerals coming from the Montclus and Vergol sections. In each section, kaolinite proportion fluctuations were standardized between 0 and 1 to remove any local effect. The horizontal band represents the time-interval during which the strontium isotope curve remains stable, (from Martinez *et al.*, in press).**

based on the identification of the 405-kyr eccentricity on a $\delta^{13}C$ signal (Sprovieri *et al.*, 2006), thus strengthening the time scale proposed here (Fig. 1).

To compare the age of the onset of the Weissert Event with the onset of Paraná-Etendeka LIP, we combined radioisotopic ages accurately dated in the Berriasian and Hauterivian stages (Mahoney *et al.*, 2005; Aguirre-Urreta *et al.*, 2008a) with duration estimates of Berriasian and Hauterivian stages (Rio *et al.*, 1989; Sprenger & Ten Kate, 1993; Sprovieri *et al.*, 2006; Gréselle, 2007) and the time scale we propose here for the Valanginian Stage. The start of the Weissert Event ranges between 140.2 and 136.8 Ma, with a mean age of ~137 Ma (Fig. 2). This is ~3 myr years older than the onset of the Paraná-Etendeka, starting at 134.3 ± 0.8 Ma (Janasi *et al.*, 2011), and thus a link between the two events is unlikely. Instead, following Westermann *et al.* (2010), we propose that a massive continental organic carbon storage accompanied by a demise in the carbonate platform factory was responsible for the $\delta^{13}C$ positive shift.

The pause in the $^{87}Sr/^{86}Sr$ increase is still observed in the Upper Valanginian. It is concomitant with decreasing kaolinite contents in the Vocontian Basin and hiatus or condensed intervals in most of Northwestern Europe and Western tethyan sections (Fig. 1; Hoedemaeker & Herngrenn, 2003; Bonin *et al.*, 2012). This pause in the Sr-isotope increase is thus attributed to a strong decrease in detrital supply maybe linked to a global arid climate in the Late Valanginian. In addition, a cooling interval is suggested in the Upper Valanginian based on decreasing atmospheric pCO_2, faunal turnovers, geochemistry and facies together with the occurrence of glendonite (Walter, 1991; Reboulet & Atrops, 1995; Gröcke *et al.*, 2005; McArthur *et al.*, 2007; Price & Nunn, 2010; Bonin *et al.*, 2012). The prominent record of the obliquity in the *O. (O.) nicklesi* and *C. furcillata* subzones may reflect a stronger polar dynamic control on the global climate and sea level (Boulila *et al.*, 2011). This is consistent with the hypothesis of a cooling trend, which may have been significant enough to trigger limited production of polar ice.

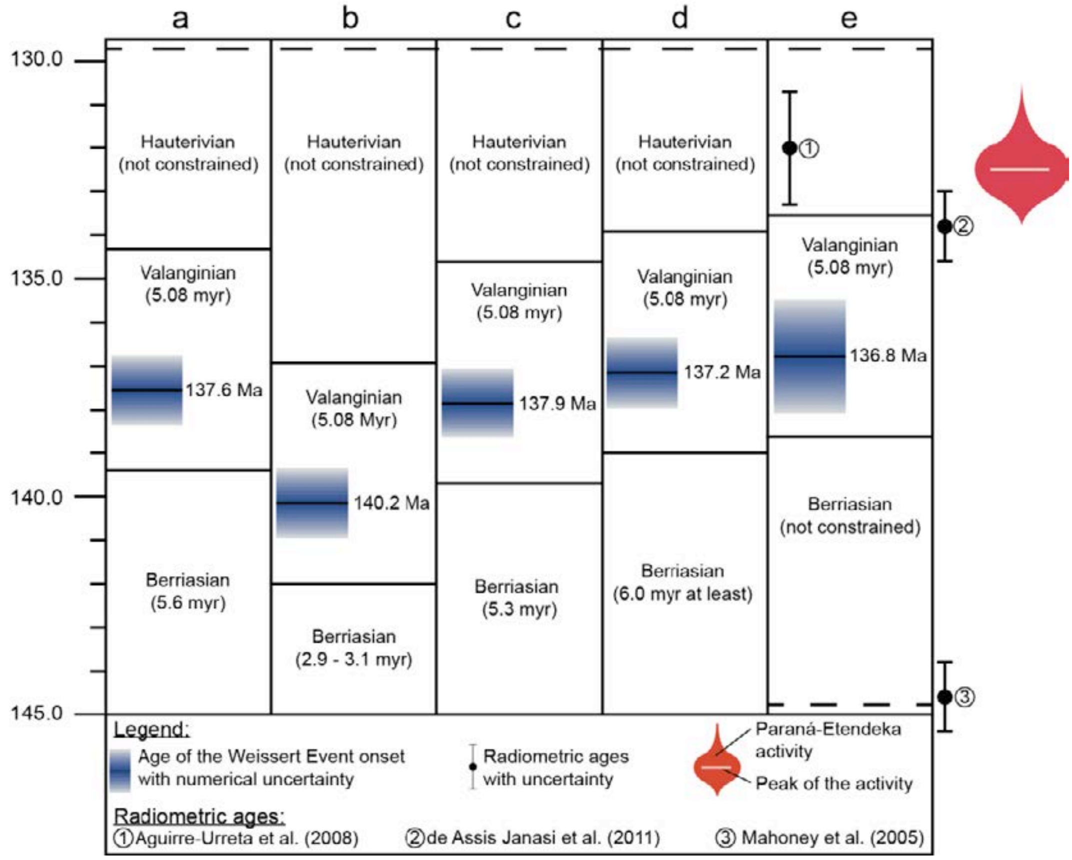

Fig. 2: **Compilation of GTS2012, radio-isotopic and cyclostratigraphic data for the Berriasian, Valanginian and Hauterivian stages with comparison between ages for the Weissert Event and emplacement of the Paraná–Etendeka Trap. Duration of the Valanginian Stage and duration from the Weissert Event to Valanginian Stage boundaries are from this study. A) to D) The age of the base of the Berriasian is 145.0 ± 0.8 Ma, the uncertainty for the age of the Weissert event onset is ±0.8 Ma, like the uncertainty on the age provided by Mahoney *et al.* (2005). A) Duration of the Berriasian is based on field cycle counting in the Vocontian Basin (Rio *et al.*, 1989). B) Duration of the Berriasian is based on spectral analyses from $CaCO_3$ content in pelagic alternations from Southeastern Spain (Sprenger & Ten Kate, 1993). C) Duration of the Berriasian Stage is from the Pacific seafloor spreading model (Gradstein *et al.*, 2012). D) Duration of the Berriasian Stage is based on field cycle counting in the Jura and Helvetic platforms (Gréselle, 2007). E) U–Pb SHRIMP age is obtained in the Neuquén Basin (Aguirre-Urreta *et al.*, 2008a) and correlated to the end of the Weissert excursion using calcareous nannofossil and carbon-isotope stratigraphy (Aguirre-Urreta *et al.*, 2005; Aguirre-Urreta *et al.*, 2008b). Duration from the end of the Weissert excursion to the top of the Valanginian Stage is based on orbital tuning (Sprovieri *et al.*, 2006), (from Martinez *et al.*, in press).**

References

Aguirre-Urreta M.B., Rawson P.F., Concheyro G.A., Bown P.R. & Ottone E.G. (2005). Lower Cretaceous (Berriasian–Aptian) biostratigraphy of the Neuquén Basin. In Veiga G.D., Spalletti L.A., Howell J.A. & Schawarz, E. (Eds), *The Neuquén Basin, Argentina.* Geological Society London, Special Publication, 252: 57–81.

Aguirre-Urreta M.B., Pazos P.J., Lazo D.G., Mark Fanning C. & Litvak V.D. (2008a). First U–Pb SHRIMP age of the Hauterivian stage, Neuquén Basin, Argentina. *Journal of South American Earth Sciences*, 26: 91-99.

Aguirre-Urreta M.B., Price G.D., Ruffell A.H., Lazo D.G., Kalin R.M., Ogle N. & Rawson P.F. (2008b). Southern hemisphere early Cretaceous (Valanginian-Early Barremian) carbon and oxygen isotope curves from the Neuquén basin, Argentina. *Cretaceous Research*, 29: 87-99.

Blanc E. (1995). Transect plate-forme-bassin dans les séries carbonatées du Berriasien supérieur et du Valanginien inférieur (domaines jurassien et nord-vocontien): chronostratigraphie-transferts des sédiments. *PhD Thesis, Université Joseph-Fourier Grenoble I*, Grenoble (unpublished).

Bonin A., Vennin E., Pucéat E., Guiraud M., Arnaud-Vanneau A., Adatte T., Pittet B. & Mattioli E. (2012). Community replacement of neritic carbonate organisms during the late Valanginian platform demise: A new record from the Provence Platform. *Palaeogeography, Palaeoclimatology, Palaeoecology*, 365-366: 57-80.

Boulila S., Galbrun B., Miller K.G., Pekar S.F., Browning J.V., Laskar J., & Wright J.D. (2011). On the origin of Cenozoic and Mesozoic "third-order" eustatic sequences. *Earth-Science Reviews*, 109: 94-112.

Bulot L.G., Thieuloy J.-P., Blanc E. & Klein J. (1992). Le cadre stratigraphique du Valanginien supérieur et de l'Hauterivien du Sud-Est de la France: définition des biochronozones et caractérisation de nouveaux biohorizons. *Géologie Alpine*, 68: 13-56.

Cleveland W.S. (1979). Robust locally weighted regression and smoothing scatterplots. *Journal of the American statistical association*, 74: 829-836.

Cotillon P. (1971). Le Crétacé inférieur de l'arc subalpin de Castellane entre l'Asse et le Var: stratigraphie et sédimentologie. *Bureau de Recherches Géologiques et Minières*. 313 p.

Cotillon P. (1987). Bed-scale cyclicity of pelagic Cretaceous successions as a result of world-wide control. *Marine geology*, 78: 109-123.

Duchamp-Alphonse S., Fiet N., Adatte T. & Pagel M. (2011). Climate and sea-level variations along the northwestern Tethyan margin during the Valanginian C-isotope excursion: Mineralogical evidence from the Vocontian Basin (SE France). *Palaeogeography, Palaeoclimatology, Palaeoecology*, 302: 243-254.

Erba E., Bartolini A. & Larson R. L. (2004). Valanginian Weissert oceanic anoxic event. *Geology*, 32: 149-152.

Fesneau C. (2008). *Enregistrement des changements climatiques dans le domaine Téthysien au Valanginien.* PhD Thesis, Université de Bourgogne, Dijon (unpublished).

Fesneau C., Deconinck J.-F., Pellenard P. & Reboulet S. (2009). Evidence of aerial volcanic activity during the Valanginian along the northern Tethys margin. *Cretaceous Research*, 30: 533-539.

Föllmi K.B., Weissert H., Bisping M. & Funk H. (1994). Phosphogenesis, carbon-isotope stratigraphy, and carbonate-platform evolution along the Lower Cretaceous northern Tethyan margin. *Geological Society of America Bulletin*, 106: 729-746.

Giraud F., Beaufort L. & Cotillon P. (1995). Periodicities of carbonate cycles in the Valanginian of the Vocontian Trough: a strong obliquity control. *Geological Society, London, Special Publications*, 85: 143-164.

Gradstein F.M., Ogg J.G., Schmitz M.D. & Ogg G.M. (2012). A Geologic Time Scale 2012. *Elsevier BV*, Amsterdam, 1144 pp.

Greselle B. (2007). *Impact des variations paléoclimatiques sur la sédimentation carbonatée au Valanginien.* PhD Thesis, Université Claude Bernard-Lyon I, Lyon (unpublished).

Gréselle B. & Pittet B. (2010). Sea-level reconstructions from the Peri-Vocontian Zone (South-east France) point to Valanginian glacio-eustasy. *Sedimentology*, 57: 1640-1684.

Gröcke D.R., Price G.D., Robinson S.A., Baraboshkin E.Y., Mutterlose J. & Ruffell A.H. (2005). The Upper Valanginian (Early Cretaceous) positive carbon-isotope event recorded in terrestrial plants. *Earth and Planetary Science Letters*, 240: 495-509.

Hoedemaeker P.J. & Herngreen G.F.W. (2003). Correlation of Tethyan and Boreal Berriasian - Barremian strata with emphasis on strata in the subsurface of the Netherlands. *Cretaceous Research*, 24: 253-275.

Huang Z., Ogg J G. & Gradstein F.M. (1993). A quantitative study of Lower Cretaceous cyclic sequences from the Atlantic Ocean and the Vocontian Basin (SE France). *Paleoceanography*, 8: 275-291.

Janasi V.D.A., De Freitas V.A. & Heaman L.H. (2011). The onset of flood basalt volcanism, Northern Paraná Basin, Brazil: A precise U–Pb baddeleyite/zircon age for a Chapecó-type dacite. *Earth and Planetary Science Letters*, 302: 147-153.

Kemper E., Rawson P.F. & Thieuloy J.-P. (1981). Ammonites of Tethyan ancestry in the early Lower Cretaceous of North-West Europe. *Palaeontology*, 24: 251-311.

Laskar J., Fienga A., Gastineau M. & Manche H. (2011). La2010: a new orbital solution for the long-term motion of the Earth. *Astronomy & Astrophysics*, 532: A89.

Littler K., Robinson S.A., Bown P.R., Nederbragt A.J. & Pancost R.D. (2011). High sea-surface temperatures during the Early Cretaceous Epoch. *Nature Geoscience*, 4: 169-172.

Mahoney J.J., Duncan R.A., Tejada M.L.G., Sager W.W. & Bralower T J. (2005). Jurassic-Cretaceous boundary age and mid-ocean-ridge–type mantle source for Shatsky Rise. *Geology*, 33: 185-188.

Mann M.E. & Lees J.M. (1996). Robust estimation of background noise and signal detection in climatic time series. *Climatic Change*, 33: 409-445.

Martinez M., Deconinck J.-F., Pellenard P., Reboulet S. & Riquier L. (2013). Astrochronology of the Valanginian Stage from reference sections (Vocontian Basin, France) and palaeoenvironmental implications for the Weissert Event. *Palaeogeography, Palaeoclimatology, Palaeoecology*. (in press). doi: 10.1016/j.palaeo.2013.02.021.

Martinez M., Pellenard P., Deconinck J.-F., Monna F., Riquier L., Boulila S. & Moiroud M. (2012). An orbital floating time scale of the Hauterivian/Barremian GSSP from a magnetic susceptibility signal (Río Argos, Spain). *Cretaceous Research*, 36: 106-115.

McArthur J.M., Janssen N.M.M., Reboulet S., Leng M.J., Thirlwall M.F. & Van De Schootbrugge B. (2007). Palaeotemperatures, polar ice-volume, and isotope stratigraphy (Mg/Ca, $\delta^{18}O$, $\delta^{13}C$, $^{87}Sr/^{86}Sr$): The Early Cretaceous (Berriasian, Valanginian, Hauterivian). *Palaeogeography, Palaeoclimatology, Palaeoecology*, 248: 391- 430.

Moiroud M., Martinez M., Deconinck J.-F., Monna F., Pellenard P. & Riquier L. (2012). High-resolution clay mineralogy as a proxy for orbital tuning: Example of the Hauterivian-Barremian transition in the Betic Cordillera (SE Spain). *Sedimentary Geology*, 282: 336-346.

Price G.D. & Nunn E.V. (2010). Valanginian isotope variation in glendonites and belemnites from Arctic Svalbard: Transient glacial temperatures during the Cretaceous greenhouse. *Geology*, 38: 251-254.

Reboulet S. & Atrops F. (1995). Rôle du climat sur les migrations et la composition des peuplements d'ammonites du Valanginien supérieur du bassin vocontien (S-E de la France). *Geobios*, Mémoire spécial 18: 357-365.

Reboulet S. & Atrops F. (1999). Comments and proposals about the Valanginian-Lower Hauterivian ammonite zonation of south-eastern France. *Eclogae Geologicae Helvetiae*, 92: 183-198.

Reboulet S., Rawson P.F., Moreno-Bedmar J.A., (reporters), *et al*. (20 co-authors) (2011). Report on the 4th International Meeting of the IUGS Lower Cretaceous Ammonite Working Group, the “Kilian Group”(Dijon, France, 30th August 2010). *Cretaceous Research*, 32: 786-793.

Rio M., Ferry S. & Cotillon P. (1989). Périodicités dans les séries pélagiques alternantes et variations de l'orbite terrestre. Exemple du Crétacé inférieur dans le Sud-Est de la France. *Comptes rendus de l'Académie des sciences, série 2*, 309: 73-79.

Sprenger A. & Ten Kate W.G. (1993). Orbital forcing of calcilutite-marl cycles in southeast Spain and an estimate for the duration of the Berriasian stage. *Geological Society of America Bulletin*, 105:807-818.

Sprovieri M., Coccioni R., Lirer F., Pelosi N. & Lozar F. (2006). Orbital tuning of a lower Cretaceous composite record (Maiolica Formation, central Italy). *Paleoceanography*, 21: PA4212.

Thomson D. J. (1982). Spectrum estimation and harmonic analysis. *Proceedings of the IEEE*, 70: 1055-1096.

Thomson D. J. (1990). Quadratic-inverse spectrum estimates: applications to palaeoclimatology. *Philosophical Transactions: Physical Sciences and Engineering*, 332: 539-597.

Van De Schootbrugge B., Föllmi K.B., Bulot L.G. & Burns S.J. (2000). Paleoceanographic changes during the early Cretaceous (Valanginian–Hauterivian): evidence from oxygen and carbon stable isotopes. *Earth and Planetary Science Letters*, 181: 15-31.

Walter B. (1991). Changement de faunes de bryozoaires dans le Valanginien supérieur des Alpes-de-Haute-Provence. Parallélisme avec la crise observée dans le Jura à la même époque. *Cretaceous Research*, 12: 597-606.

Westermann S., Föllmi K. B., Adatte T., Matera V., Schnyder J., Fleitmann D., Fiet N., Ploch I. & Duchamp-Alphonse S. (2010). The Valanginian δ_{13}C excursion may not be an expression of a global oceanic anoxic event. *Earth and Planetary Science Letters*, 290: 118-131.

Worldwide asymmetric distribution of Boreal, Tethyan, Austral dinoflagellates: palaeoceanographic reconstruction of Southern Ocean and impact of the palaeogeography on the northern sea-surface temperature gradients for Aptian and Albian

Edwige Masure[1], Bruno Vrielynck[2]

[1]UPMC Univ Paris 06, CR2P - UMR 7207 CNRS, MNHN, Univ Paris 06, 4, place Jussieu, 75005 Paris, France; E-mail: edwige.masure@upmc.fr
[2] UPMC Univ Paris 06, ISTEP - UMR 7193 CNRS, Univ Paris 06, 4 place Jussieu, 75005 Paris, France; E-mail: bruno.vrielynck@upmc.fr

The sea surface temperatures (SST) are the most problematic aspects of the greenhouse period. The inferred palaeotemperatures obtained from isotopic analysis on planktonic foraminifera indicated that the high-latitude SST from the Southern Ocean could have been warm as 16-20°C at 60°S (DSDP site 511) in the Late Albian (Huber *et al*., 1995). This is an extraordinary temperatures for 60°S and during a decade results have been overlooked. Warm high-latitude SST of Southern Ocean have been confirm by Bice *et al.* (2003) for upper Turonian (30-32°C at 60°S) and Jenkyns *et al.* (2012) for Middle Jurassic-Early Cretaceous. Bice *et al.* (2003) and Takashima *et al.* (2006) using models suggest Late Cretaceous asymmetric SST gradient with warmer high latitudes in the Southern Ocean. Dealing with the biogeography of dinoflagellate cysts as paleotemperature proxy (Masure and Vrielynck, 2009) indicate that warmer high latitude SST existed during Late Albian in the Southern Ocean.

Extant dinoflagellates are organisms sensitive to temperature and salinity; each species lives in a given ranges of climatic and environmental conditions. Their cysts delineate climatic belts (Marret and Zonneveld, 2003) and are excellent proxies of sea-surface conditions with the best analogue method for quantitative quaternary palaeoceanographic reconstruction (de Vernal *et al*., 2001). Best analogue method applied to recent dinocysts cannot be applied to Mesozoic cysts since the ecological behaviours (temperature and salinity ranges) of extinct motile dinoflagellates – producing the fossilized cysts – are unknown.

Compiling 87 articles and using a Geographical Information System (GIS), Masure and Vrielynck (2009) have mapped worldwide biogeography of 38 dinoflagellates and have demonstrated Cretaceous bioclimatic belts. Late Albian Tropical, Subtropical, Boreal, Austral, bipolar and cosmopolitan species have been identified. Asymmetric distribution of warm subtropical and colder species (i.e. Boreal, Austral, Subpolar species) on the two hemispheres suggest asymmetric SST gradient.

For comparison with Albian assemblages, 32 Aptian species derived from 36 studies from the northern hemisphere and 14 ones from the southern hemisphere have been encountered (Masure *et al.*, 2013). Asymmetric distribution from 40°N to 70°S of subtropical Tethyan species demonstrates same asymmetric Aptian and Late Albian SST gradients with warmer high latitude sea surface water of the Southern Ocean. The SST gradients are stronger in the northern hemisphere than in the southern hemisphere. For Aptian, 3 belts are defined in the northern hemisphere and 1 in the southern hemisphere, for Albian, dinocysts delineate 4 belts in the northern hemisphere and 3 in the southern hemisphere according the selected cysts.

We note that Aptian and Late Albian Subtropical and Subpolar dinoflagellates met and mixed at 35-40°N in the northern hemisphere, while they mixed along 30° to 70°S and 50° to 70°S palaeolatitudes respectively in the southern hemisphere. The dissimilarity between narrow mixing belts in the northern hemisphere and broad mixing belts in the southern hemisphere is noteworthy and questionable. The mixing of Tethyan and Austral dinoflagellates suggest co-occurrence of warm and cold currents. It is difficult to accept that in the high latitudes of the Southern Ocean Tethyan subtropical and Austral species (i.e. bipolar species) lived together during the Austral summer. We would have to imagine that Tethyan and Austral species lived in different water masses suggesting a structure of the ocean different from the current structure. Hay (2008) suggested that the ocean circulation would be accomplished through mesoscale eddies which could carry warmth to the polar regions.

In contrast, the mixing belt is narrow in the northern hemisphere, why? During Early Aptian – Late Albian warming and sea level rise (Haq *et al.*,1988), Boreal species sensitive to temperature migrated from the western European Basins (35°N) to higher latitudes (55°N) through the shallow proto-North Atlantic and the Greenland-Norwergian Seaway connecting the Arctic Ocean. While Tethyan species did not migrate staying in the southern part of the proto-North Atlantic at 40°N. We suggest that the northern part of the proto-North Atlantic and the Greenland-Norwergian Seaway might have been barriers until Late Albian for oceanic Tethyan dinoflagellates stopped either by the shallow water column or temperature and salinity constraints. We can speculate that in this northern part of the world the oceanic heat transport was halted by continental masses located between the Tethys, Central Atlantic and Arctic Oceans while the heat transport in the Southern Hemisphere was not so limited.

In conclusion, warm high-latitudes SSTs of the Southern Ocean is now well established from the Middle Jurassic up to Turonian, and the asymmetric Cretaceous SST gradients have been demonstrated. The mixing of Tethyan and Austral dinoflagellates in high-latitudes of Southern Ocean along 20° suggest co-occurrence of warm and cold currents as warm and cold mesoscale eddies. The palaeogeography of the northern hemisphere impacts the SST gradient and water masses exchanged between the proto-North Atlantic and the Arctic Ocean are limited until the Late Albian.

References

Bice K.L., Huber B.T. & Norris R.D. (2003). Extreme polar warmth during the Cretaceous greenhouse? Paradox of the late Turonian δO^{18} record at Deep Sea Drilling Project Site 511. *Paleoceanography*, 18, 2: 1031.

De Vernal A., Henry M., Matthiessen J., Mudie P.J., Rochon A., Boessenkool K., Eynaud F., Grosfjeld K., Guiot J., Hamel D., Harland R., Head M.J., Kunz-Pirrung M., Levac E., Loucheur V., Peyron O., Pospelova V., Radi T., Turon J.-L., Voronina E. (2001). Dinoflagellate cyst assemblages as tracers of sea-surface conditions in the northern North Atlantic, Arctic and sub-Arctic seas: the new "*n=677*" database and application for quantitative paleoceanographical reconstruction. *Journal of Quaternary Science*, 16: 681.

Hay W.W. (2008). Evolving ideas about the Cretaceous climate and ocean circulation. *Cretaceous Research*, 29, 725-753.

Haq Bilal U., Hardenbol J. & Vail P. (1988). Chronology of fluctuating sea levels since the Triassic. *Science*, 235: 1156-1166.

Huber B.T., Hodell D.A. & Hamilton C.P. (1995). Middle-Late Cretaceous climate of the southern high latitudes, stable isotopic evidence for minimal equator-to-pole thermal gradients. *Geological Society of America Bulletin*, 107: 1164-1191.

Jenkyns H.C., Schouthen-Huibers L., Schouten S. & Sinninghe Damsté J.S. (2012). Warm Middle Jurassic-Early Cretaceous high-latitude sea-surface temperatures from the Southern Ocean. *Climate of the Past*, 8: 215-226.

Marret F. & Zonneveld K.A.F. (2003). Atlas of modern organic-walled dinoflagellate cyst distribution. *Review of Palaeobotany and Palynology*, 125(1-2): 1-200.

Masure E. & Vrielynck B. (2009). Late Albian dinoflagellate cyst paleobiogeography as indicator of asymmetric sea surface temperature gradient on both hemispheres with southern high latitudes warmer than northern ones. *Marine Micropaleontology*, 70: 120-133.

Masure E., Aumar A.-M. & Vrielunck B. (2013). World palaeogeography of Aptian and Late Albian dinoflagellates cysts: Implications for sea surface temperature gradient and palaeoclimate. In Lewis J.M., Marret F. & Bradley L. (Eds), *Biological and Geological Perspectives of Dinoflagellates.* The Micropalaeontological Society, Special Publications. Geological Society, London, (in press)

Takashima R., Nishi H., Huber B.T. & Leckie M.R. (2006). Greenhouse World and the Mesozoic ocean. *Oceanography*, 19: 82-92.

Climate Response to CO_2-forcing in a Paleo-Icehouse

Isabel P. Montañez[1], Christopher J. Poulsen[2]

[1]Geology Department, University of California-Davies, Shields Avenue, Davies, CA 95616, U.S.A.; E-Mail: ipmontanez@ucdavis.edu
[2]Dept. of Earth and Environmental Sciences, 3026 C.C. Little Building, University of Michigan, Ann Arbor, MI 48109, U.S.A.; E-Mail: poulsen@umich.edu

At the current rate of global C emissions (~9 or 10 Pg yr^{-1}) (Friedlingstein *et al.*, 2010) and without substantial mitigation efforts, atmospheric CO_2 is projected to increase by the end of this century to levels (potentially between 600 and >900 ppmv; Solomon *et al.*, 2007) not previously experienced on Earth since the onset of our current glacial state, over 34 million years ago (NRC 2011). If observations of historic changes in climate and ecosystems under rising, but generally low, atmospheric CO_2 levels are any indication, a future high-CO_2 icehouse world will be drastically different than today (IPCC 2007, Barnowsky *et al.*, 2012). How different is an open question. Insight into how the Earth system will function in such an evolving and high CO_2 environment resides in the deep-time records of past climate and ecosystem response to greenhouse gas-forced warming. This archive is unique in that it is the only empirical source of the climate and biotic response to greenhouse gas forcing at the high levels to which Earth is destined. Ice cores, tree ring, deep-sea sediment and speloethem records have been invaluable for understanding climate under glacial and modern conditions of the Pleistocene but lack the temporal range to sample past times of greenhouse gas-forced climate change. The climate of the past few 1000s to 100s of 1000s of years has been characterized by atmospheric CO_2 contents 30% lower than present-day, stable ice and permafrost in both polar regions, and CO_2 and temperature changes during climate transitions up to two orders of magnitude slower than those of the past few decades (NRC 2011). Deep-time records are not perfect analogues for the future in part because no such analog exists. In turn climate models are not perfect representations of the climate system. But, like climate models, the deep-time archive provides insight into fundamental climate processes, and specifically the system response to evolving CO_2 levels that cannot be gleaned from the more recent record of our existing glacial state.

Icehouses, such as our current glacial state, account for a small portion of Earth's history. The last period of bipolar glacial conditions, prior to the onset of the Cenozoic icehouse, was the late Paleozoic (340 to 280 Mya). Glacial conditions persisted for 10s of millions of years (Veevers & Powell, 1987, Frakes *et al.* 1992) under the lowest atmospheric CO_2 levels and possibly highest O_2 concentrations of the Phanerozoic (Berner, 2006). Supercontinental configuration and lower solar luminosity created boundary conditions that were significantly different than present-day. Despite these differences, this geologic archive provides the opportunity to study climate processes and feedbacks in the system in response to changing atmospheric CO_2 concentrations and major terrestrial ecosystem shifts. The late Paleozoic was the time of the evolution and expansion of the oldest known paleotropical wetland forests (Cleal & Thomas, 2005). Recent studies of the late Paleozoic ice age (herein referred to as the LPIA) document a dynamic glaciation history characterized by repeated, short-lived (<1 to ~8 my), and possibly severe glacial events (Soreghan G.S. *et al.*, 2008) separated by substantially diminished ice (Isbell *et al.*, 2003, 2012; Fielding *et al.*, 2008). Other studies, building on decades of prior research effort, provide insight into the complex response of sea level, atmospheric and oceanic circulation, and lower latitude climate to the waxing and waning of high-latitude glacial ice and likely varying atmospheric greenhouse gas levels (e.g., Soreghan *et al.*, 2002; Soreghan MJ. *et al.*, 2008; Montañez *et al.*, 2007; Poulsen *et al.*, 2007; Birgenheier *et al.*, 2010; Eros *et al.*, 2012). Similarly, paleobiologic studies reveal a biosphere far less stable than previously believed, one characterized by complex floral and faunal restructuring that accompanied and, in some cases, likely influenced climate at this time (Powell, 2007; Clapham & James, 2008; DiMichele *et al.*, 2009; Horton *et al.*, 2010; McGhee *et al.*, 2012). Notably, the demise of this icehouse in the Middle Permian provides a unique view of the transition of a vegetated and metazoan world from a glacial state to fully greenhouse conditions (Gastaldo *et al.*, 1996; Montañez *et al.*, 2007).

Three areas of study are particularly compelling for insight into the climate and ecosystem response of the late Paleozoic icehouse to perturbation, including deglaciation. These include: (1) The role of atmospheric CO_2 in forcing climate change and the dynamic glaciation history relative to other drivers (e.g., paleogeography, oceanic gateways, tectonically induced variation in the equilibrium line altitude for ice, and ocean circulation). (2) How the geographic extent and volume of continental ice varied with changes in forcings and, in turn, the magnitude of glacioeustatic response to such variation. (3) To what forcing(s) did low-latitude climate primarily respond and by what mechanisms were such changes linked to higher latitude glaciation and glacioeustasy. Moreover, what role did the vast wetland forests of the paleotropics play in driving climate change. In this presentation, we address these issues through data-model comparisons for the LPIA.

***CO_2-forcing and glaciation history*:** Our recent proxy-based and modeling studies suggest that atmospheric CO_2 varied substantially *throughout* the LPIA and may have played a primary role in its dynamic glaciation and climate history. Ongoing paleosol carbonate- and stomatal-based reconstruction of atmospheric CO_2 defines variations from lows of 100-300 ppmv to highs of 700-1200 ppmv on a sub- to multi-million year time-scale (Montañez *et al*., 2007; Garello *et al*., 2012, Montañez and McElwain, unpublished data — CO_2 concentrations that greatly exceed those of the Cenozoic icehouse (≤435 ppmv; Pagani *et al*., 2010; Foster *et al*., 2012). Changes in atmospheric CO_2 concentration were coincident with major changes in sea level and inferred periods of substantial growth and contraction of ice sheets. Our climate-ice sheet models for the LPIA (Horton & Poulsen, 2009; Horton *et al*., 2010) further indicate that CO_2 was the fundamental driver for the building and demise of the ice sheets. Other factors, including topography, may have been locally important. Field and model evidence argue for smaller total ice volumes (~20×10^6 km^3) than previously suggested distributed within multiple ice centers and support the possibility of bipolar glaciation at times (Montañez & Poulsen, 2013). Moreover, the inferred sea level history (Eros *et al*., 2012) and paleo-atmospheric pCO_2 reconstructions (Montañez *et al*., 2007; Montañez & McElwain unpublished data) for the Permo-Carboniferous suggest a stepped nature to the onset of the LPIA (late Mississippian) and its demise 60 million years later (Early Permian). Together with the temporal distribution of ice centers constrained by model results and geologic data, this suggests threshold behavior, likely involving changes in atmospheric pCO_2 and orbital forcing analogous to that during the initiation of the Cenozoic icehouse (Montañez & Poulsen, 2013).

***Ice volume changes and glacioeustasy*:** A recent compilation (Rygel *et al*., 2008) of estimates of eccentricity-scale sea-level fluctuations, inferred from cyclothems, stratigraphic relationships and incised valleys, and geochemical proxies from low-latitude Permo-Carboniferous successions, illustrates the substantial variability in the magnitudes of eustatic change through the LPIA. Although estimated magnitudes range from 10 to 200+ m, inferred magnitudes greater than ~50 m may be problematic given the growing support for smaller total ice volume and numerous ice centers from which small ice sheets and glaciers emanated coupled with the insensitivity of massive ice sheets to orbital forcing (Montañez & Poulsen, 2013). Our modeling efforts (Horton *et al*., 2010) using an atmospheric general circulation model coupled to a three-dimensional ice-sheet model simulate smaller ice volumes (~20×10^6 km^3 with CO_2 values of 560 ppmv) distributed as multiple ice centers that compare well to maximum estimates based on glacigenic deposits, but generate orbitally-forced ice volume changes equivalent to ~25 m of sea-level change. Notably, simulated ice sheets with much larger volumes do not ablate during warm summer orbits due to their high and thus very cold surfaces and thus present a 'too-large-to-fail' paradox —these ice sheets sequester sufficient water to account for the large glacioeustatic changes inferred from cyclothems, but are too large and stable to respond to orbital forcing. Feedbacks in the late Paleozoic climate system, including changes in greenhouse gas levels, dust loading, and vegetation-climate feedbacks, likely factored largely into the waxing and waning of the ice sheets as model results reveal that orbitally-forced insolation changes alone were insufficient to drive substantial expansion and contraction of Gondwanan ice sheets (Horton *et al*., 2010). Lastly, temporal variability in the magnitudes of glacioeustasy is expected given that ice volume and stability would have differed between glacial events and intermittent periods of contraction.

***Climate Linkages*:** Teleconnections between high-latitude ice sheet behavior and low-latitude atmospheric dynamics during the late Paleozoic have been proposed in large part based on reconstructed shifts in tropical continental climate in synch with eccentricity-scale (10^4 yr) glacial-interglacial cycles (e.g., Soreghan, 1994; Rankey, 1997; Soreghan *et al*., 2002; Cecil *et al*., 2003; Olszewski & Patkowsky, 2008; Soreghan MJ *et al*., 2008). With the discovery of discrete 10^6-year glacial events and intermittent glacial minima has come evidence of contemporaneous low-latitude climate shifts at a comparable timescale (e.g., Feldman *et al*., 2005; Birgenheier *et al*., 2009; Allen *et al*., 2011; Eros *et al*., 2012). Data-model comparisons highlight how the nature of low-latitude climate change may have varied with the time-scale of change and in response to specific forcings. Climate models for the LPIA further suggest that long-term changes in low-latitude precipitation were likely controlled by atmospheric CO_2 levels. Although ice volume, glacioeustasy, and low-latitude precipitation may fluctuate on similar orbital timescales, our climate simulations indicate that they need not be mechanistically linked (Horton *et al.*, 2012), contrary to what has been widely inferred for the late Paleozoic ice age.

At the eccentricity time-scale or less, it is likely that feedbacks played an important role. Documented shifts in the composition of paleotropical flora between inferred glacial and interglacial states of the LPIA within eccentricity-paced cycles (Falcon-Lang 2004; Falcon-Lang & DiMichele 2010; DiMichele *et al.*, 2010) and on million-year time-scales (Cleal & Thomas 2005; Montañez *et al.*, 2007; DiMichele *et al.*, 2009), highlight the potential importance of vegetation-climate feedbacks, in particular under evolving CO_2 levels, to have exerted an influence on regional to global climate and C and water cycling. Our modeling also predicts major variation in tropical vegetation with climate and the *potential* for vegetation feedbacks to have influenced the late Paleozoic climate system (Poulsen *et al.*, 2007; Horton *et al.,* 2010, 2012; Montañez & Poulsen 2013). These findings underscore the need for further data-model studies involving better resolved LPIA conditions in order to fully understand the origin and timing of continental climate change and the nature of possible low-high latitude linkages during glaciated periods and intermittent periods of glacial minima (i.e., glacial-interglacial cycles of eccentricity to million-year scale).

References

Allen J.P., Fielding C.R., Gibling M.R. & Rygel M.C. (2011). Fluvial response to paleo-equatorial climate fluctuations during the late Paleozoic ice age. *Geological Society of America, Bulletin*, 123: 1524-1538.

Barnosky A.D., Hadly E.A., Bascompte J. and 19 others. (2012). Approaching a state shift in Earth's biosphere. *Nature*, 486: 52-58.

Berner R.A. (2006). GEOCARBSULF: A combined model for Phanerozoic atmospheric O_2 and CO. *Geochimica et Cosmochimica Acta*, 70: 5653-5664.

Birgenheier L.P., Fielding C.R., Rygel M.C., Frank T.D. & Roberts J. (2009). Evidence for dynamic climate change on sub-10^6-year scales from the late Paleozoic glacial record, Tamworth Belt, New South Wales, Australia. *Journal of Sedimentary Research*, 79: 56-82.

Birgenheier L.P., Frank T.D., Fielding C.R. & Rygel M.C. (2010). Coupled carbon isotopic and sedimentological records from the Permian system of eastern Australia reveal the response of atmospheric carbon dioxide to glacial growth and decay during the late Palaeozoic Ice Age. *Palaeogeography, Palaeoclimatology, Palaeoecology*, 286:178-193.

Cecil B.C., Dulong F.T, West R.R., Stamm R., Wardlaw B. & Edgar N.T. (2003). Climate controls on the stratigraphy of a Middle Pennsylvanian cyclothem in North America. In: Cecil C.B. & Edgar N.T. (Eds), *Climate Controls on Stratigraphy.* SEPM Special Publication, 77: 151–182.

Clapham M.E & James N.P. (2008). Paleoecology of Early-Middle Permian marine communities in eastern Australia: Response to global climate change in the aftermath of the late Paleozoic ice age. *Palaios*, 23: 738-750.

Cleal C.J. & Thomas B.A, (2005). Palaeozoic tropical rainforests and their effect on global climates: Is the past the key to the present? *Geobiology*, 3: 13–31.

Dimichele W.A., Montañez I.P., Poulsen C.J. & Tabor N.J. (2009). Climate and vegetational regime shifts in the late Paleozoic ice age earth. *Geobiology*, 7: 200-226.

Dimichele W.A., Cecil B., Montañez I.P. & Falcon-Lang H. (2010). Cyclic changes in Pennsylvanian paleoclimate and effects on floristic dynamics in tropical Pangaea. *International Journal of Coal Geology*, 83: 329-344.

Eros J.M., Montañez I.P., Osleger D.A., Davydov V.I., Nemyrovska T., Poletaev V. & Zhykalyak M.V. (2012). Sequence Stratigraphy and Onlap History, Donets Basin, Ukraine: Insight into Late Paleozoic Ice Age dynamics. *Palaeogeography, Palaeoclimatology, Palaeoecology*, 313-314: 1-25.

Falcon-Lang H.J. (2004). Pennsylvanian tropical rain forests responded to glacial-interglacial rhythms. *Geology*, 32: 689-692.

Falcon-Lang H.J. & Dimichele W.A. (2010). What happened to the coal forests during Pennsylvanian glacial phases? *Palaios*, 25: 611-617.

Feldman H.R., Franseen E.K., Joeckel R.M. & Heckel P.H. (2005). Impact of longer-term modest climate shifts on architecture of high-frequency sequences (c &clothems), Pennsylvanian of Mid-continent U.S.A. *Journal of Sedimentary Research*, 75: 360–368.

Fielding C.R., Frank T.D., Birgenheier L.P., Rygel M.C., Jones A.T. & Roberts J. (2008). Stratigraphic imprint of the Late Palaeozoic Ice Age in eastern Australia: A record of alternating glacial and non-glacial climate regime. *Journal Geological Society of London*, 165: 129-140.

Fischbein S.A., Joeckel R.M. & Fielding C.R. (2009). Fluvial-estuarine reinterpretation of large, isolated sandstone bodies in epicontinental cyclothems, Upper Pennsylvanian, northern Mid-continent, USA, and their significance for understanding late Paleozoic sea-level fluctuations. *Sedimentary Geology*, 216: 15-28.

Foste G.L., Lear C.H. & Rae J.W.B. (2012). The evolution of pCO_2, ice volume and climate during the middle Miocene. *Earth and Planetary Science Letters*, 341-344: 243-254.

Frakes L.A., Francis J.E. & Syktus J.I. (1992). Climate Modes of the Phanerozoic. *Cambridge: Cambridge University Press*, Cambridge. 274 p.

Friedlingstein P., Houghton R.A., Marland G., Hackler J., Boden T.A., Conway T.J., Canadell J.G., Raupach M.R, Ciais P. & Le Quéré C. (2010). Update on CO_2 emissions. *Nature Geoscience*, 3: 811-812.

Garello D., Montañez I.P., Barclay R.S., McElwain J.C., Byrd A. & Dimichele W.A. (2012). Carboniferous atmospheric CO_2 and climate: An integrated fossil cuticle and paleosol carbonate analysis (abst). *Geological Society of America. Abstracts and Programm.* Charlotte, NC.

Gastaldo R.A., Dimichele W.A. & Pfefferkorn H.W. (1996). Out of the icehouse into the greenhouse: a Late Paleozoic analog for modern global vegetational change. *GSA Today*, 6: 1–7.

Horton D.E., Poulsen C.J. & Pollard D. (2007). Orbital and CO_2 forcing of Late Paleozoic continental ice sheets. *Geophysical Research Letters*, 34: L19708.

Horton D.E. & Poulsen C.J. (2009). Paradox of late Paleozoic glacioeustasy. *Geology*, 37: 715-718.

Horton D.E., Poulsen C.J. & Pollard D. (2010. Influence of high-latitude vegetation feedbacks on late Paleozoic glacial cycles. *Nature Geoscience*, 3: 572-577.

Horton D.E., Poulsen C.J., Montañez I.P. & Dimichele W.A. (2012). Eccentricity-paced late Paleozoic climate change. *Palaeogeography, Palaeoclimatology, Palaeoecology*, 331-332: 150-161.

IPPC (Solomon S., Qing D., Manning M. & 27 Others). (2007). Technical summary. In: Solomon S., Qin D., Manning M., Chen Z., Marquis M., Averyt K.B., Tignor M. & Miller H.L. (Eds), *Climate change 2007: The physical science basis. Contribution of Working Group I to the fourth assessment report of the Intergovernmental Panel on Climate Change*. Cambridge University Press, Cambridge, UK.

Isbell J.L., Miller M.F., Wolfe K.L. & Lenaker P.A. (2003). Timing of late Paleozoic glaciation in Gondwana: Was glaciation responsible for the development of northern hemisphere cyclothems? In Chan M.A. & Archer A.W. (Eds), *Extreme Depositional Environments: Mega End Members in Geologic Time*. Geological Society of America, Special Publication, 370: 5-24.

Isbell J.L., Henry L.C., Gulbranson E.L., Limarino C.O., Fraiser M.L., Koch Z.J., Ciccioli P.I. & Dineen A.A. (2012). Glacial paradoxes during the late Paleozoic ice age: Evaluating the equilibrium line altitude as a control on glaciation. *Gondwana Research*, 22: 1-19.

Montañez I.P. & Poulsen C.J. (2013). The Late Paleozoic Ice Age: An evolving icehouse paradigm. *Annual Reviews in Earth and Planetary Sciences*, 41: 24.1-24.28.

Montañez I.P., Tabor N.J., Niemeier D., Dimichele W.A., Frank T.D., Fielding C.R., Isbell J.L., Birgenheier L.P. & Rygel M.C. (2007). CO_2-forced climate instability and linkages to tropical vegetation during late Paleozoic deglaciation. *Science*, 315: 87-91.

Nrc 2011 (Montañez I.P., Norris R.D., Algeo T., Chandler M.A., Johnson K.R., Kennedy M.J., Kent D.V., Kiehl J.T., Kump L.R., Ravelo A.C. & Turekian K.K.). Understanding Earth's deep past. Lessons for our climate future. *The National Academies Press*, Washington D.C., 161 pp.

Olszewski T.D. & Patzkowsky M.E. (2008). Icehouse climate and eustasy recorded in a low-latitude epeiric platform: Alternating climate regimes in the Pennsylvanian-Permian succession of the North American mid-continent. In: Holmden C. & Pratt B.R. (Eds), *Dynamics of Epeiric Seas: Sedimentological, Paleontological and Geochemical Perspectives.* Geological Association of Canada, Special Paper, 48: 1-17.

Pagani M., Liu Zh., Lariviere J. & Ravelo A.C. (2010). High Earth-system climate sensitivity determined from Pliocene carbon dioxide concentrations. *Nature Geoscience*, 3: 27–30.

Poulsen C.J., Pollard D., Montañez I.P. & Rowley D. (2007). Late Paleozoic tropical climate response to Gondwanan deglaciation. *Geology*, 35: 771-774.

Powell M.G. (2007). Latitudinal diversity gradients for brachiopod genera during late Palaeozoic time: links between climate, biogeography and evolutionary rates. *Global Ecology and Biogeography*, 16: 519-528.

Rankey E.C. (1997). Relations between relative changes in sea level and climate shifts: Pennsylvanian−Permian mixed carbonate-siliciclastic strata, western United States. *Geological Society of America, Bulletin*, 109: 1089-1100.

Rygel M.C., Fielding C.R., Frank T.D. & Birgenheier L.P. (2008). The magnitude of late Paleozoic glacioeustatic fluctuations: A synthesis. *Journal of Sedimentary Research*, 78: 500-511.

Soreghan G.S. (1994). The impact of glacioclimatic change on Pennsylvanian cyclostratigraphy. In Embry A.F., Beauchamp B. & Glass D.J. (Eds), *Pangea - Global Environments and Resources*. Canadian Society of Petroleum Geologists, Memoir, 17: 523-543.

Soreghan G.S., Elmore R.D. & Lewchuk M.T. (2002). Sedimentological record of western Pangean climate in upper Paleozoic loessite. *Geological Society of America, Bulletin*, 114: 1019–1035.

Soreghan G.S., Soreghan M.J., Poulsen C.J., Young R.A., Eble C.F., Sweet D.E. & Davogustto O.C. (2008). Anomalous cold in the Pangaean tropics. *Geology*, 36: 659-662.

Soreghan M.J., Soreghan G.S. & Hamilton M.A. (2008). Glacial-interglacial shifts in atmospheric circulation of western tropical Pangaea. *Palaeogeography, Palaeoclimatology, Palaeoecology*, 268: 260-272.

Veveers J.J. & Powell C.A. (1987). Late Paleozoic glacial episodes in Gondwanaland reflected in transgressive-regressive depositional sequences in Euramerica. *Geological Society of America, Bulletin*, 98: 475-487.

Evolution of neodymium isotopic signature of seawater during the Late Cretaceous: new insights on oceanic circulation changes

Mathieu Moiroud[1], Emmanuelle Pucéat[1], Yannick Donnadieu[2], Germain Bayon[3], Jean-François Deconinck[1]

[1]UMR CNRS 6282 Biogéosciences, Université de Bourgogne, 6 bd Gabriel, 21000 Dijon, France
[2]UMR CEA/CNRS, 1572 Laboratoire des Sciences du Climat et de l'Environnement, CE Saclay, Orme des Merisiers, Bât. 701, 91191 Gif sur Yvette Cedex, France
[3]Département Géosciences Marines, Ifremer, 29280 Plouzané, France

Changes in oceanic circulation during the Late Cretaceous have been inferred from the neodymium isotopic composition (ε_{Nd}) of fish remains, which reflects the signature of past seawater (Robinson *et al.*, 2010; MacLeod *et al.*, 2011). However the nature of these changes remains controversial, mainly due to insufficient temporal and spatial coverage of Nd isotope data. Data from continental margins in particular remain scarce for the Cretaceous (Pucéat *et al.*, 2005; Soudry *et al.*, 2006), yet such records would help to discuss the origin of the changes depicted in deep and intermediate water masses (changes in the location of deep water production vs. changes in the composition of water in the source area).

This work aims at reconstructing the signature of neritic and oceanic water ε_{Nd} during the Late Cretaceous/Early Paleogene in potential areas of deep water sinking and seaways linking different oceans. For this purpose, samples of fish remains, foraminifera and detrital fraction have been recovered in Late Cretaceous to Paleocene sediments from both oceanic and neritic sites. The DSDP sites 152 (Nicaraguan Rise), 258 (Naturaliste Plateau, southwestern Australia), 323 (Bellingshausen Abyssal Plain), and ODP sites 690 (Maud Rise) and 700 (East Georgia Basin, South Atlantic) were selected to obtain oceanic data. Samples from Wyoming, Texas, New Jersey, Chile, Seymour Island (Antarctic Peninsula), Egypt and Hokkaidō (northern Japan) supplied neritic material.

Part of the results primarily points out a decreasing trend after the Cenomanian-Turonian interval, previously observed in the Atlantic and the Indian sector of the Southern Ocean (Murphy and Thomas, 2012; Robinson *et al.*, 2012) and a general increasing trend during the Maastrichtien and the Paleocene, but also documents the first Cretaceous ε_{Nd} data for the Southern Pacific, the continental margins of North America and Japan, and the Panama and Drake passages. Nevertheless, further comparisons with ε_{Nd} data available in the literature and climate modelling are required to tentatively explain the oceanic circulation during the Late Cretaceous.

References

MacLeod K.G., Londoño C.I., Martin E.E., Jiménez Berrosco Á. & Basak C. (2011). Changes in North Atlantic circulation at the end of the Cretaceous greenhouse interval. *Nature Geoscience*, 4: 779-782.

Murphy D.P. & Thomas D.J. (2012). Cretaceous deep-water formation in the Indian sector of the Southern Ocean. *Paleoceanography*, 27: PA1211.

Pucéat E., Lécuyer C. & Reisberg L. (2005). Neodymium isotope evolution of NW Tethyan upper ocean. *Earth and Planetary Science Letters*, 236: 705-720.

Robinson S.A., Murphy D.P., Vance D. & Thomas D.J. (2010). Formation of 'Southern Component Water' in the Late Cretaceous: evidence from Nd-isotopes. *Geology*, 38 (10): 871-874.

Robinson S.A. & Vance D. (2012). Widespread and synchronous change in deep-ocean circulation in the North and South Atlantic during the Late Cretaceous. *Paleoceanography*, 27: PA1102.

Soudry D., Glenn C.R., Nathan Y., Segal I. & Vonderhaar D.L. (2006). Evolution of Tethyan phosphogenesis along the northern edges of the Arabian-African shield during the Cretaceous-Eocene as deduced from temporal variations of Ca and Nd isotopes and rates of P accumulation. *Earth-Science Reviews*, 78: 27-57.

Impact of large igneous provinces: a modeling approach

Mickael Mussard[1], Frédéric Fluteau[1], Guillaume Le Hir[1], Yves Goddéris[2], Olivier Boucher[3], Vincent Courtillot[1]

[1]Institut de Physique du Globe and Université Paris-Diderot, Sorbonne Paris Cité, 1 rue Jussieu, Paris, France
[2]Géosciences Environnement Toulouse (GET), Observatoire Midi Pyrénées, Université de Toulouse, CNRS, IRD, 14 avenue E. Belin; F- 31400 Toulouse, France
[3]Laboratoire de Météorologie Dynamique, IPSL, CNRS/UPMC, Paris, France

The temporal synchronism between mass extinctions and the emplacement of large igneous provinces suggests a causal connection between the two. However, the mechanisms linking volcanism and mass extinctions are not well understood. We know, from the studies of recent and historical volcanic eruptions, that the sulfur dioxide injected in the atmosphere, and subsequently converted into sulfate aerosols, modifies the Earth's radiative budget and favors global cooling of the Earth's surface during the year(s) following the eruption. In case of trap volcanism, the impact on climate and environment is more complex. It depends on both the tempo (and dynamics) of eruptions and the nature and amount of volatiles released. Among the volatiles released during the emplacement of traps, we focus on the impact of SO_2 and CO_2 more specifically.

Recent studies on the Deccan traps (Chenet *et al*., 2008, 2009), the Karoo traps (Moulin *et al*., 2011) and the Siberian traps (Pavlov *et al*., 2011) provided high-resolution constraints on the tempo of emplacement through the analysis of the secular geomagnetic variations recorded by lava flows (used as a relative chronometer; the absence of secular geomagnetic variations recorded in successive lava flows suggests an outpouring in less than ~100 yrs). In the case of the Deccan traps, Chenet *et al*. (2008, 2009) proposed using this procedure that the 3500-m-thick lava pile of the Main Province was erupted in some 30 volcanic pulses (successive volcanic eruptions having not recorded secular geomagnetic variation) and some 41 individual lava flow units. The total time of volcanic activity may have not exceeded 10 kyr over a 400 kyr-long period of trap emplacement. With some assumptions about the geometry of lava flow units and volcanic pulses, Chenet *et al*. (2008, 2009) estimated that a volcanic pulse may have released 0.1 Gt/yr to 1 Gt/yr of SO_2 and 0.1 to 2 Gt/yr of CO_2, such releases lasting about a century.

To quantify the impact of a trap emplacement on the Earth's climate and its environment, the CO_2 and SO_2 inputs within the atmosphere have been modeled using a global biogeochemical cycle box model (COMBINE, Goddéris & Joachimski 2004) coupled with a climate model, wherein CO_2 and SO_2 amounts are constrained by data extracted from Chenet *et al*. (2008, 2009). For short-live processes occurring into the atmosphere, the formation and evolution of sulphate aerosol is modeled by 3 equations: the SO_2 oxydation, the liquid aerosol formation and the gravitational sedimentation from the stratosphere (Miles *et al*, 2003, Pierazzo *et al*, 2003). To assess the climate forcing due to the related loading of liquid aerosols, our model uses a relationship calculated using a General Circulation Model (GCM) (Robock *et al*. 2009, Fluteau pers.com). Long-lived processes are also included: over continents sulphate are supposed to react with carbonates and silicates, into the oceans sulphate act on the alkalinity budget and carbonate saturation state. Finally the oceanic primary productivity is computed as a function of all theses environmental changes (Behrenfeld & Falkowski 1997, Chen & Durbin, 1994).

Various parameters (amounts of CO_2 and SO_2, rates of release, duration of a volcanic pulse or duration quiescence period, etc) have been investigated. Preliminary tests, using Deccan traps constraints (0.5kyrs of duration) show that:

1) A short and important cooling is associated to single pulse due to the SO_2 converted into aerosols. If the pCO_2 increases during the traps emplacement, the warming is hidden by the SO_2 cooling which directly intercept the incoming energy coming from the Sun.

2) At a long-term scale, the succession of pulses significantly decreases the efficiency of the weathering over continents, which reduces the CO_2 consumption. This effect enhances the CO_2 build-up into the atmosphere caused by volcanoes emissions. In consequence, at the end of the trap emplacement, when aerosols are completely removed, a significant warming occurs, a result in agreement with geological records (Tobin *et al*. 2012).

3) A continuous release of CO_2 and SO_2 fails in reproducing any of the environmental perturbations able to cause a significant drop of marine productivity. Contrastingly, intense degassing peaks lead to a breakdown of biological primary productivity. This last result may be the missing link between traps emplacements and mass extinctions.

References

Behrenfeld M J. & Falkowski P. G. (1997). Photosynthetic rates derived from satellite-based chlorophyll concentration. *Limology and Oceanography*, 42(1): 1-20.

Chen C.Y & Durbin E.G. (1994). Effects of pH on the growth and carbon uptake of marine phytoplankton. *Marine Ecology Progress Series*, 109: 83–94

Chenet A.L., Quidelleur X., Fluteau F. & Courtillot V. (2007). 40K-40Ar dating of the main Deccan large igneous province: Further evidence of KTB age and short duration. *Earth and Planetary Science Letters*, 263: 1-15, doi:10.1016/j.epsl.2007.07.011.

Chenet A.L., Fluteau F., Courtillot V., Gérard M. & Subbarao K.V. (2008). Determination of rapid Deccan eruptions across the Cretaceous- Tertiary boundary using paleomagnetic secular variation: Results from a 1200-m-thick section in the Mahabaleshwar escarpment. *Journal of Geophysical Research*, 113: B04101, doi:10.1029/2006JB004635.

Chenet A. L., Courtillot V., Fluteau F., Gérard M., Quidelleur X., Khadri S.F.R., Subbarao K.V. & Thodarson T. (2009). Determination of rapid Deccan eruptions across the Cretaceous-Tertiary boundary using paleomagnetic secular variation: 2. Constraints from analysis of eight new sections and synthesis for a 3500-m-thick composite section. *Journal of Geophysical Research*, 114: B06103, doi:10.1029/2008JB005644.

Godderis Y. & Joachimski M.M. (2004). Global change in the Late Devonian: modelling the Frasnian/Famennian short-term carbon isotope excursions. *Palaeogeography, Palaeoclimatology, Palaeoecology*, 202(3-4): 309-329.

Miles G.M., Grainger R.G. & Highwoode J. (2003). Volcanic Aerosols, the significance of volcanic eruption strength and frequency for climate. *Quaterly Journal of the Royal Meterological Society*, 128: 1–999, doi: 10.1256/qj.

Moulin M., Fluteau F., Courtillot V., Marsh J., Delpech G., Gérard M. & Jay E.A. (2011). An Attempt to Constrain the Age, Duration and Eruptive History of the Karoo Flood Basalt: the Naude's Nek Section (South Africa). *Journal of Geophysical Research*, 116: B07403, 27 pp., doi:10.1029/2011JB008210.

Pavlov V.E., Fluteau F., Veselovskiy R. V., Fetisova A. M. & Latyshev A.V. (2011). Secular Geomagnetic Variations and Volcanic Pulses in the Permian-Triassic Traps of the Norilsk and Maimecha-Kotui Provinces. *Izvestiya, Physics of the Solid Earth*, 47(5) 402–417.

Pierazzo E., Hahmann A.N. & Sloan L.C. (2003). Chicxulub and climate: radiative perturbations of impact-produced S-bearing gases. *Astrobiology*, 3(1): 99-118.

Robock A., Ammann C.M., Oman L., Shindell D., Levis S. & Stenchikov G. (2009). Did the Toba volcanic eruption of ~74 ka B.P. produce widespread glaciation? *Journal of Geophysical Research*, 114: D10107, doi:10.1029/2008JD011652.

Tobin T.S., Ward P.D., Steig E.J., Olivero E.B., Hilburn I.A., Mitchell R.N., Diamond M.R., Raub T.D. & Kirschvink J.L. (2012). Extinction patterns, $\delta^{18}O$ trends, and magnetostratigraphy from a southern high-latitude Cretaceous–Paleogene section: Links with Deccan volcanism. *Palaeogeography, Palaeoclimatology, Palaeoecology*, 350–352: 180–188, doi:10.1016/j.palaeo.2012.06.029.

Are the global Ordovician-Silurian climate changes really recorded in the $\delta^{18}O$ isotope signal?

Elise Nardin

Géosciences Environnement Toulouse (GET), Observatoire Midi Pyrénées, Université de Toulouse, CNRS, IRD, 14 avenue E. Belin; F- 31400 Toulouse-France, E-mail: elise.nardin@get.obs-mip.fr

The early Palaeozoic climate has historically been described as warm and equable, except for the brief glacial event restricted to the Hirnantian (latest Ordovician). However this hypothesis has been disputed with the progressive discoveries of geological evidences of a long-term cooling trend through the Ordovician-Silurian period punctuated by the Hirnantian-Aeronian glacial event: (1) a general rise in calcitic and aragonitic shell $\delta^{18}O$ (Veizer *et al*., 1999) and conodont biogenic apatite $\delta^{18}O$ (Trotter *et al*., 2008), (2) a more steep pole to equator climatic gradient (Boucot *et al*., 2004; Vandenbroucke *et al*., 2010), (3) the sedimentologic records of cooler conditions before the Hirnantian glacial spike itself (Fortey & Cocks, 2005; Díaz-Martínez *et al*., 2007; Ghienne *et al*., 2007; Lehnert *et al*., 2010; Loi *et al*., 2010), and (4) the mean tropical sea surface temperature decrease from the Middle Ordovician to the middle Silurian modelled with a coupled climate-biogeochemical numerical model (Nardin *et al*., 2011). Therefore the historical hypothesis of an early Palaeozoic greenhouse climate punctuated by a brief glacial event (Hirnantian) appears to be disproved. More precisely, the occurrence of at least five glacial periods has been identified on the sedimentologic record (e.g. glaciomarine diamictites) through the Hirnantian-Sheinwoodian period (Ghienne *et al*., 2007; Brand *et al*., 2006). Two studies, based on $\Delta 47$ palaeothermometer used to characterize the Hirnantian glacial peak, suggest an extension of its duration from the mid Katian (with no sedimentologic record discovered yet) to the mid Rhuddanian and strong variations in the seawater $\delta^{18}O$ ($\delta^{18}O_{sw}$) (Finnegan *et al*., 2011; Rosenau *et al*., 2012). Three colder periods, cold enough to cause at least the development of glaciers in high latitude, are supposed in the early Katian, the early Sheinwoodian, the mid Ludfordian based on strong sea-level falls in areas without major tectonic activity, but no glaciologic record (Saltzman & Young, 2005; Buggisch *et al*., 2010; Jeppsson & Aldridge, 2000; Kozłowski & Sobien, 2012; Kaljo *et al*., 1997). Moderate to strong positive $\delta^{13}C_{carb}$ excursions support these glacial to cold events. In addition major lithologic change (carbonate precipitation) on the peri-Gondwanan platforms and massive faunal migrations from tropical to higher latitude areas suggest a relatively warm episode prior to the Hirnantian-Rhuddanian glaciation (the so-called Boda Event; Fortey & Cocks, 2005). Finally recent studies emphasized two possible colder periods in the late Floian and in the middle Darriwilian based on duration of stratigraphic sequences and associated strong sea-level falls in South Africa and Jordan (Turner *et al*., 2011; Turner *et al*., 2012, respectively). Beside the large databases (Veizer *et al*., 1999; Trotter *et al*., 2008) independent $\delta^{18}O$ measurements incredibly increased in the last few years for the Ordovician-Silurian period (e.g., Azmy *et al*., 1998; Buggisch *et al*., 2010; Rosenau *et al*., 2012; Samtleben *et al*., 2000; Wenzel *et al*., 2000; Wheeley *et al*., 2012; Lehnert *et al*., 2010; Žigaité *et al*., 2010). Next challenges are 1) to compile and homogenise all independent $\delta^{18}O$ measurements on biogenic carbonate and apatite and 2) to confront the fluctuations of the resulting global signal, when considering $\delta^{18}O$ as palaeothermometer, to the supposed cold to glacial periods during the Ordovician-Silurian period. The major defiance here is to endorse or dispute hypothetic cold and warm periods, suggested on $\delta^{13}C$ negative excursions and/or on steep sea-level falls. Expected outcomes are 1) the distinction between local and climatic events, 2) the refinement of their timing (when did the icehouse period start and stop?), and 3) the improvement of the understanding of the early Palaeozoic climate (e.g., long early Palaeozoic Ice Age vs. long Greenhouse Age).

The first step of this study was to inventory isotopic ($\delta^{13}C_{carb}$), stratigraphic (sea-level fluctuations and sequence durations) and sedimentologic (e.g., glacial markers, carbonate and evaporite sediments) records in order to precise the timing and the geographical extension of the different inferred cold or warm periods. The second step was to compile exhaustive databases of $\delta^{18}O$ measurements on biogenic carbonates (articulate brachiopod, ostracode and trilobite shells) and on biogenic apatite (conodont and inarticulate brachiopod shell) based on independent geochemical published studies. Sampling sites were spatialized. Facies categories (e.g., lagoonal facies) were established to characterize each isotopic sample. All data points were temporally situated at the biozone scale and instantaneously reordered (assuming a constant sedimentation rate within a biozone) following to the last International Stratigraphic Chart (ICS; Cohen *et al*., 2013) and recalibrated according to the last used geochemical standards (Lécuyer *et al*., 1996; Pucéat *et al*., 2010). The third step was to use the compiled $\delta^{18}O$ measurements and the $\delta^{18}O$ values taken from the major databases (Veizer *et al*., 1999; Trotter *et al*., 2008) as palaeothermometer using equations given by Pucéat *et al*. (2010) for conodont apatite material, by Lécuyer *et al*. (1996) for inarticulate brachiopod phosphatic shell, and by Kim and O'Neil (1997) for articulate brachiopod carbonate shell. Major uncertainty concerns the reconstruction of the $\delta^{18}O_{sw}$ (Veizer *et al*., 1997; Wallmann 2001; Jaffrés *et al*., 2007; Nardin *et al*., 2011). In this study four hypotheses have been considered: 1) $\delta^{18}O_{sw}$ varying from -1 (ice-free world) and 0 (iced world); based on the quaternary values (Duplessy *et al*., 2002), 2) $\delta^{18}O_{sw}$ varying from -1 (ice-free world) and 0 (iced world) extended to 1 for the late Ordovician-early Silurian glacial peak; based on the quaternary values (Duplessy *et al*., 2002), 3) $\delta^{18}O_{sw}$ varying through time according to the reconstructed values from the Δ47 measures (Finnegan *et al*., 2011; Rosenau *et al*., 2012), and 4) $\delta^{18}O_{sw}$ varying through time according to the modelled values from Wallmann (2001). Databases built on conodont apatite, articulate brachiopod carbonate and inarticulate brachiopod phosphate were analysed independently and then compared.

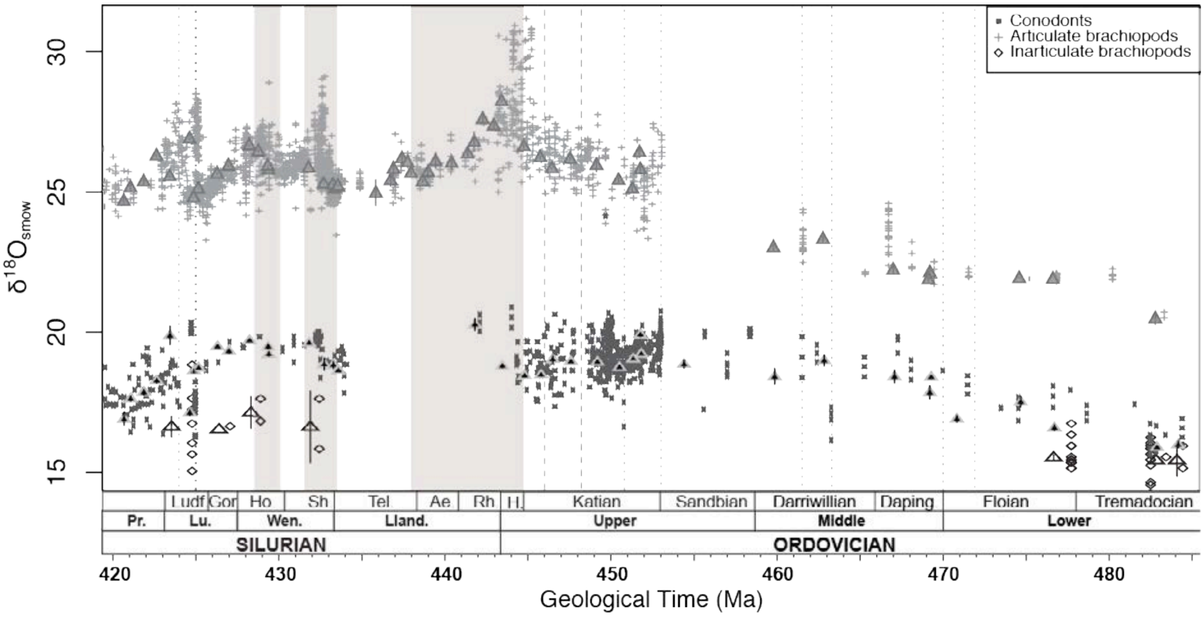

Fig. 1: **Distribution of the $\delta^{18}O$ measures on conodont apatite, inarticulate brachiopod phosphatic and articulate brachiopod carbonate shells through the Early Palaeozoic. Are superimposed the median values per biozone for each category. Are drawn in grey the glacial phases recorded in the sedimentologic record, in loosely dotted lines, the Boda Event, and in contracted dotted lines, the hypothetic cold episodes inferred from $\delta^{13}C$ and/or from sea-level falls.**

The analysis of the geographic distribution of sampling sites show that most of them were located in the tropical zone trough the whole study period. $\delta^{18}O$ data compiled for this study match in the timing and the amplitude with the databases of Veizer *et al*. (1999) and Trotter *et al*. (2008). Preliminary results on the compiled databases confirm the increase of $\delta^{18}O$, from the Tremadocian to the Dapingian for the $\delta^{18}O_{phos}$ signal and to the late Katian for the $\delta^{18}O_{carb}$ signal (Fig. 1). Both signals reach a plateau, which is interrupted by positive peaks in the Hirnantian-low Rhuddanian, the early-middle Sheinwoodian, the middle Homerian and the early Ludfordian for both signals. Those peaks are registered in all categorized environments. The identified peaks seem to confirm most of the inferred glacial or cold periods, even those with no sedimentologic record. However the long increase of both signals in the Lower and Middle Ordovician does not reflect the hypothetic cold episodes in the late Floian and the early Darriwilian (Turner *et al*., 2011, 2012). The supposed warm Boda Event is not highlighted in the compiled isotopic signals (Fig. 1).

Strong discrepancies have been detected between the temperatures calculated from the $\delta^{18}O_{carb}$ (articulate brachiopods) and from the $\delta^{18}O_{phos}$ (conodont and inarticulate brachiopods) for the Early-Middle Ordovician (from 20 to 10°C through time), whatever the assumption on the $\delta^{18}O_{sw}$. For instance, using the first assumption on the $\delta^{18}O_{sw}$ (Duplessy *et al*., 2002), temperature calculated with the $\delta^{18}O_{carb}$ decrease from 65°C to 50°C while those calculated with the $\delta^{18}O_{phos}$ decrease from 45°C to 35°C. Then the three signals are more consistent from the Darriwilian to the Pridoli, giving between 30 and 45°C for tropical SST with slight decreases of few degrees during the inferred cold periods.

Several questions rise from the present results. Inarticulate brachiopods are expected to represent semi-endobenthic fauna living near shore whereas articulate brachiopods typify epibenthic fauna living on shallow to deep-water platform. Conodont animals were supposed to have a nektobenthic to pelagic mode of life in epicontinental seas (Rigo & Joachimski, 2010). Temperatures calculated from conodont apatite $\delta^{18}O$ should therefore be higher than those calculated from brachiopod $\delta^{18}O$. Temperatures reconstructed from conodont and inarticulate brachiopods are homogeneous and lower than temperatures reconstructed from articulate brachiopods, using the same $\delta^{18}O_{sw}$ during the Ordovician period. Therefore the reconstructed values might not reflect temperature through the water column but they might be tied to the type of material used when measuring $\delta^{18}O$. Reconstructed Early-Mid Ordovician $\delta^{18}O_{carb}$ and $\delta^{18}O_{phos}$ temperatures using $\delta^{18}O_{sw}$ =-1 are far too high to allow normal marine life (Ross, 1995). In addition to inevitable diagenetic influence on the $\delta^{18}O$ measurements, the hypotheses on the $\delta^{18}O_{sw}$ may be not representative of the early Phanerozoic Earth system. Similar calculations with $\delta^{18}O_{sw}$=-3 suggest more 'reasonable' temperatures ranging between 45°C and 35°C ($\delta^{18}O_{carb}$) and between 40°C and 30°C ($\delta^{18}O_{phos}$) for the Early-Middle Ordovician period. This confirms previous discussions about the reconstruction of the $\delta^{18}O_{sw}$ (Veizer *et al*., 1997; Wallmann, 2001; Jaffrés *et al*., 2007) and the need of further studies.

References

Azmy K., Veizer J., Bassett M.G. & Copper P. (1998). Oxygen and carbon isotopic composition of Silurian brachiopods: implications for coeval seawater and glaciations. *Geological Society of America Bulletin*, 110: 1499–1512.

Boucot A.J., Xu C. & Scotese C.R. (2004). Phanerozoic climatic zones and paleogeography with a consideration of atmospheric CO_2 level: *Paleontological Journal*, 38: 115–122.

Brand U., Azmy K. & Veizer J. (2006). Evaluation of the Salinic I tectonic, Cancaniri glacial and Ireviken biotic events: Biochemostratigraphy of the Lower Silurian succession in the Niagara Gorge area, Canada and U.S.A. *Palaeogeography, Palaeoclimatology, Palaeoecology*, 241: 192–213.

Buggisch W., Joachimski M.M., Lehnert O., Bergström S., Repetski J.E. & Webers G.F. (2010). Did intense volcanism trigger the first Late Ordovician icehouse? *Geology*, 38, 327–330.

Cohen K. M., Finney S. & Gibbard P.L. (2013). International Chronostratigraphic Chart v 2013/01. ICS.

Diaz-Martinez E. & Grahn Y. (2007). Early Silurian glaciation along the western margin of Gondwana (Peru, Bolivia and Northern Argentina): Palaeogeographic and geodynamic setting. *Palaeogeography, Palaeoclimatology, Palaeoecology*, 245: 62–81.

Duplessy J.-C., Labeyrie L. & Waelbroeck C. (2002). Constraints on the ocean oxygen isotopic enrichment between the Last Glacial Maximum and the Holocene: Paleoceanographic implications. *Quaternary Science Reviews*, 21: 315–330.

Finnegan S., Heim N.A., Peters S.E. & Fischer W.W. (2012). Climate change and the selective signature of the Late Ordovician mass extinction. *Proceedings of the National Academy of Sciences*, 109: 6829–6834.

Fortey R.A. & Cocks L.R.M. (2005). Late Ordovician global warming: The Boda event. *Geology*, 33: 405–408.

Ghienne J.-F., Le Heron D.P., Moreau J., Denis M. & Deynoux M. (2007). The Late Ordovician glacial sedimentary system of the North Gondwana platform. In: Hambrey M.J, Christoffersen P., Glasser N.F. & Hubbard B. (Eds), *Glacial Sedimentary Processes and Products.* International Association of Sedimentologists, Special Publications, 39: 295–319.

Jaffrés J.B.D., Shields G.A. & Wallmann K. (2007). The oxygen isotope evolution of seawater: A critical review of a long-standing controversy and an improved geological water cycle model for the past 3.4 billion years. *Earth-Science Reviews*, 83: 83–122.

Jeppsson L. & Aldridge R.J. (2000). Ludlow (late Silurian) oceanic episodes and events. *Journal of the Geological Society, London*, 157: 1137–1148.

Kaljo D., Kiipli T. & Martma T. (1997). Carbon isotope event markers through the Wenlock-Pridoli sequence at Ohesaare (Estonia) and Priekule (Latvia). *Palaeogeography, Palaeoclimatology, Palaeoecology*, 132, 211–223.

Kim S.-T. & O'Neil J.R. (1997). Equilibrium and nonequilibrium oxygen isotope effects in synthetic carbonates. *Geochimica et Cosmochimica Acta*, 64: 3461–3475.

Kozłowski W. & Sobień K. (2012). Mid-Ludfordian coeval carbon isotope, natural gamma ray and magnetic susceptibility excursions in the Mielnik IG-1 borehole (Eastern Poland) - Dustiness as a possible link between global climate and the Silurian carbon isotope record. *Palaeogeography, Palaeoclimatology, Palaeoecology*, 339-341: 74–97.

Lécuyer C., Grandjean P. & Emig C.C. (1996). Determination of oxygen isotope fractionation between water and phosphate from living lingulids: potential application to palaeoenvironmental studies. *Palaeogeography, Palaeoclimatology, Palaeoecology*, 126: 101–108.

Lehnert O., Männik P., Joachimski M.M., Calner M. & Frýda J. (2010). Palaeoclimate perturbations before the Scheinwoodian glaciation: a trigger for extinctions during the "Ireveken Event." *Palaeogeography, Palaeoclimatology, Palaeoecology*, 296: 320–331.

Loi A., Ghienne J.F., Dabard M.-P., Paris F., Botquelen A., Christ N., Elaoud-Debbaj Z., Gorini A., Vidal M, Vilet B. & Destombes J. (2010). The Late Ordovician glacio-eustatic record from a high-latitude storm-dominated shelf succession: The Bou Ingarf section (Anti-Atlas, Southern Morocco). *Palaeogeography, Palaeoclimatology, Palaeoecology*, 296: 332–358.

Nardin E., Goddéris Y., Donnadieu Y., Le Hir G., Blakey R.C., Pucéat E. & Aretz M. (2011). Modeling the early Paleozoic long-term climatic trend. *Geological Society of America Bulletin*, 123: 1181–1192.

Puceat E., Joachimski M.M., Bouilloux A., Monna F., Bonin A., Motreuil S., Mornières P., Hénard S., Mourin J., Dera G. & Quesnes D. (2010). Revised phosphate-water fractionation equation reassessing paleotemperatures derived from biogenic apatite. *Earth and Planetary Science Letters*, 298: 135–142.

Rigo M. & Joachimski M.M. (2010). Palaeoecology of Late Triassic conodonts: Constraints from oxygen isotopes in biogenic apatite. *Acta Palaeontologica Polonica*, 55: 471–478.

Rosenau N.A., Herrmann A.D. & Leslie S.A. (2012). Conodont apatite δ18O values from a platform margin setting, Oklahoma, USA: Implications for initiation of Late Ordovician icehouse conditions. *Palaeogeography, Palaeoclimatology, Palaeoecology*, 315-316: 172–180.

Ross D.A. (1995). Introduction to Oceanography. *Harper Collins College Publishers*. New York,

Saltzman M.R. & Young S.A. (2005). Long-lived glaciation in the Late Ordovician? Isotopic and sequence-stratigraphic evidence from Western Laurentia. *Geology*, 33: 109–112.

Samtleben C., Munnecke A. & Bickert T. (2000). Development of facies and C/O istopes in transects through the Ludlow of Gotland: evidence for global and local influences on a shallow-marine environment. *Facies*, 43: 1–38.

Trotter J.A., Williams I.S., Barnes C.R., Lecuyer C. & Nicoll R.S. (2008). Did Cooling Oceans Trigger Ordovician Biodiversification? Evidence from Conodont Thermometry. *Science*, 321: 550–554.

Turner B., Armstrong H.A. & Holt P. (2011). Visions of ice sheets in the early Ordovician greenhouse world: Evidence from the Peninsula Formation, Cape Peninsula, South Africa. *Sedimentary Geology*, 236: 226–238.

Turner B.R., Armstrong H.A., Wilson C.R. & Makhlouf I.M. (2012). High frequency eustatic sea-level changes during the Middle to early Late Ordovician of southern Jordan: Indirect evidence for a Darriwilian Ice Age in Gondwana. *Sedimentary Geology*, 251-252: 34–48.

Vandenbroucke T.R.A., Armstrong H.A., Williams A., Paris F., Zalaslewicz J.A., Sabbe K., Nolvak J., Challands T.J., Verniers J. & Servais T. (2010). Polar front shift and atmospheric CO2 during the glacial maximum of the Early Paleozoic icehouse. *Proceeding of the National Academy of Sciences USA*, 109: 14983–14986.

Veizer J., Ala D., Azmy K., Bruckschen P., Buhl D., Bruhn F., Carden G.A.F., Diener A., Ebneth S. & Goddéris Y. (1999). $^{87}Sr/^{86}Sr$, $\delta^{13}C$ and $\delta^{18}O$ evolution of Phanerozoic seawater. *Chemical Geology*, 161(1-3): 59-88.

Veizer J., Bruckschen P., Pawellek F., Diener A., Podlaha O.G., Carden G.A.F., Jasper T., Korte C., Strauss H., Azmy K. & Ala D. (1997). Oxygen isotope evolution of Phanerozoic seawater. *Palaeogeography, Palaeoclimatology, Palaeoecology*, 132: 159–172.

Wallmann K. (2001). The geological water cycle and the evolution of the d18O values. *Geochimica et Cosmochimica Acta*, 65: 2469–2485.

Wenzel B., Lécuyer C. & Joachimski M.M. (2000). Comparing oxygen isotope records of Silurian calcite and phosphate - δ18O composition of brachiopods and conodonts. *Geochimica et Cosmochimica Acta*, 64: 1859–1872.

Wheeley J.R., Smith M.P. & Boomer, I. (2012). Oxygen isotope variability in conodonts: implications for reconstructing Palaeozoic palaeoclimates and palaeoceanography. *Journal of the Geological Society*, 169: 239–250.

Žigaité Ž., Joachimski M.M., Lehnert O. & Brazauska A. (2010). $\delta^{18}O$ composition of conodont apatite indicates climatic cooling during the Middle Pridoli. *Palaeogeography, Palaeoclimatology, Palaeoecology*, 294: 242–247.

Isotopic and mineralogical evidence for atmospheric oxygenation in 2.76 Ga old paleosols

Pascal Philippot[1], Yoram Teitler[1], Martine Gérard[2], Pierre Cartigny[1], Elodie Muller[1], Nelly Assayag[1], Guillaume Le Hir[1], Frédéric Fluteau[1]

[1]Institut de Physique du Globe and Université Paris-Diderot, Sorbonne Paris Cité, 1 rue Jussieu, Paris, France
[2]Institut de Minéralogie et de Physique de la Matière Condensée, Univ Paris Jussieu, IRD, 75252 Paris, France

Recent chemical and isotopic data from Archean marine sediments indicates that alteration of continental surfaces have contributed a substantial fraction of the flux of redox-sensitive elements (S, Cr, Mo) to the ocean several hundreds of millions of years prior to the Great Oxidation Event (GOE; between 2.45 and 2.32 Ga). However, controversies regarding the factors controlling these deliveries have highlighted the problems of identifying a reliable proxy of continental surface alteration during the Archean. Unlike marine proxies, which are indirect climatic records, paleosols, which form at the atmosphere-lithosphere interface, can provide direct constraints on the weathering processes at the time of formation. Here we present new sulfur isotope and mineralogical data from the reference 2.76 Ga old Mount Roe Basalt paleosols at Whim Creek (Western Australia). The data are from new lithofacies that were not documented in previous studies. These lithofacies contain a Fe^{3+}-montmorillonite, calcite and sulfate mineralogical assemblage and display enrichments in Cr and Mo compared to the original basalt. Sulfur isotope analysis of microscopic sulfate inclusions preserved in Fe^{3+}-montmorillonite and calcite yielded $\delta^{34}S$, $\Delta^{33}S$ and $\Delta^{36}S$ values that are different from the field of mass independent (MIF) Archaean sulfates. $\Delta^{33}S$ values overlap the field of post-Archaean, mass dependent (MDF) terrestrial materials. In a $\Delta^{33}S$-$\Delta^{36}S$ diagram, sulfates plot away from the MIF slope ~-1 defined by Archaean samples and overlap the MDF slope of ~ -7 defined by post-2.32-Ga old sulfides. The large range of $\delta^{34}S$ (up to 20‰) between different samples indicates that S-isotope heterogeneities are preserved on a small scale. Such heterogeneities are best explained by repeated cycles of microbial sulfate reduction producing sulfides followed by the re-oxidation of sulfides into sulfates during oxidative weathering and/or microbial oxidation of microbially-derived ^{34}S-depleted sulfides. These results suggest that the concentrations of free oxygen in the Late Archaean climate system has increased, at least transiently, to levels similar to the GOE.

Orbitally forced sequences in the Lower Carboniferous and the onset of Carboniferous glaciations at the Tournaisian Viséan boundary

Edouard Poty, Bernard Mottequin, Julien Denayer

Unité de paléontologie animale et humaine, Université de Liège, Allée du 6 août, Bâtiment B18, Sart-Tilman, B 4000 Liège 1, Belgium. E-mail: e.poty@ulg.ac.be; bmottequin@ulg.ac.be; julien.denayer@ulg.ac.be

Investigations realized in the Belgian Tournaisian and Viséan to record the sedimentary cycles allowed to the recognition of eustatic third-order cycles (Hance *et al*., 2002), which were later extended to Poland and South China. Most of them could correspond to excentricity cycles, of about 2.4 Ma (Poty *et al*., 2013). Shorter cycles were also recognized and differences in their nature and stratigraphic distribution were enhanced. The Lower Tournaisian (Hastarian substage) and the lower part of the Upper Tournaisian (Ivorian substage) show only short cycles, not grouped in bundles, considered as due to only one orbital parameter corresponding to precession cycles (Poty *et al*., 2013). They correspond to alternations in monsoon and dryer climates, without strong marked changes in the sea level. Similar cycles are recognized in the rest of the Upper Tournaisian.

The latest Tournaisian third-order sequence (sequence 4 of Hance *et al*., 2002) is characterized by a very high high-stand system tract, and a flooding of lowlands previously emerged (« Avins event » of Poty, 2007). This very high-sea level caused good connections between marine basins, and thus favours the widespread of foraminifers, brachiopods and corals, through Australia, Japan, China, and the rest of Eurasia. Its falling stage systems tract is characterized by a very strong fall in the sea-level and is considered as corresponding to the development of an ice-cap and to a heralding change to the Carboniferous climate with glaciations. This low sea-level persisted during the earliest Viséan, and the third-order sequence 5 of Hance *et al*. (2002) never reached the shallow marine platforms previously covered by the latest Tournaisian sea. It is from the base of this third-order sequence 5 that a marked fourth (obliquity) and/or fifth-order (eccentricity) cyclicity developed. These latter sequences are the same than the ones recorded in the Middle (Livian substage) and the Upper Viséan (Warnantian substage). The transition between the Tournaisian monsoon climate and the Viséan climate with glaciations is well documented in sections in the Dinant vicinity where the Tournaisian precession cycles passe to eustatic obliquity-excentricity cycles.

Therefore, it can be concluded that the onset of the Carboniferous glaciations is as early as the Early Viséan and not in the Late Viséan as usually considered.

References

Hance L., Poty E., & Devuyst F.X. (2002). Sequence stratigraphy of the Belgian Lower Carboniferous - tentative correlation with the British Isles. In: Hills L.V., Henderson C.M. & Bamber E.W. (Eds), *Carboniferous and Permian of the World.* Memoir Canadian Society of Petroleum Geologists, 19: 41-51.

Poty E. (2007). The Avins event: a remarkable worldwide spread of corals at the end of the Tournaisian (Lower Carboniferous). In: Hubmann B. & Piller W.E. (Eds), *Fossil corals and sponges; Proceedings of the 9th International Symposium on Fossil Cnidaria and Porifera, Graz 2003*. Schriftenreihe der Erdwissenschaftlichen Kommissionen, Österreichische Akademie der Wissenschaften, 17: 231-249.

Poty E., Mottequin B. & Denayer J. (2013). An attempt of time calibration of the Lower Tournaisian (Hastarian Substage) based on orbitally forced sequences. In: International Field Symposium « The Devonian and Lower Carboniferous of northern Gondwana ». Abstract Book. *Document de l'Institut Scientifique, Rabat*, 26: 105-107.

Climate sensitivity in the pre-Cenozoic world

Christopher J. Poulsen, Richard P. Fiorella

Dept. of Earth and Environmental Sciences, 3026 C.C. Little Building, University of Michigan, Ann Arbor, MI 48109, U.S.A.; E-Mail: poulsen@umich.edu

Earth's climate sensitivity—a measure of the equilibrium response of Earth's temperature to a change in radiative forcing—has received considerable attention because of its implications for future climate (e.g. IPCC, 2007). In the context of modern climate change, climate sensitivity has generally been restricted to the response of fast feedbacks (i.e. water vapor, sea ice, clouds, upper ocean) in the Climate system. The full climate sensitivity, referred to as Earth system sensitivity, has been recognized to also include slow feedbacks (i.e. ice sheets, deep ocean, vegetation, geochemical cycles) and can be Substantially greater than the sensitivity based solely on fast feedbacks (e.g. Hansen *et al*., 2008; Lunt *et al*., 2009; Pagani *et al*., 2009). In theory, reconstructions of coeval temperature and CO_2 can provide an estimate of Earth system sensitivity and have been used to argue for high sensitivities in the past (Royer *et al*., 2012).

Whether these estimates are relevant to the modern climate system is largely unknown since there is little understanding of how climate sensitivity has varied through Earth history. In theory, palaeoclimate simulations may provide some insights into this issue (e.g. Donnadieu *et al*., 2006); however, few systematic analyses of climate sensitivity have been conducted and published results are often difficult to compare due to differences between andincomplete reporting of boundary conditions. An exception to this is studies of snowball Earth initiation, which have tended to systematically explore broad ranges of boundary conditions (e.g. Poulsen *et al*., 2001; Poulsen, 2004; Voigt and Marotzke, 2009; Abbot *et al*., 2011; Yang *et al*., 2012).

In this contribution, we report on a suite of experiments conducted using NCAR's CAM3.1 to explore the role of geography on snowball Earth initiation (Fiorella and Poulsen, submitted). We test four different continental arrangements: (a) an aquaplanet with no land (AQP), (b) an equator-centered rectangular supercontinent extending to 43°N/S and spanning 130 degrees in longitude (hereafter RECT), (c) a Marinoan (~635 Ma) continental reconstruction with two large tropical continents (hereafter MAR), and (d) modern continental configuration with topography removed (hereafter MOD-NT). For each experiment, either the total solar irradiance relative to modern (TSI; with fixed CO_2 of 280 ppm) or atmospheric CO_2 level (with TSI of 94%) is reduced until ice covers Earth's surface.

Our results indicate that initiation of a snowball Earth in CAM3.1 is highly sensitive to prescribed geography and occurs at approximately 91 (AQP), 87 (MOD), 85 (MAR), and 84% (RECT) solar luminosity or, if solar luminosity is fixed, at approximately 25 (AQP), 1 (MOD), and <0.1 ppmv CO2 (MAR, RECT) (Fig. 1). In these experiments, the climate sensitivity varies because continental configuration alters the partitioning of energy within the climate system. In the absence of land, the AQP simulation has higher cloud fractions and greater verticallyintegrated specific humidity. Though the surface initially has lower albedo, it receives less energy from direction radiation and is more reliant on greenhouse forcing. As radiative forcing is reduced through a decrease in TSI or CO_2 in the AQP simulation, greenhouse forcing decreases nonlinearly with temperature, giving rise to high climate sensitivity. In contrast, geographies (MAR, RECT) with large tropical landmasses receive higher net shortwave radiation at the surface despite a higher surface albedo because of the near absence of clouds over landmasses. In addition, land-ocean thermal contrasts drive strong circulations that work to saturate the marine boundary layer. As a result of these differences, climate sensitivity is substantially lower.

To substantiate our findings, we also quantify feedback strengths in these simulations using the radiative kernel method (Soden *et al*., 2008). This analysis indicates that water vapor and albedo feedbacks dominate the response to radiative forcing and vary across the four simulations and as a function of radiative forcing. In sum, our results demonstrate that climate sensitivity can be affected by atmospheric dynamics, varies with mean climate state, and is likely to have changed through Earth history due to continental drift and other factors.

Following on these initial results, we are developing (and intend to present) a second suite of simulations that quantify the role of Paleozoic and Mesozoic palaeogeography on climate sensitivity to variations in atmospheric CO_2 and surface conditions including vegetation and topography. If our initial simulations are

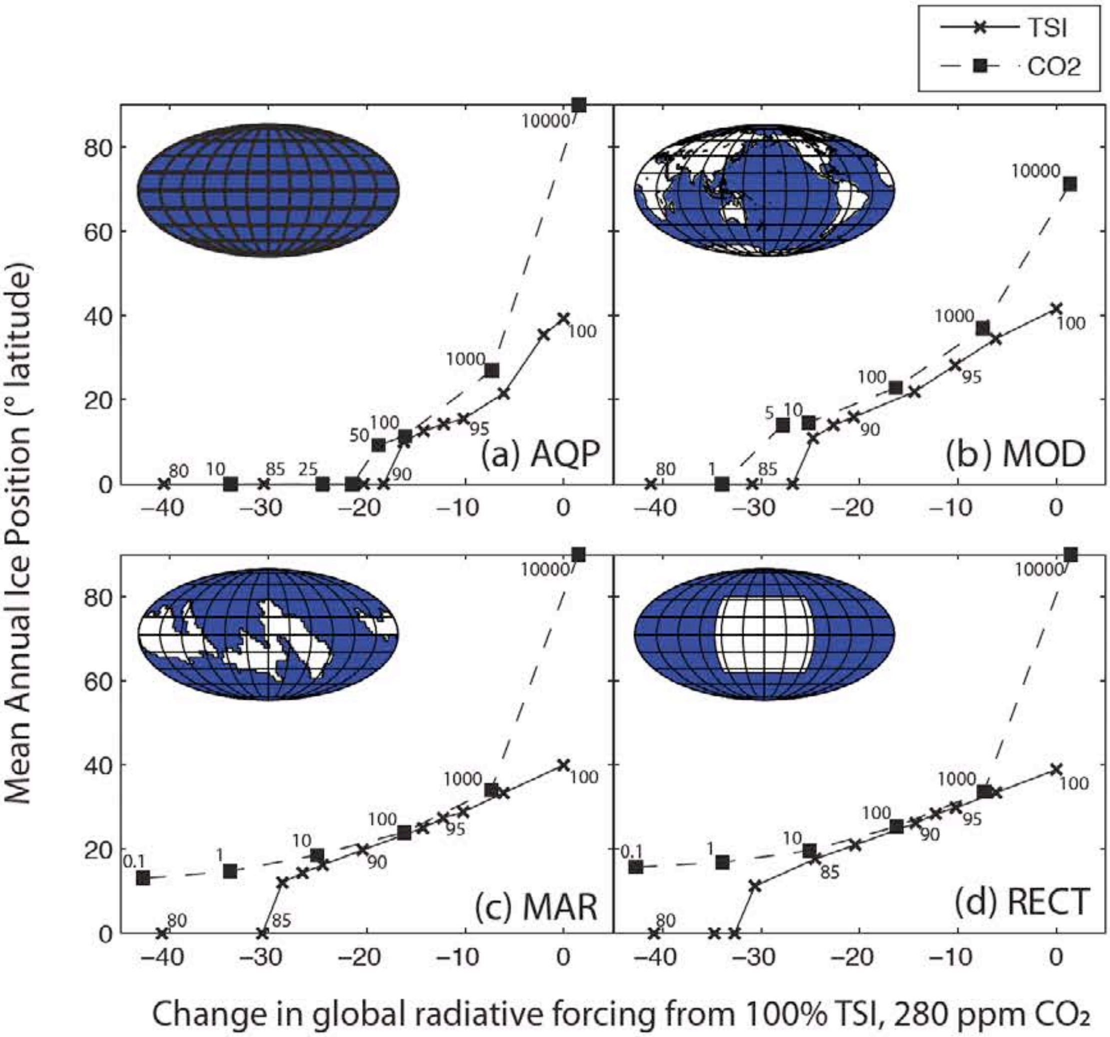

Fig. 1: **Comparison of annual ice line position as a function of geography (a-d) and radiative forcing (Wm^{-2}). Direct comparison of CO2 and TSI forcing is facilitated by calculating change in radiative forcing from a common reference simulation (with 100% TSI and 280 ppm CO_2) for each geography. Note that (a) the climate response to changes in radiative forcing varies as a function of geography; and (b) for the same global forcing, snowball states are more readily simulated with reductions in TSI than CO_2, a trend which is principally related to differences in the distribution of radiative forcing.**

representative, we expect that climate sensitivity has varied through the Phanerozoic as a function of both palaeogeography and mean climate state. This work will lead to a fuller recognition of the variability and evolution of climate sensitivity through Earth history.

References

Abbot D.S., Voigt A. & Koll D. (2011). The Jormungand global climate state and implications for Neoproterozoic glaciations. *Journal Geophysical Research*, 116(D18): D18103, doi:10.1029/2011JD015927.

Donnadieu Y., Pierrehumbert R., Jacob R., & Fluteau F. (2006). Modelling the primary control of paleogeography on Cretaceous climate. *Earth and Planetary Science Letters*, 248(1-2): 426–437, doi:10.1016/j.epsl.2006.06.007.

Hansen J., Sato M., Kharecha P., Beerling D., Berner R., Masson-Delmotte V., Pagani M., Raymo M., Royer D. & Zachos J. (2008). Target atmospheric CO_2: Where should humanity aim? *Open Atmospheric Science Journal*, 2(15): 217–231.

Lunt D.J., Haywood A.M., Schmidt G.A., Salzmann U., Valdes P.J. & Dowsett H.J. (2009). Earth system Sensitivity inferred from Pliocene modelling and data. *Nature Geoscience*, 3(1): 60–64, doi:10.1038/ngeo706.

Pagani M., Liu Z., Lariviere J. & Ravelo A.C. (2009). High Earth-system climate sensitivity determined from Pliocene carbon dioxide concentrations. *Nature Geoscience*, 3(1): 27–30, doi:10.1038/ngeo724.

Poulsen C.J. (2004). Factors that inhibit snowball Earth simulation. *Paleoceanography*, 19(4): 11, doi:10.1029/2004PA001056.

Poulsen C.J., Pierrehumbert R.T. & Jacob, R.L. (2001). Impact of ocean dynamics on the simulation of the Neoproterozoic "snowball Earth", *Geophysical Research Letters*, 28(8): 1575-1578.

Royer D.L., Pagani M. & Beerling D.J. (2012). Geobiological constraints on Earth system sensitivity to CO2 during the Cretaceous and Cenozoic. *Geobiology*, 10(4), 298–310: doi:10.1111/j.1472-4669.2012.00320.x.

Soden B.J., Held I.M., Colman R., Shell K.M., Kiehl J.T. & Shields C.A. (2008). Quantifying Climate Feedbacks using radiative Kernels. *Journal of Climate*, 21(14): 3504–3520, doi:10.1175/2007JCLI2110.1.

Voigt A., & Marotzke J. (2009). The transition from the present-day climate to a modern Snowball Earth. *Climate Dynamics*, 35: 1–19, doi:10.1007/s00382-009-0633-5.

Yang J., Peltier W.R. & Hu Y. (2012). The Initiation of Modern "Soft Snowball" and 'Hard Snowball' Climates in CCSM3. Part I: The Influences of Solar Luminosity, CO_2 Concentration, and the Sea Ice/Snow Albedo Parameterization. *Journal of Climate*, 25(8): 2711–2736, doi:10.1175/JCLI-D-11-00189.1.

The Aptian evaporites of the central segment of the South Atlantic: geodynamic context and climatic implications

Cécile Robin[1], Anne-Claire Chaboureau[1,2,3], François Guillocheau[1], Yannick Donnadieu[2], Sébastien Rohais[3]

[1]Géosciences Rennes – UMR6118, Université de Rennes 1, Campus de Beaulieu, 263 av. du Général Leclerc, Rennes 35042 Cedex, France; E-Mail: cecile.robin@univ-rennes1.fr, francois.guillocheau@univ-rennes1.fr, anne-claire.chaboureau@lsce.ipsl.fr
[2] Laboratoire des Sciences du Climat et de l'Environnement, CNRS-CEA, CEA Saclay, Orme des Merisiers, Bat. 701, 91191 Gif-sur-Yvette Cedex, France; E-Mail: yannick.donnadieu@lsce.ipsl.fr
[3]IFP Energies nouvelles, 1 et 4 Avenue de Bois-Préau, 92852 Rueil-Malmaison, France; E-Mail: sebastien.rohais@ifpen.fr

For a long time, evaporitic sequences have been interpreted as indicative of an arid climate. Such systematic interpretations led to the suggestion that the Central segment of the South Atlantic (20–0° S) was characterized by an arid climate during the upper Aptian. Indeed, synchronous to this period that corresponds to the rifting and to the opening of this part of the South Atlantic, a large evaporitic sequence spreads out from the equator to 20°S.

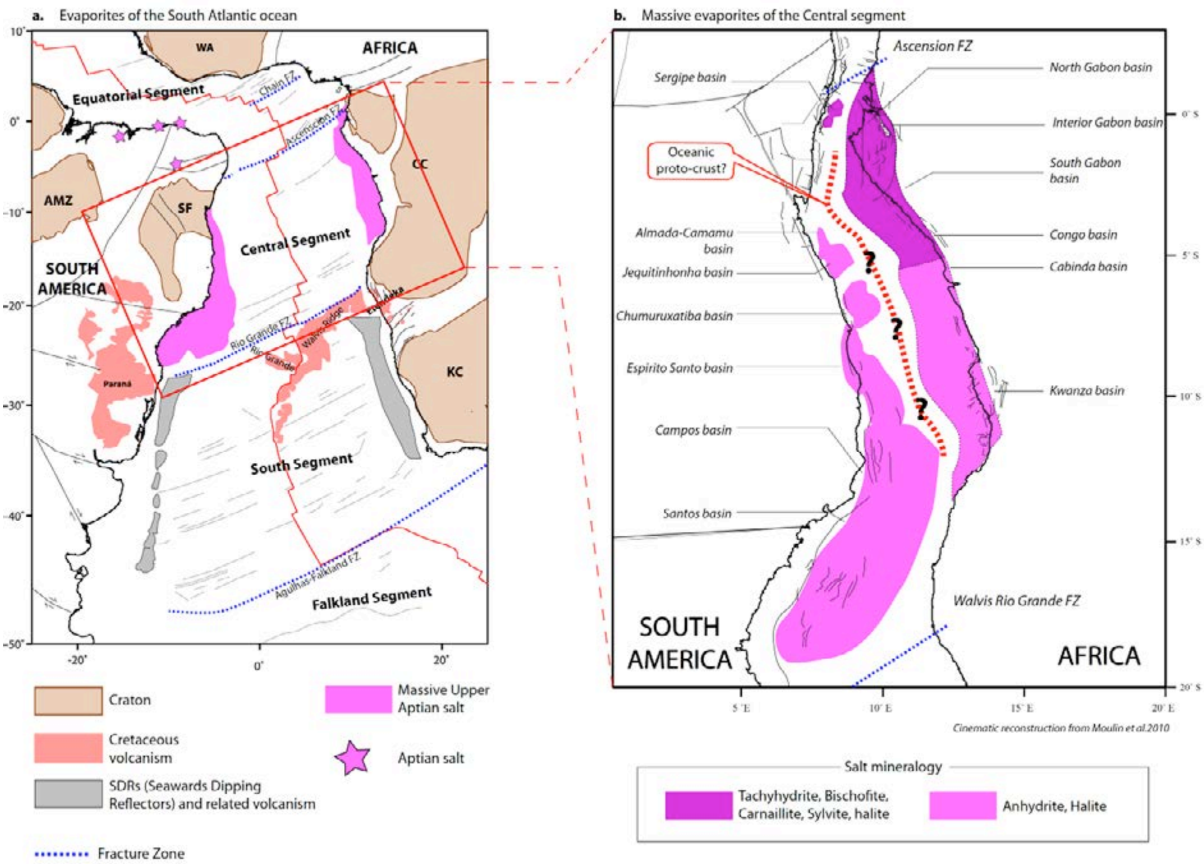

Fig. 1: **(a) Location of the Central segment and the salt sequence along the Brazilian and African margin (WA, West Africa Craton; CC, Congo Craton; KC, Kalahari Craton; AMZ, Amazonia Craton; SF, Sao Francisco Craton; FZ, Fracture Zone); (b) Mineralogy of the massive evaporites in the Central segment, at time of filing, (Chaboureau *et al*., 2012a)**

This observation raises majors questions: what was the incidence of the rifting on the climate? And what were the roles of these two processes on the sedimentary dynamic and particularly during the salt deposit? In this purpose a numerical modeling approach was chosen and three major steps were followed: (1) paleogeographic synthesis, (2) climate modeling, and (3) stratigraphic modeling. The geodynamic processes that control the opening of the central segment of the South Atlantic Ocean (between the Walvis Ridge and the Ascension FZ) are debated. We discuss the timing of the sedimentary and tectonic evolution of the Early Cretaceous rift by drawing eight palaeogeographic and geodynamic maps from the Berriasian to the Middle-Late Aptian, based on a biostratigraphic (ostracodes and pollen) chart recalibrated on absolute ages (chemostratigraphy, interstratified volcanics, Re-Os dating of the organic matter). The central segment of the South Atlantic is composed of two domains, with a two phases evolution of the pre-drift ("rifting") times (Chaboureau *et al*., 2012a): a rift phase, characterized by tilted blocks and growth strata, followed by a sag basin (Fig. 2). The southern domain includes the Namibe, Santos and Campos Basins.

The northern domain extends from the Espirito Santo and North Kwanza Basins, in the south, to the Sergipe-Alagoas and North Gabon Basins to the north. Extension started in the northern domain during the Late Berriasian (Congo-Camamu Basin to the Sergipe-Alagoas-North Gabon Basins) and migrated southward. At that time, the southern domain was not a subsiding domain (emplacement of the Parana-Etendeka Trapp). Extension started in this southern domain during the Early Barremian (Fig. 2). The rift

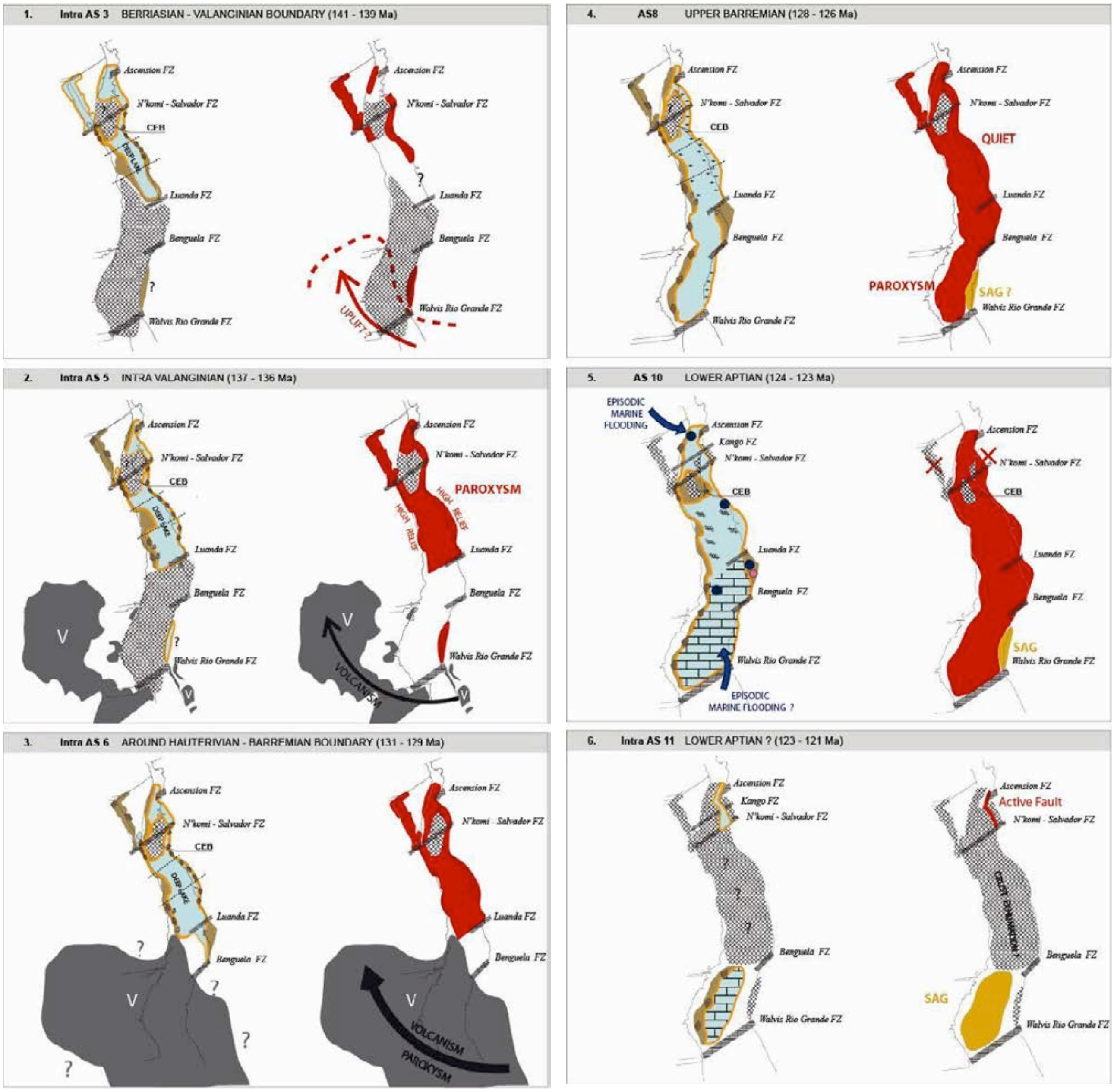

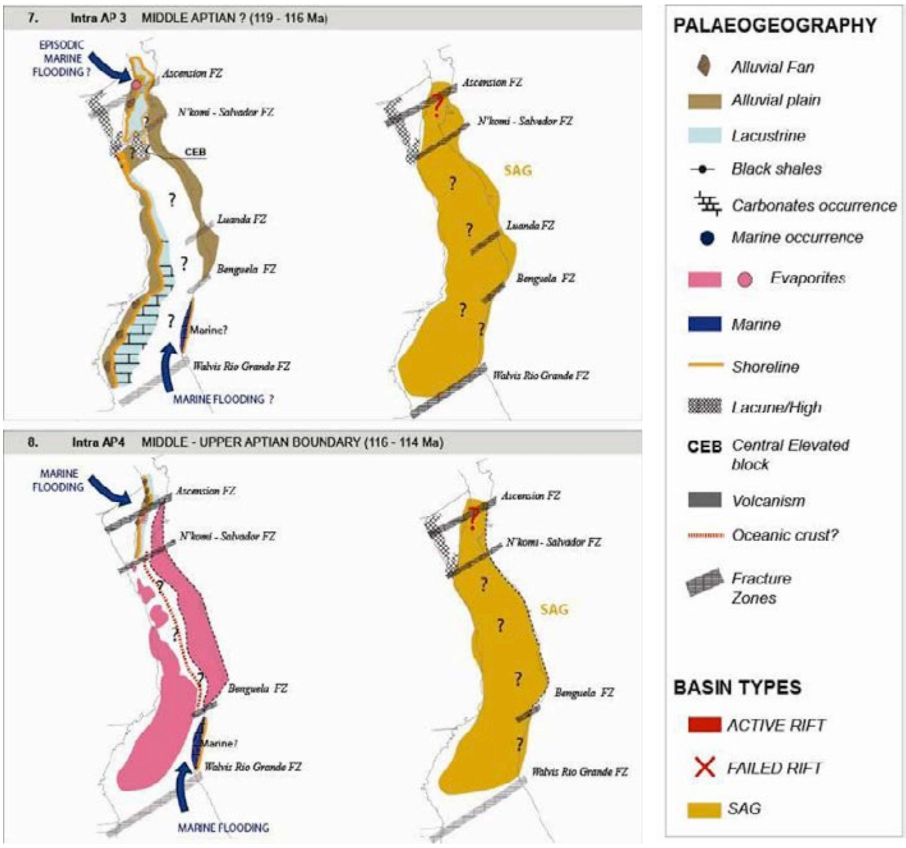

Fig. 2: **Summary palaeogeographic and geodynamic maps in eight stages from the Berriasian-Valanginian boundary (intra ostracode biozone AS3) to the Middle-Upper Aptian boundary (intra biozone AP4) (Chaboureau *et al.*, 2012a).**

phase is shorter in the south (5-6 Ma, Barremian to base Aptian) than in the north (19 to 20 Myr, Upper Berriasian to base Aptian). The sag phase is of Middle to Late Aptian age. In the northern domain, this transition corresponds to a hiatus of Early to Middle Aptian age. From the Late Berriasian to base Aptian, the northern domain evolves from a deep lake with lateral highs to a shallower organic-rich one with no more highs. The lake migrates southward in two steps, until the Valanginian at the border between the northern and southern domains, until the Early Barremian, north of Walvis Ridge.

Using the fully ocean atmosphere coupled model FOAM, we test the potential for the Aptian geography to produce an arid area over the Central segment. Sensitivity to the altitude of the rift shoulders separating the Africa and the South America cratons, to the water depth of the Central segment and to the drainage pattern have been performed. Using seawater salinity as a diagnostic, our simulations show that the southern part of the Central segment is characterized by very high salinity in the case of catchment areas draining the water out of the Central segment. Conversely, whatever the boundary conditions used, the northern part of the Central segment remains humid and salinities are very low. Hence, we conclude that the evaporites deposited in the southern part of the Central segment may have been controlled by the climate favouring aridity and high saline waters (Fig. 3). In contrast, the evaporites of the northern part can hardly be reconciled with the climatic conditions occurring there and may be due to hydrothermal sources (Chaboureau *et al.*, 2012b). Our interpretations are in agreement with the gradient found in the mineralogical compositions of the evaporites from the North to the South, i.e. the northern evaporites are at least 4 times more concentrated than the southern one.

Finally, stratigraphic modeling revealed the importance of taking into account (1) of this seasonality pattern and (2) of the paleogeography of the Central segment. The interaction between the three thematic has clarified the importance of the control factors for the formation of evaporites. Thus, (1) the climate played a major role in providing favorable climatic conditions due to the seasonnality, but (2) the rift has been the primary control factor by allowing a subsidence for marine connection and income of salt for deposition of evaporites in a restricted basin.

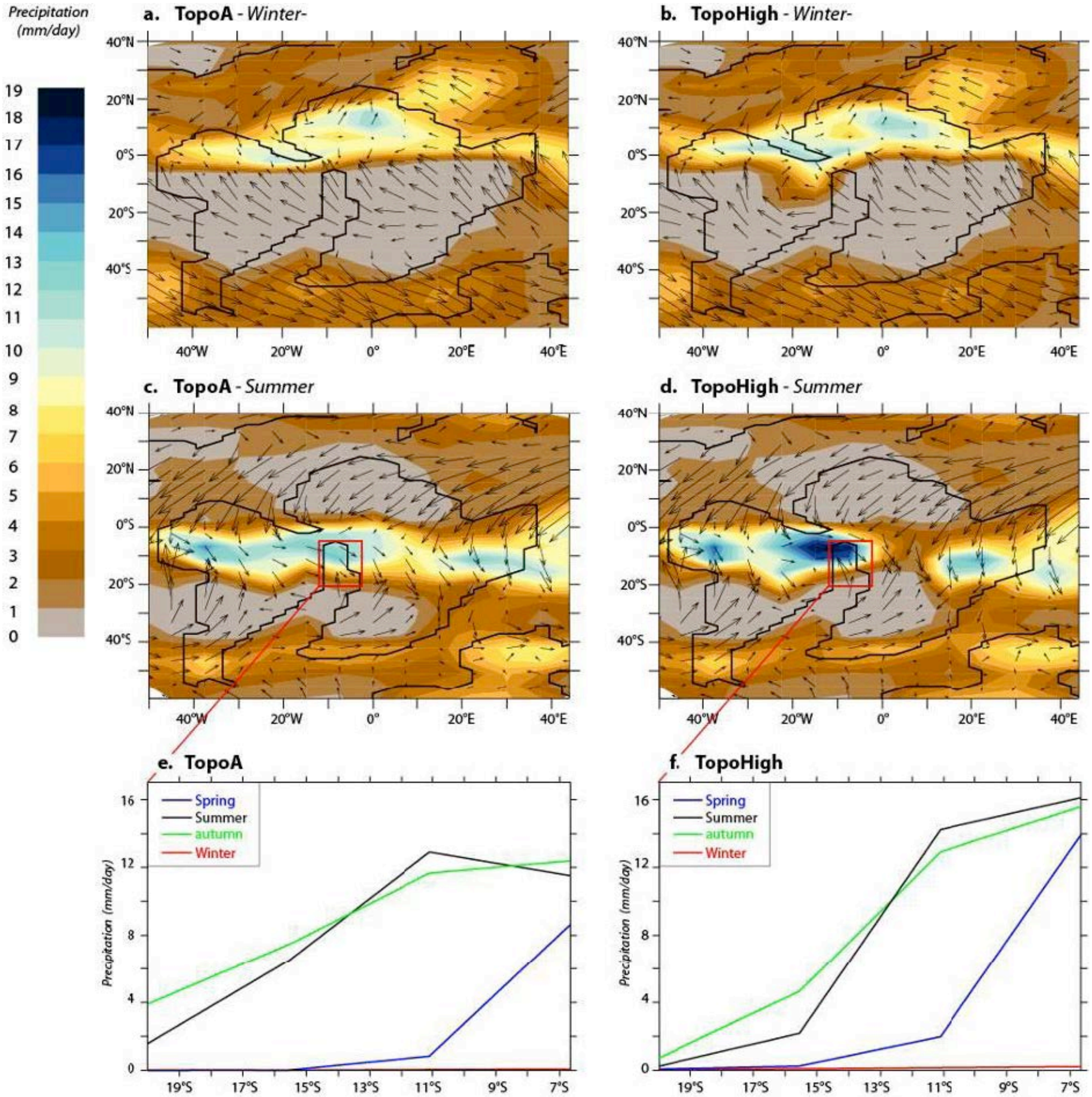

Fig. 3: **Seasonal average precipitations (mm.day-1). a) for the TopoA in austral winter (DJF); b) for the TopoHigh in austral Winter; c) for the TopoA in austral summer (JJA); d) for the TopoHigh in austral summer. Latitudinal evolution of the seasonal average precipitation (mm.day-1) in the Central segment (between 10° W and 5°W) e) for the TopoA and f) for the TopoHigh (Chaboureau *et al.*, 2012b).**

References

Chaboureau A.-C., Guillocheau F., Robin C., Rohais S., Moulin, M. & Aslanian D. (2012a). Paleogeographic evolution of the central segment of the South Atlantic during Early Cretaceous times: Paleotopographic and geodynamic implications. *Tectonophysics*, in Press.

Chaboureau A.-C., Donnadieu Y., Sepulchre P., Robin C., Guillocheau F. & Rohais S. (2012b). The Aptian evaporites of the South Atlantic: a climatic paradox? *Climate of the Past*, 8: 1047-1058.

Pre-Cenozoic atmospheric CO_2: some new developments with proxies and the long-term carbon cycle model GEOCARB, and implications for climate sensitivity

Dana L. Royer

Department of Earth and Environmental Sciences, Wesleyan University, Middletown, Connecticut 06459, USA; E-Mail: droyer@wesleyan.edu

The last thirty years have witnessed an explosion in the amount of information regarding the atmospheric CO_2 content during the pre-Cenozoic. Multiple long-term carbon cycle models of ever increasing sophistication have been established for estimating paleo- CO_2, and multiple proxies have been developed that, to date, have provided nearly 400 independent estimates of atmospheric CO_2 for the pre-Cenozoic. I focus here on three recent advances: a new CO_2 proxy appropriate for the pre-Cenozoic based on stomatal geometry and $\delta^{13}C$; new constraints on the uncertainty of CO_2 estimates from the long-term carbon cycle model GEOCARB; and inferences of high climate sensitivity to CO_2 during both glacial and non-glacial times. Estimates of atmospheric CO_2 concentration for the Phanerozoic Eon are based on a variety of proxies, but quantitative reconstructions for the pre-Cenozoic come overwhelmingly from one approach, the $\delta^{13}C$ of pedogenic carbonate. One proxy for reconstructing CO_2 during the late Cretaceous and Cenozoic relies on an empirical relationship between stomatal distributions and CO_2, but estimates are unbounded above ~500-1000 ppm and are limited to only a handful of calibrated species. A related stomatal ratio approach can be readily applied to pre-Cenozoic fossils, but the CO_2 estimates are semi-quantitative at best. A new approach has been developed for estimating paleo- CO_2 using the well-validated equation for leaf gas exchange: $c_a = A / (g_c \times [1 - c_i/c_a])$, where c_a = atmospheric CO_2 (µmol mol^{-1}), c_i= leaf intercellular CO_2 (µmol mol^{-1}), A = photosynthetic rate (µmol m^{-2} s^{-1}), and g_c = total operational conductance to CO_2 diffusion from the atmosphere to sites of photosynthesis within the leaf (mol m^{-2} s^{-1}). c_i/c_a can be estimated from the carbon isotopic fractionation between atmospheric CO_2 and the leaf, g_c from stomatal size and density, and A from extant analogs. This mechanistic approach avoids the unbounded errors in extrapolative methods and is applicable to most fossil material bearing stomata, therefore opening up much of the 400 Myr paleobotanical record for analysis. The new approach, validated against direct measurements and ice core records, produces CO_2 estimates for the Phanerozoic that are in close agreement with most recent reconstructions, but with typically less uncertainty. Critically, this method presents the opportunity to rapidly generate many pre-Cenozoic CO_2 estimates: all that is required are simple measurements of stomatal geometry and density, the $\delta^{13}C$ of leaf tissue and paleoatmosphere, and some basic physiological metrics from an extant member of the same order or family as the fossil material.

The long-term carbon cycle model GEOCARB is widely used to estimate atmospheric CO_2 levels during the Phanerozoic. Input parameters in GEOCARB are either time dependent (e.g., seafloor spreading rates; marine carbonate $\delta^{13}C$) or assumed to be time invariant (e.g., activation energy for silicate mineral dissolution; rate of chemical weathering by gymnosperms relative to angiosperms). Bob Berner, the model's author, assessed the sensitivity on estimated CO_2 of each time-dependent variable by comparing a standard model run with one where the variable remains fixed at its present-day value; the sensitivity of each time-invariant constant was quantified by running the model with several value choices across its likely range. The combined effect of uncertainty in all parameters on estimated CO_2 was gauged qualitatively by expert knowledge; these errors were hand-drawn on figures and considered "best guesses". In an effort to better quantify the uncertainty in CO_2 estimates from the GEOCARB model, a Monte Carlo resampling framework was used to produce more realistic distributions of estimated CO_2 based on variance in input parameters both singly and in combination. In support of Berner's earlier interpretations, uncertainties in estimated CO_2 are most sensitive to our current knowledge of variance in seafloor spreading rates and the effect of vascular plants on chemical weathering rates. Relative to the last sensitivity analysis by Berner (for the GEOCARBIII model), uncertainties here are better constrained for the Paleozoic but less constrained for the Mesozoic. Critically, a synthesis of CO_2 proxy data match well with the GEOCARB simulations, boosting confidence that our general knowledge of Phanerozoic CO_2 is reasonably secure. A striking pattern over the last decade is that CO_2 estimates from both proxies and the GEOCARB model have come down, especially those during hothouse times (and this includes estimates from the new stomatal-based method already presented). There is scant evidence, for example, for CO_2 levels exceeding 1500 ppm during much of the Mesozoic. In contrast, paleotemperature records have largely remained the same or (especially for the tropics) warmed up. This makes explaining these globally-warm times more difficult, and may imply a high long-term climate sensitivity to CO_2. Although both CO_2 and temperature records have appreciable uncertainty, a close scrutiny of these records points to long-term climate sensitivity sometimes exceeding 3°C for a CO_2 doubling, which is the benchmark value commonly assumed based on the analysis of present-day and near-present-day ("short-term") climate. It is not clear what factors were responsible for amplifying climate sensitivity above the canonical value during these globally-warm times, but it may be related to cloud dynamics and other trace greenhouse gases. During times with significant ice growth, which includes the Permo-Carboniferous, more compelling evidence exists for a long-term climate sensitivity exceeding 6°C. These interpretations come from analyzing Neogene climates as well as optimizing the fit for the Phanerozoic between GEOCARB and CO_2 proxies by adjusting the climate sensitivity input parameter in GEOCARB. The principal mechanism for amplifying climate sensitivity nearly two-fold is likely related to the ice-albedo feedback associated with continental ice sheets, an effect not considered by present-day global climate models. These calculations of long-term climate sensitivity are most appropriate for studies that integrate over long timescales (10^4+ yrs), and thus are appropriate for most geologic studies. Critically, the association of globally-warm temperatures with only moderately-elevated CO_2 levels has important implications for our long-term future.

On the reliability of paired carbon isotope as a p_{CO2} proxy in the Ediacarian Araras platform, Brazil

Pierre Sansjofre[1,2], Magali Ader[1], Ricardo I.F. Trindade[3], Alfonso C.R. Nogueira[4]

1 IPGP, Université Paris 7, France; correspondance: E-mail: ader@ipgp.fr
2 MCGill University, Monteral, Canada
3 IAG, Universidad de São Paulo, Brazil
4 Universidad federal Do Para, Brazil

The snowball Earth model accounts for many of the typical geological and geochemical features of the Marinoan glaciation deposits (~635Ma) and of their overlying cap carbonate (Hoffman *et al.*, 1998). Melting this snowball Earth would have required a massive increase of the atmospheric carbon dioxide content (pCO_2), which is consistent with Boron and Oxygen-isotope data (Kasemann *et al.*, 2005; Bao *et al.*, 2008). Recently however, we proposed instead a low atmospheric pCO_2 in the aftermath of the deglaciation (Sansjofre *et al.*, 2011). Our interpretation is based on paired carbon isotope data obtained on cap carbonates from Mirassol d'Oeste section (Ediacarian Araras platform, Brazil), together with previous results from cap carbonates of the Doushantuo Formation (South China) and Zhamoketi Formation (North China) (Jiang *et al.*, 2010; Shen *et al.*, 2008). All three data sets showed low $\Delta^{13}C_{carb\text{-}org}$ (= $\delta^{13}C_{carb}$ - $\delta^{13}C_{org}$) values of 23.6±0.8‰. We made the case that these anomalously low values are best interpreted as resulting from a decrease in the photosynthetic fractionation factor (ε_p), which can be related to an atmospheric pCO_2 lower than 3000 ppmv at the time of cap carbonate deposition.

Since then, we obtained new paired carbon isotope data for three other sections of the Araras platform in order to constrain further this interpretation. Tangara da Serra section represents an equivalent of the previously studied Mirassol d'Oeste section. It gives access to the upper part of the cap dolostone (Mirassol d'Oeste Formation) and the lower part of the cap limestone (Guia Formation) both deposited in relatively shallow waters. The results obtained on this section are consistent with those previously obtained for Mirassol d'Oeste section in that they show low $\Delta^{13}C_{carb\text{-}org}$ of 21±1‰. Carmelo and Copacel sections give access to the whole Guia Formation with deeper water deposits. Their $\Delta^{13}C_{carb\text{-}org}$ values are comprised between 27 and 32‰, with occurrences of lower values reaching 24‰.

This new data set is broadly consistent with a low atmospheric pCO_2 scenario in the glaciation's aftermath, followed by a return to higher pCO_2. In details, however some features indicate that the occurrences of the low $\Delta^{13}C_{carb\text{-}org}$ are restricted to shallow depositional environments. To be compatible with a first order control of $\Delta^{13}C_{carb\text{-}org}$ by pCO_2 this requires a strong temperature decrease towards the basin. Two alternate hypotheses can be invoked: (i) a shallow water early diagenetic process inducing a $\delta^{13}C_{org}$ increase and a $\delta^{13}C_{carb}$ decrease or (ii) primary producers presenting lower ε_p in spite of high pCO_2 conditions and possibly inducing carbonate precipitation out of isotope equilibrium with the seawater DIC. Both the diagenetic event and the primary producers would remain to be constrained.

References

Bao H., Lyons J.R. & Zhou C. (2008). Triple oxygen isotope evidence for elevated CO2 levels after the Neoproterozoic glaciation. *Nature*, 453: 504-506.

Hoffman P.F. & Schrag D.P. (2002). The snowball Earth hypothesis: testing the limits of global change. *Terra Nova*, 14: 129-155.

Jiang G., Wang X., Shi X., Zhang S., Xiao S. & Dong J. (2010). Organic carbon isotope constraints on the dissolved organic carbon (DOC) reservoir at the Cryogenian–Ediacaran transition. *Earth and Planetary Science Letters*, 299:159-168.

Kasemann S.A., Hawkesworth C.J., Prave A.R., Fallick A.E. & Pearson P.N. (2005). Boron and calcium isotope composition in Neoproterozoic carbonate rocks from Namibia: evidence for extreme environmental change. *Earth and Planetary Science Letters*, 231: 73-86.

Shen B., Xiao S., Kaufman A.J., Bao H., Zhou C. & Wang H. (2008). Stratification and mixing of a post-glacial Neoproterozoic ocean: Evidence from carbon and sulfur isotopes in a cap dolostone from northwest China. *Earth and Planetary Science Letters*, 265: 209-228.

Sansjofre P., Ader M., Trindade R.I.F., Elie M., Lyons J., Cartigny P. & Nogueira A.C.R. (2011). A carbon isotope challenge to the snowball Earth. *Nature*, 478: 93-96.

Sources and Abundance of Permian Loess Deposition in Tropical Western Pangaea: Implications for Dust Generation and Atmospheric Circulation

Gerilyn Soreghan[1], Nicholas Heavens[2], Michael Soreghan1

[1]School of Geology, University of Oklahoma, Norman OK, U.S.A. 73019; E-Mail: lsoreg@ou.edu, msoreg@ou.edu
[2]Department of Atmospheric and Planetary Sciences, Hampton University, Hampton, VA, U.S.A., 23668; E-Mail: nicholas.heavens@hamptonu.edu

Loess and associated dust deposits are well recognized and studied as both an archive and agent of climate and climate change for Earth's late Cenozoic record. These archives include loess deposits as well as dust (generally <10 µm) recovered from ocean- and ice-cores records. Exclusive of volcanogenic processes, the particles that compose loess and dust can be generated by physical and/or chemical weathering, and inheritance from pre-existing material (e.g., siltstone, tuff, diatomaceous material), and are sourced (emitted) from regions characterized by a deficit in effective moisture for at least part of the year.

Records from (primarily) Quaternary time demonstrate that major sources and sinks for silt- and clay-sized eolian detritus are extra-tropical: loess occurs in regions generally higher than ~30o, and dust in regions generally higher than ~15o. Generation regions are generally associated with either 1) physical weathering driven by glaciation, producing glacial loess deposits in high-mid latitude regions, or 2) deflation of ephemeral lacustrine and fluvial systems in low-mid latitude (desert) regions. Dust remains poorly known in Earth's past prior to the Cenozoic, but is increasingly recognized in the form of paleoloess deposits, and (epeiric) marine strata that accumulated isolated from fluvio-deltaic influx. Deposits in continental and marine strata indicate widespread deposition of loess and dust in western tropical Pangaea during the Late Carboniferous-Permian. These indicators of tropical atmospheric dustiness are highly unusual when compared with the demonstrably extra-tropical loess and dust of the Cenozoic. Here, we report on the growing recognition of voluminous dust deposits preserved in the Permian record of the western-central U.S. (western tropical Pangaea), the source for that loess, and implications for tropical paleoclimate.

Fine-grained redbeds occur and locally predominate in Permian strata throughout the western U.S. extending to the limits of Permian preservation in the central U.S. Within the Anadarko basin of Oklahoma (central U.S.), the Permian section, which reaches in excess of 2000 m in the subsurface, consists in outcrop of fine-grained redbeds bearing characteristics of predominantly loess deposition. If continued study confirms these as loess, they represent the thickest such deposits yet documented in Earth's record. These units consist predominantly of red mudstone and siltstone in commonly massive units, but sedimentary structures and bedding that signal aqueous processes (e.g. laminations, ripples) have led most to infer deltaic or tidal deposition. The absence of channel systems to deliver the sediment, as well as the predominantly massive and laterally continuous character and the fine grain size signal wind transport, implying that these units record sustained eolian deposition overprinted at times by subaqueous (e.g., lacustrine and marginal marine) deposition. Some units also contain eolian or eolianmarine (eolian-transported but marine deposited) very fine sand, such as mid Permian units of the Permian Basin region (Texas).

Detrital zircon geochronology sheds light on possible source regions for the loess and eolian sand. These data, together with data from modal framework mineralogy, indicate that much of the loess and very fine sand originated in the relatively distant Ouachita(-Appalachian) orogenic systems, which formed part of the Central Pangaean Mountains (CPM), the collisional zone that sutured the Pangaean supercontinent. More specifically, key populations of detrital zircons, together with the remarkably (sub)arkosic mineralogy of some units pinpoints terranes south of the Ouachita suture for some of the source regions, notably the Maya/Yucatan block, now within Mexico/Central America. Loess deposits from older (Lower Permian) units of the western U.S. include sources that pinpoint the uplifts of the Ancestral Rocky Mountains. For sources emanating from the CPM, transport pathways likely involved a component of fluvial systems draining the piedmont region of the Ouachita orogenic belt, and ultimate eolian deflation of these fluvial systems within an easterly/southeasterly and seasonal westerly/northwesterly atmospheric circulation. Monsoonal transport, especially northern excursions of the ITCZ during northern hemisphere summers, would have facilitated transport from terranes south of the Ouachita-Marathon suture in present-day

Mexico and Central America These results show that 1) Loess and associated dust was being sourced from rocks that included crystalline basement, 2) multiple sources were involved, but especially sources in the core of the Central Pangaean Mountains.

The tropical setting of these units is remarkably non-uniformitarian. Possible causes and consequences of this massive loess/dust record may include (1) partial glacial genesis of silt in the CPM, (2) precipitation suppression in the vicinity of the CPM due to glacial stability at relatively low altitudes; (3) the action of the Pangaean mega-monsoon, and (4) particularly effective dust traps in western and central North America. Modeling constrains the erosivity (effects of winds and soil moisture) of a range of possible climate states on dust mobilization and underscores the relative difficulty of sourcing dust directly from the Central Pangaean Mountains under most circumstances. Combining data and modelling helps constrain the erodibility (sediment availability, coherence, etc.) of dust sources. Reconstructions of marine dust deposition to the south and the west of the Midcontinent region suggest glacial-interglacial timescale erodibility changes were similar to those seen in the Midcontinent in the last 20,000 years, when this region was at a much higher latitude.

Evidence for continental and sea ice in Siberian Arctic during the Pliensbachian-Toarcian (Early Jurassic)

Guillaume Suan[1], Jean-Michel Brazier[1], Boris L. Nikitenko[2], Laurent Simon[3]

[1]Laboratoire de Géologie de Lyon, UMR CNRS 5276, Université Lyon 1, Ecole Normale Supérieure de Lyon, Campus de la Doua, Bât. Géode, F-69622 Villeurbanne Cedex, France; E-Mail: guillaume.suan@univ-lyon1.fr
[2]Institute of Petroleum Geology and Geophysics, Siberian Branch of Russian Academy of Sciences, Ac. Koptyg av.3, Novosibirsk 90, 630090, Russia
[3]Université de Lyon, UMR5023 Laboratoire d'Ecologie des Hydrosystèmes Naturels et Anthropisés, Université Lyon 1, ENTPE, CNRS, 6 rue Raphaël Dubois, F-69622 Villeurbanne, France

Various records suggest that the Mesozoic, one of the warmest intervals of the Phanerozoic eon, was punctuated by several rapid cooling events that were possibly accompanied by the growth of high latitude glaciers. Nevertheless, in the absence of direct evidence for polar ice, these glaciations remains highly debated and large uncertainties exist about the linkage amongst sea level, climate and biotic changes in the Mesozoic greenhouse world. For instance, the growth and decay of both glacial and sea ice have been proposed as key drivers of global oceanographic and biotic changes that took place close to the Pliensbachian-Toarcian transition (~183 million years ago; Early Jurassic), but evidence for ice during this interval remains elusive. In this study we present new geochemical (organic carbon isotopes, total organic carbon contents) and sedimentological (sand contents and quartz sand microtextures) data from Pliensbachian-Toarcian fine-grained marine sediments exposed along the Kelimyar River in northern Siberia (Russia) to reconstruct polar climate dynamics during this key interval of the Mesozoic greenhouse world. Our data reveal that a significant proportion of the isolated quartz sands have microtextures diagnostic of glacially induced high mechanical stress during most of the studied interval. The ubiquity of subaqueous transport microtextures indicates that most of these glacial grains were not raf ted by icebergs but likely originated from isolated Alpine glaciers and were subsequently transported by rivers. In addition, the presence of large rounded boulders and isolated sand grains in the otherwise fine-grained successions suggests sediment rafting by sea-ice and implies that the Arctic shelves were at least periodically covered by ice throughout the latest Pliensbachian-earliest Toarcian interval. Interestingly, sites with higher sand contents show dramatically reduced organic carbon contents, implying that productivity and organic matter flux to the seafloor might have been modulated by spatial and temporal changes in sea-ice coverage.

Development of Devonian platform deposits in the central Carnic Alps: Facies, biodiversity and geochemistry

Thomas J. Suttner, Erika Kido

University of Graz, Institute of Earth Sciences (Geology and Palaeontology), Heinrichstrasse 26, A-8010 Graz, Austria; E-Mail: thomas.suttner@uni-graz.at; erika.kido@uni-graz.at

The Early to Middle Devonian shallow marine sequence of the central Carnic Alpsis best exposed between Mount Seewarte some few hundred meters south of Lake Wolayer (Austria) and Forcella Monumenz near CimaPlottaon the Italian side of the Carnic chain (Hubmann *et al*., 2003; Schönlaub *et al*., 2004). It consists of the neritic Rauchkofel Limestone (Lochkovian to Pragian) at the base of Mount Seewarte which is followed by the Hohe Warte Lst (Pragian), Seewarte Lst (Pragian to Emsian?), Lambertenghi Lst (Emsian?), Spinotti Lst including the *Amphipora* Lst at its top (Eifelian to Givetian), and the Kellergrat Reef Lst (Givetian to Frasnian?).

In general the sequence starts with some few lithoclastic horizons and crinoidal limestones (organisms: brachiopods, gastropods, echinoderms, conodonts) followed by a short interval of dark gray nodular limestone bearing phosphatic shells of *Opsiconidion* and some few conodonts in the Lochkovian, and well-bedded crinoidal grainstones and a thick unit of massive bright gray frame- and rudstones (dominating skeletal components: calcareous algae, stromatoporoids, tabulate and rugose corals) during the Pragian. These units are succeeded by laminated dark gray to black limestones that are rich in algae, bryozoans, ostracodes and large specimens of gastropods and interpreted as lagoonal deposits. Above deposited are a series of loferite cycles that consist of dolomitized microbial laminites, some levels of birds-eye limestone, rimmed-grain grainstones, oncoidal limestone intervals, and few palaeosol horizons. Within grainstone beds abundant high trochospiral gastropods, brachiopods, bivalves, ostracodes, small solitary rugose corals and some stromatoporoid colonies are observed. Overlying these cyclically deposited sediments another unit of massive bright gray limestones exposes mainly small bioherms of tabulate and rugose corals at its base, a relatively thick horizon dominated by stromatoporoids in the middle and peritidal sediments such as birds-eye limestone and microbial laminites that are followed by intervals of *Amphipora* biostroms towards the top of the formation. At Forcella Monumenz, close to the top of the Spinotti Limestone, a brachiopod horizon mainly consisting of specimens assigned to *Stringocephalus burtini* occurs. The interval dominated by *Amphipora* is overlain by reef deposits of the Kellergrat Reef Lst that is rich in solitary rugose corals, tabulates, single, up to half a meter large stromatoporoid colonies, echinoderms and brachiopods. Conodonts derived from crinoidal debris layers intercalated between 10-20 cm thick frame- and rudstone-layers of this unit exposed at the abandoned quarry near Val di Collina indicate a Givetian age.

The geochemical record of $\delta_{13}C$ isotopes shows several excursions along the Lower-Middle Devonian sequence. The first minor positive shift is identified directly at the S/D boundary. A second one in the early Pragian (*steinachensis* Zone) which is represented by a breccia horizon that bears mega-clasts of up to 10 m in diameter (Fig.1). A third one occurs near the top of the Lambertenghi Lst (positive shift from about 1.4 ppm to 3.3 ppm is observed), which is followed by a relatively even record of values around 1.5 ppm (base of Spinotti Lst). This change in carbon isotope record is linked with changed environmental conditions from peritidal deposits to a several hundred meters thick interval of massive limestone dominated by stromatoporoids and rugose corals. Early Givetian carbon isotope values of the Kellergrat Reef Lst plot around 2.5 ppm (with slight shifts of about 0.4 ppm). Additionally first datasets on the magnetic susceptibility of limestone beds across the entire sequence are obtained for the Rauchkofel Lst, the HoheWarte Lst and the Lambertenghi Lst.

This is a contribution to FWF P23775-B17, IGCP 596and IGCP 580.

References

Hubmann B., Pohler S., Schönlaub H.P. & Messner F.(2003). Paleozoiccoral-sponge bearing successions in Austria. *Berichte der Geologischen Bundesanstalt*, 61: 1-91.

Schönlaub H.P., Histon K. & Pohler S. (2004). The Palaeozoic of the Carnic Alps. In Schönlaub H.P. (Ed.) *Field Trip CarnicAlps Guidebook. June 23-24, 2004, Carinthia Austria*. Geologische Bundesanstalt, 40, 2-32.

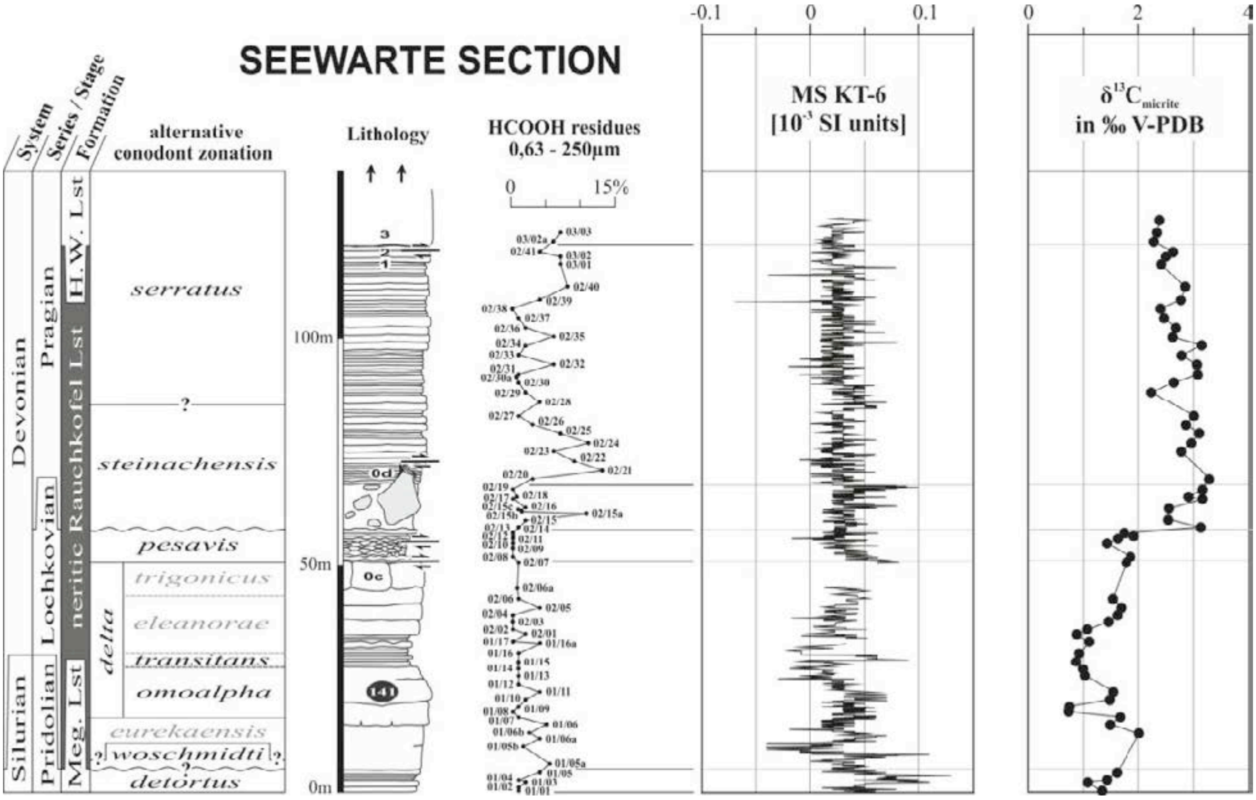

Fig. 1: **MS and carbon isotope trends of the Early Devonian Rauchkofel Lst and Hohe Warte Lst.**

Investigating the Paleoproterozoic glaciations with 3-D climate modeling

Yoram Teitler[1], Guillaume Le Hir[1], Frédéric Fluteau[1], Yannick Donnadieu[2], Pascal Philippot[1]

[1]Institut de Physique du Globe and Université Paris-Diderot, Sorbonne Paris Cité, 1 rue Jussieu, Paris, France
[2] Laboratoire des Sciences du Climat et de l'Environnement (LSCE),, CNRS-CEA-UVSQ, 91191 Gif-sur-Yvette, France

Although the solar constant at the end of the Archean did not exceed 80% of its present day value (Sagan & Mullen, 1972; Gough, 1981), Earth's surface remained unfrozen during most of the Archean and Proterozoic eons. During the first 3 billions of years of Earth's history, only two discrete glacial epochs have been reported: the 2.9 Ga old Pongola glacial (Young *et al*., 1998) and the 2.45-2.22 Ga Paleoproterozoic glaciations where 3 successive ice-ages are recorded (Bekker *et al*., 2003; Erikkson *et al*., 2011; Young *et al*., 1998). The ubiquitous formation at low latitude of glaciogenic rocks associated with these Paleoproterozoic ices ages indicates that a significant cooling occurred between 2.45 and 2.22 Ga leading to the first global glacial epoch (Kopp *et al*., 2005). The onset of such extreme climatic conditions is *canonically* considered to be the result of the collapse of atmospheric CH_4 induced by the Great Oxygenation Event (GOE) (e.g., Kopp *et al*., 2005). Using the classical assumption that the Earth's cooling was related to the collapse of atmospheric methane concentrations (Catling *et al*., 2007; Pavlov *et al*., 2003), we used a General Circulation climate Model (GCM), FOAM (Fast Ocean Atmosphere Model, Jacob, 1997) to investigate the role of atmospheric CH_4 on climate sensitivity to determine needed conditions to initiate snowball Earth glaciations at the Archean-Paleoproterozoic boundary. The use of a GCM, instead of one dimensional climate models (Kasting, 1987), allows us to (1) evaluate the crucial role of the ice-albedo feedback during climate cooling, (2) determine the spatial constraints on surface temperatures and sea ice extent and (3) test the relevance of different scenarios of pCH_4 evolution (Catling *et al*., 2007; Pavlov *et al*., 2000). Using Archean-Paleoproterozoic boundary conditions (distribution of continental masses, seawater salinity and Earth rotation rate), we performed sensitivity experiments to a combination of pCO_2 ranging from 1.6 10^{-3} bar to $2.7.10^{-2}$ bar and pCH_4 ranging from 4 ppmv (4.10^{-6} bar) to 1000 ppmv (10^{-3} bar) in agreement with geologic data and chemical models (Catling *et al*., 2007; Pavlov *et al*., 2003; Sheldon 2006). We show that a mild to warm climate may exist since the Late Archean even under moderate atmospheric levels of CO_2 (< $2.6.10^{-2}$ bar) and pCH_4 (<10 ppmv). In addition, we show that an abrupt pCH_4 collapse (from 1000 to 4ppmv), associated to the GOE, not comply with geological constraints to explain the initiation a global glaciation. Instead of the *canonical* scenario suggesting that Paleoproterozoic ices ages resulted of the collapse of atmospheric CH_4, here we propose that both CO_2 and CH_4 have decreased. Considering that the CH_4 collapse occurred immediately after the first glacial event, our simulations suggest that the pCO_2 must have dropped below 5.10^{-3} PAL to trigger a snowball Earth. This may be possible through the enhancement of silicate weathering after 2.5 Ga (Kump and Barley, 2007) combined to a potential shutdown of volcanism from 2.45 to 2.20 Ga (Condie *et al*., 2009). Initiating the second and third glacial events requires that the CO_2 concentrations remain lower than $1.3.10^{-2}$ bar. A final conclusion is that the return to stable, mild to warm climate after 2.2 Ga is related to the rise of atmospheric CO_2 (>2.10^{-2} bar) at constant low pCH_4, possibly linked to enhanced volcanic activity and /or moderate silicate weathering.

References

Catling D.C., Claire M.W. & Zahnle K.J. (2007). Anaerobic methanotrophy and the rise of atmospheric oxygen. *Philosophical Transactions of the Royal Society of London A*, 365, 1867-1888.

Condie K. C., O'Neil C. & Aster R.C. (2009). Evidence and implications for a widespread magmatic shutdown for 250 My on Earth. *Earth and Planetary Science Letters*, 282: 294–298.

Eriksson P.G., Lenhardt N., Wright D.T., Mazumder R. & Bumby A.J. (2011). Late Neoarchaean Palaeoproterozoic supracrustal basin-fills of the Kaapvaal craton: Relevance of the supercontinent cycle, the "Great Oxidation Event" and "Snowball Earth"? *Marine and Petroleum Geology*, 28: 1385-1401.

Gough D. O. (1981). Solar interior structure and luminosity variations. *Solar Physics*, 74: 21-34.

Kasting J.F. (1987). Theoretical constraints on oxygen and carbon-dioxide concentrations in the Precambrian atmosphere. *Precambrian Research*, 34(3-4): 205-229.

Kopp R.E., Kirschvink J.L., Hilburn I.A. & Nash C.Z. (2005). The paleoproterozoic snowball Earth: A climate disaster triggered by the evolution of oxygenic photosynthesis. *PNAS*, 102: 11131-11136.

Kump L.R. & Barley M.E. (2007). Increased subaerial volcanism and the rise of atmospheric oxygen 2.5 billion years ago. *Nature*, 448: 1033-1036.

Pavlov A.A., Kasting J.F., Brown L.L., Rages K.A. & Freedman R. (2000). Greenhouse warming by CH_4 in the atmosphere of early Earth. *Journal of Geophysical Research*, 105 (E5): 11981–990.

Pavlov A.A., Hurtgen M.T., Kasting J.F. & Arthur M.A. (2003). Methane-rich Proterozoic atmosphere? *Geology*, 31: 87-90.

Sagan C. & Mullen G. (1972). Earth and Mars: Evolution of atmospheres and surface temperatures. *Science*, 177: 52-56.

Sheldon N.D. (2006). Precambrian paleosols and atmospheric CO_2 levels. *Precambrian Research*, 147: 148-155.

Young G. M., Von Brunn V., Gold D.J.C. & Minter W.E.L. (1998). Earth's Oldest Reported Glaciation: Physical and Chemical Evidence from the Archean Mozaan Group (2.9 Ga) of South Africa. *Journal of Geology*, 106: 523–538.

Responses of marine ecosystems to climate change during the Late Palaeozoic to Early Mesozoic

Richard J. Twitchett

School of Geography, Earth and Environmental Sciences, Plymouth University, United Kingdom; E-Mail: richard.twitchett@plymouth.ac.uk

The transition from the Late Palaeozoic to Early Mesozoic was a time of profound biological and climatic changes. A number of biotic crises characterize this interval, all of which are associated with evidence of global warming and concomitant environmental changes in both the terrestrial and marine realms. Marine ecosystems and organisms responded to these changes in a number of ways, and there are several responses that are common to all of the main events studied thus far despite differences in the scale and magnitude of these changes. This presentation will briefly outline the similarities and differences between the key events of the studied interval, based on current published data, and will provide a short summary of future potential research directions.

The four key events studied are as follows:

1. Late Permian mass extinction event: As first demonstrated by Kearsey *et al*. (2009), and later supported by Joachimski *et al*. (2012) and Sun *et al*. (2012), the Late Permian extinction event is associated with dramatic global warming of some 8-10°C. Concomitant environmental changes are well known and include the expansion of anoxic dead zones in the oceans (e.g. Wignall and Twitchett, 1996; Grice *et al*., 2005) and greatly elevated weathering rates on land that led to enhanced sedimentation rates in shelf settings (Algeo & Twitchett, 2010) amongst others (Algeo *et al*., 2011). Key ecological changes include a near synchronous collapse of marine and terrestrial ecosystems (e.g. Twitchett *et al*., 2001); dramatic size reduction in all marine groups studied thus far (e.g. Twitchett, 2007; He *et al*., 2010; Metcalfe *et al*., 2011); significant reduction in burrow size and depth (Twitchett, 1999; 2007); significant reduction in epifaunal tiering with the loss of high tier suspension feeders (e.g. Twitchett, 1999; 2006). Ecosystem rebuilding and ecological recovery from this event varied between regions (Twitchett *et al*., 2004; 2006; Hoffman *et al*., 2011) and depositional settings (Beatty *et al*., 2008), and was globally more complex and nuanced than recent overly simplistic models such as that of Chen and Benton (2012) suggest.
2. Smithian-Spathian event: this biotic crisis occurred within the Early Triassic and has thus far only been recorded in pelagic and/or nektobenthic organisms such as conodonts and ammonoids (Stanley, 2009). As hypothesized by Galfetti *et al*. (2007) and as shown by Sun *et al*. (2012), this event is associated with a rise in global temperatures. Few high resolution ecological studies of the Smithian-Spathian event have hitherto been undertaken, although Chen *et al*. (in press) demonstrate that conodonts, at least, underwent dramatic temporary size reduction through this event. Ongoing and future studies should determine whether patterns of ecological collapse and recovery are similar to those following other global warming events.
3. Late Triassic mass extinction event: One of the first mass extinction events to be intimately linked to CO2 rise and global warming, this event also records a near synchronous collapse of marine and terrestrial ecosystems (Mander *et al*., 2013). Recorded ecological changes are similar to those recorded through the Late Permian event (Mander *et al*., 2008), including a temporary reduction in infaunal and epifaunal tiering, and a temporary reduction in burrow size and depth, but recovery was much faster after the Late Triassic event and completed within the Hettangian in all localities and settings thus far studied (e.g. Twitchett & Barras, 2004; Barras & Twitchett, 2007; Mander *et al*., 2008), although there is a need for more local ecological studies.
4. Early Toarcian extinction event: Danise *et al*. (2013) recently published the most complete and detailed quantitative ecological assessment of marine community dynamics through this global warming event. Their data demonstrate the intimate association between biofacies, sealevel, temperature and oxygen levels, and show strong similarity with ecological changes that occur during modern hypoxic events, albeit at vastly different temporal scales. It is clear, however, that extinctions occurred even in areas unaffected by oceanic anoxia (Gomez & Goy, 2011). Other ecological changes include size reduction in some, though not all, marine invertebrate groups (e.g. Morten & Twitchett, 2009).

In summary, current data demonstrate that the key biotic crises of the Late Palaeozoic to Early Mesozoic are all related to global warming, and associated with similar oceanographic changes. The resulting ecological changes that occurred in marine ecosystems show strong similarities between events, although there is a clear need for many more local-scale, high resolution, quantitative studies to better elucidate patterns of global change.

References

Algeo T.J. & Twitchett, R.J. (2010). Anomalous Early Triassic sediment fluxes due to elevated weathering rates and their biological consequences. *Geology*, 38: 1023-1026.

Algeo T.J., Chen Z.-Q., Fraiser M.L. & Twitchett R.J. (2011). Terrestrial–marine teleconnections in the collapse and rebuilding of Early Triassic marine ecosystems. *Palaeogeography, Palaeoclimatology, Palaeoecology*, 308: 1-11.

Barras C.G. & Twitchett R.J. (2007). Response of the marine infauna to Triassic-Jurassic environmental change: ichnological data from southern England. *Palaeogeography, Palaeoclimatology, Palaeoecology*, 244: 223-241.

Beatty T.W., Zonneveld J-P. & Henderson C.M. (2008). Anomalously diverse early Triassic ichnofossil assemblages in northwest Pangea: a case for a shallow-marine habitable zone. *Geology*, 36: 771-774.

Chen Y., Twitchett R.J., Jiang H., Richoz S., Lai X., Yan C., Sun Y., Liu X. & Wang. Size variation of conodonts during the Smithian-Spathian (Early Triassic) global warming event. *Geology*, (in press).

Chen Z-Q. & Benton M.J. (2012). The timing and pattern of biotic recovery following the end-Permian mass extinction. *Nature Geoscience*, 5: 375-383.

Danise S., Twitchett R.J., Little C.T.S. & Clémence M-E. (2013). The Impact of Global Warming and Anoxia on Marine Benthic Community Dynamics: an Example from the Toarcian (Early Jurassic). *PLoS ONE* 8(2): e56255.

Galfetti T., Hochuli P.A., Brayard A., Bucher H., Weissert H. & Vigran J.O. (2007). Smithian-Spathian boundary event: Evidence for global climatic change in the wake of the end-Permian biotic crisis. *Geology*, 35, 291–294.

Gomez J.J. & Goy A. (2011) Warming-driven mass extinction in the Early Toarcian (Early Jurassic) of northern and central Spain. Correlation with other time-equivalent European sections. *Palaeogeography, Palaeoclimatology, Palaeoecology*, 306: 176–195.

Grice K., Cao C., Love G.D., Böttcher M.E., Twitchett R.J., Grosjean E., Summons R.E., Turgeon S.C., Dunning W. & Jin Y. (2005). Photic zone euxinia during the Permian-Triassic Superanoxic Event. *Science*, 307: 706-709.

He W.-H., Twitchett R.J., Zhang Y., Shi G.R., Feng Q.-L., Yu J.-X., Wu S.-B. & Peng X.-F. (2010). Controls on body size during the Late Permian mass extinction event. *Geobiology*, 8: 391-402.

Hofmann R., Goudemand N., Wasmer M., Bucher H. & Hautmann M. (2011). New trace fossil evidence for an early recovery signal in the aftermath of the end-Permian mass extinction. *Palaeogeography, Palaeoclimatology, Palaeoecology*, 310: 216-226.

Joachimski M.M., Lai X., Shen S., Jiang H., Luo G., Chen B., Chen J. & Sun Y. (2012). Climate warming in the latest Permian and the Permian–Triassic mass extinction. *Geology*, 40: 195-198.

Kearsey T., Twitchett R.J., Price G.D. & Grimes S.T. (2009). Isotope excursions and palaeotemperature estimates from the Permian/Triassic Boundary in the Italian Dolomites. *Palaeogeography, Palaeoclimatology, Palaeoecology*, 279: 29-40.

Mander L., Twitchett R.J. & Benton M.J. (2008). Palaeoecology of the Late Triassic extinction event in the SW UK. *Journal of the Geological Society, London*, 165: 319–332.

Mander L., Kürschner W.M. & McElwain J.C. (2013). Palynostratigraphy and vegetation history of the Triassic–Jurassic transition in East Greenland. *Journal of the Geological Society of London*, 170: 37-46.

Metcalfe B., Twitchett R.J. & Price-Lloyd N. (2011). Size and growth rate of 'Lilliput' animals in the earliest Triassic. *Palaeogeography, Palaeoclimatology, Palaeoecology*, 308: 171-180.

Morten S.D. & Twitchett R.J. (2009). Fluctuations in the body size of marine invertebrates through the Pliensbachian-Toarcian extinction event. *Palaeogeography, Palaeoclimatology, Palaeoecology*, 284: 29-38.

Sun Y.D., Joachimski M., Wignall P.B., Yan C.B., Chen Y.L., Jiang H.S., Wang L.N. & Lai X.L. (2012). Lethally hot temperatures during the Early Triassic Greenhouse. *Science*, 338: 366–370.

Stanley S.M. (2009). Evidence from ammonoids and conodonts for multiple Early Triassic mass extinctions. *Proceedings of the National Academy of Sciences of the USA*, 106: 15264–15267.

Twitchett R.J. (1999). Palaeoenvironments and faunal recovery after the end-Permian mass extinction. *Palaeogeography, Palaeoclimatology, Palaeoecology*, 154, 27-37.

Twitchett R.J. (2006). The palaeoclimatology, palaeoecology and palaeoenvironmental analysis of mass extinction events. *Palaeogeography, Palaeoclimatology, Palaeoecology*, 232, 190-213.

Twitchett R.J. (2007). The Lilliput effect in the aftermath of the end-Permian extinction event. *Palaeogeography, Palaeoclimatology, Palaeoecology*, 252: 132-144.

Twitchett R.J. & Barras C.G. (2004). Trace fossils in the aftermath of mass extinction events. In McIlroy, D. (Ed), *The Application of Ichnology to Palaeoenvironmental and Stratigraphic Analysis*. Geological Society, London, Special Publications, 228: 397-418.

Twitchett R.J., Krystyn L., Baud A., Wheeley J.R. & Richoz S. (2004). Rapid marine recovery after the end-Permian mass extinction event in the absence of marine anoxia. *Geology*, 32, 805-808.

Twitchett R.J., Looy C.V., Morante R., Visscher H. & Wignall P.B. (2001). Rapid and synchronous collapse of marine and terrestrial ecosystems during the end-Permian mass extinction event. *Geology*, 29, 351-354.

Wignall P.B. & Twitchett R.J. (1996). Oceanic anoxia and the end-Permian mass extinction. *Science*, 272, 1155-1158.

Hydrocarbon seepage and transient Mesozoic climate change

Bas van de Schootbrugge[1], Guillaume Suan[2]

[1]Institute of Geosciences, Goethe University Frankfurt, Altenhöferallee 1, 60438 Frankfurt am Main, Germany; E-Mail: van.de.Schootbrugge@em.uni-frankfurt.de
[2]Laboratoire de Géologié de Lyon: Terre, Planète, Environnement, UMR CNRS 5276 Université Claude Bernard, Lyon1, 2 rue Raphaël Dubois, 69622 Villeurbanne Cedex, France; E-Mail: guillaume.suan@univ-lyon1.fr

Natural hydrocarbon seepage is a process by which asphalt, petroleum, and/or gas (e.g. methane, carbon dioxide) are expulsed from the sedimentary pile and become exposed to oxidation in the overlying ocean waters or the atmosphere. It is occurring today on a worldwide scale and there is ample evidence that, in accordance with uniformitarian principles, this was also the case in Earth history. The expulsed carbon plays an important role in perturbing the global carbon cycle and the ocean-atmosphere system if the release is both on a massive scale and rapid. For example, the destabilization of sea floor methane gas hydrates, documented by a >3 per mille global negative carbon isotope excursion, is thought to have triggered the Palaeocene-Eocene Thermal Maximum (55 Ma). Similar negative carbon isotope excursions occur throughout the Mesozoic and most are associated with the deposition of black shales and/or crises in the biosphere. Key examples include the end-Permian (252 Ma) and end-Triassic (201 Ma) mass-extinction events, as well as the Toarcian (183 Ma) and Aptian (120 Ma) Oceanic Anoxic Events (OAEs), all of which have been linked to the massive and rapid release of methane from sea floor gas hydrates. In some cases, such as the Toarcian OAE, high-resolution carbon isotope records document a series of smaller negative excursions that have been interpreted to reflect an orbitally-controlled release of methane to the atmosphere. Despite a general increase in data density over the past 10 years, we review a number of unresolved issues that are crucial to the understanding of past hydrocarbon seepage and its role in driving Mesozoic climate change. One such issue is the general lack of direct evidence for hydrocarbon seepage, in the form of microbially-mediated authigenic minerals or peculiar fossil assemblages characteristic of chemosynthetic communities. New evidence from the Early Jurassic in Germany and France suggests that such occurrences may have gone unnoticed previously. Authigenic carbonates (concretions, glendonites) with carbon isotopic signatures indicative of the anaerobic oxidation of methane are common within the Upper Pliensbachian directly preceding the Toarcian OAE. Another issue is the ambiguous nature of the carbon isotope records used to constrain both quality and quantity of hydrocarbon release. In most cases the magnitude of the negative C-isotope excursions varies depending on the type of material (bulk or skeletal carbonate, bulk or skeletal organic matter, organic molecules) analysed. However, determining which excursion reflects the exogenic carbon cycle without interferences from biological overprints is pivotal when such data are fed into carbon cycle models. Finally, a mismatch appears to exist between changes in the bio- and geosphere and the proposed release of methane. Both for the end-Triassic mass-extinction and Toarcian OAE changes in primary production (vegetation, phytoplankton) and climate preceded the changes in carbon isotope records. In these cases, methane release was an effect rather than a cause, however it may have prolonged or exacerbated ongoing changes. The trigger for these changes and for the destabilization of sea floor hydrates was likely massive flood basalt volcanism. Here we see a resemblance with current anthropogenic fossil fuel burning and future global warming: man-made warming may eventually trigger the release of large quantities of methane stored in permafrost and gas hydrates, leading to a runaway greenhouse effect.

Modelling Cretaceous and Early Eocene Climates

Paul Valdes

School of Geographical Sciences, University of Bristol, University Road, Bristol, United Kingdom; E-Mail: P.J.Valdes@bristol.ac.uk

There is now a long history of computer model simulations of climate of the Cretaceous and Early Eocene. The models predict much warmer conditions that present, but generally fail to simulate the polar and seasonal warmth indicated by the proxy climate data. The talk will discuss the role that uncertainties in palaeogeography, orbit, greenhouse gases, and internal model parameters play in addressing this model-data mismatch. Using a version of the Hadley Centre climate model we have performed a large number of simulations covering the mid and late Cretaceous and Early Eocene. Changes in palaeogeography can change local climate significantly but has relatively modest impact on equator-to-pole temperature gradient. Uncertainties in greenhouse gas concentrations and orbits can produce warmer poles, even in winter, but fail to simulate the full extent of the warmth without overheating the equator. However, we find that internal model parameters, in particular those related to clouds, can have the biggest impact on the simulation. We will discuss the implications of this result for estimates of climate sensitivity in the past and also into the future.

Reconstructing the climate of the Ordovician using zooplankton derived proxy data

Thijs R.A. Vandenbroucke[1], Carys Bennett[1,2], Chloé Amberg[1], Mark Williams[2], Howard A. Armstrong[3]

[1]Géosystèmes, UMR 8217 du CNRS, Université Lille 1, Villeneuve d'Ascq, France; E-Mail: Thijs.vandenbroucke@univ-lille1.fr; chloe.amberg@ed.univ-lille1.fr
[2]Department of Geology, University of Leicester, University Road, Leicester, LE1 7RH, United Kingdom; E-Mail: mri@leicester.ac.uk; ceb28@leicester.ac.uk
[3]Department of Earth Sciences, Durham University, Durham, United Kingdom; E-Mail: h.a.armstrong@durham.ac.uk

The Hirnantian icehouse is implicated as the causal mechanism for one of the great Phanerozoic mass extinctions. An emerging body of evidence now suggests that cooling towards the Hirnantian glacial maximum, and thus the onset of the Early Palaeozoic Ice Age (EPI), started earlier than previously assumed, during the Early Ordovician. This has fundamental importance as an early phase of cooling could provide a driving mechanism for the major changes in biodiversity during the Great Ordovician Biodiversification. In this presentation, we test this „early cooling‟ hypothesis by examining several „zooplankton‟ climate proxies including:

(i) Spatial distribution maps of Ordovician zooplankton, chitinozoans and graptolites. We have shown that Ordovician chitinozoans, like graptolites, were "mixed layer" marine zooplankton and that their global distribution was primarily controlled by variations in Sea Surface Temperature. Data on the palaeobiogeographical distribution of chitinozoan provinces during the end-Ordovician Hirnantian glaciation (440Ma) are compared to those from the pre-glacial Sandbian (460Ma). We demonstrate that severe cooling towards the Hirnantian glacial maximum resulted in (a) a steeper latitudinal temperature gradient and (b) an equator-ward shift in the position of the Hirnantian austral Polar Front from 55-70°S to 40°S. This is deduced from an expansion and diversification of the Polar fauna. These changes are equivalent to those in Pleistocene glacial maxima. Our data show that Late Ordovician surface ocean temperature gradients, and fluctuations between glacial and interglacial states, may have been more similar to modern oceans than hypothesized before. Chitinozoans and graptolites responded to climate change in a ways that are comparable to modern planktonic groups, and provide tracers of shifts in Ordovician climate belts, and ground-truth for GCM output.

(ii) The use of microfossil data to unravel the nature of 'lowstand' deposits. The Ordovician eustatic sea level curve for Baltica, based on lithological evidence from the Oslo-Asker area (Norway), includes a number of lowstands interpreted as glacioeustatic. These deposits are calcareous rhythmites, potentially recording short-term palaeoclimatological fluctuations and implying the presence of a significant ice-sheet on Gondwana. However, alternatively, these limestone-mud alterations could also be the result of diagenesis. We test both hypotheses by a bed-by-bed study of their chitinozoan content – an environmental, cyclic signal ought to be reflected in the microfauna.

(iii) Stable oxygen isotopes of the calcitic eyes of epipelagic trilobites (e.g. Carolinites) to reconstruct Sea Surface Temperatures. Current fossil-derived proxies for seawater temperature in the Ordovician are oxygen isotopes from conodont apatite and brachiopod calcite. Diagenetic alteration and the analytical techniques used are respectively problematic or still under development, and neither proxy can give a robust indication of surface-water temperature. This study assesses the potential for oxygen isotopes from the calcitic lenses of epipelagic trilobite eyes as a seawater palaeotemperature proxy. We have analysed Floian age specimens of the widespread *Carolinites* from Spitsbergen. Well-preserved eyes can be distinguished from diagenetically altered eyes using EBSD C-axis mapping, microstructure preservation and geochemistry. Well-preserved eyes have low $\delta_{18}O$ values of –8‰ to –7‰ VPDB that may signal warm sea temperatures. Data from Mid Ordovician Australian specimens (*Carolinites* and *Opipeuterella*) provide a second case study. Well-preserved eyes have low $\delta_{18}O$ values of –9‰ to –7‰ VPDB. Parallel *in situ* $\delta_{18}O$ SIMS analyses are ongoing and these data will be presented alongside the standard $\delta_{18}O$ measurements.

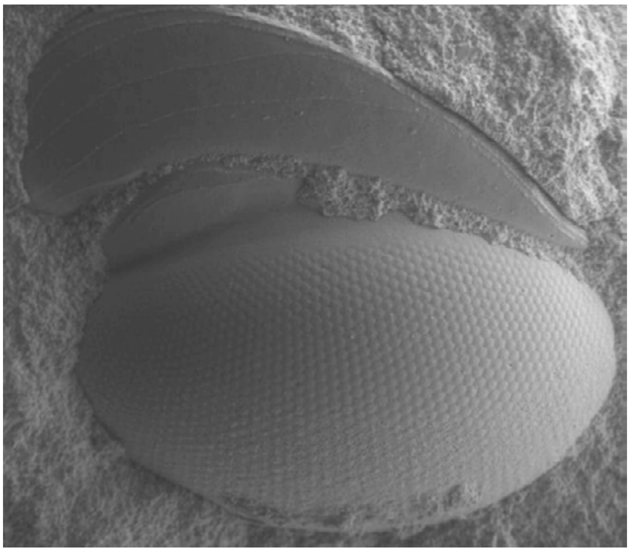

Fig. 1: **An eye of the telephinid *Opipeuterella* from the Emmanuel Formation, Canning Basin, Australia, the length of the eye is 1.8mm.**

Precipitation of aragonite crystal fans in restricted coastal areas during the Neoproterozoic Snowball Earth aftermath

Lucieth C. Vieira[1], Anne Nédélec[2], Sébastien Fabre[3], Ricardo I.F. Trindade[4], Renato Paes De Almeida[5]

[1]Instituto de Geociências, Universidade de Brasília. Campus Darcy Ribeiro. Brasília-DF, Brazil; E-Mail: lucieth@gmail.com
[2]Géosciences Environnement Toulouse (GET), Observatoire Midi Pyrénées, Université de Toulouse, CNRS, IRD, 14 avenue E. Belin; F- 31400 Toulouse-France, E-mail: anne.nedelec@get.obs-mip.fr
[3]Institut de Recherche en Astrophysique et Planétologie, Université de Toulouse, 14 avenue Edouard Belin, F-31400 Toulouse, France; E-Mail: sfabre@irap.omp.eu
[4]Instituto de Astronomia, Geofísica e Ciências Atmosférica, Universidade de São Paulo. Rua do Matão1226, Cidade Universitária, São Paulo, 05508-900, SP, Brazil; E-Mail: rtrindade@iag.usp.br
[5]Departamento de Geologia Sedimentar e Ambiental, Instituto de Geociências, Universidade de São Paulo. Rua do Lago 562, Cidade Universitária, São Paulo, 05508-900, SP, Brazil; E-Mail: rpalmeida@ig.usp.br

A striking feature of Neoproterozoic sedimentary record is related to the occurrence of glacial deposits which are covered by carbonate deposits called cap carbonates and have been identified worldwide. Usually the Neoproterozoic platform record begins by cap dolomites. In some sequences, the cap dolomites are overlaid by limestones characterized by aragonite-pseudomorph crystal fans (James *et al*., 2001; Corsetti *et al*., 2004; Hoffman *et al*., 2007; Pruss *et al*., 2008). These conspicuous, but uncommon, sea floor precipitates obviously required special conditions to form and, consequently, constitute a key point for the reconstruction of Neoproterozoic paleoenvironmental conditions.

Here we report new sedimentary and geochemical results on well preserved Neoproterozoic deposits with aragonite-pseudomorph crystal fans at the base of the Sete Lagoas Formation (central Brazil), together with a numerical model constraining aragonite crystal and micrite formation kinetics. The Sete Lagoas Formation is more than 200 m thick in the studied region, where it is composed by two shallowing-upward megacycles (Vieira *et al*., 2007). The first megacycle is made of widespread carbonates dated at *ca* 740 Ma (Pb-Pb age: Babinski *et al*., 2007). These deposits comprise tabular layers up to 30 m thick, organized in centimeter-scale cycles of lime mudstone containing aragonite pseudomorph crystal fans. They have been exploited as or ornamental stones for many years at the Sambra quarry (19°22'S, 44°21'W - SA section - Fig. 1).

Fig. 1: **Cyclic layers of micrite - aragonite crystal pairs (Sambra quarry)**

Three distinct facies containing crystals were recognized in different sections, namely (i) lime mudstone dominated facies, (ii) wave-influenced facies, and (iii) tide-influenced facies. The first one shows the highest abundance of crystal fans. It is characterized by layers of aragonite pseudomorphs crystal ranging from 5 mm to 10 cm (Fig. 1). The crystals are black to dark grey, forming bottom nucleated, upward-radiating fans, laterally connected to thin, millimetric cement-crusts. Crystal layers are covered by light-grey or red lime mudstones showing parallel to undulating lamination reflecting the irregular surface at the top of underlying crystals. The crystal/lime mudstone layer pairs show a remarkable cyclicity, especially in the SA section where they represent more than one hundred cycles (Hoppe *et al*., 2002).

The elongate morphology of the crystals with square terminations is considered to be a primary feature keeping the habitus of their aragonite precursors, but all crystals were replaced by mosaics of anhedral, equant to elongate sparry calcite. In addition to calcite, accessory mineral phases, including strontianite, celestite, barite and pyrite, were recognized. Both celestite and strontianite were likely formed during the diagenetic replacement of the Sr-rich aragonite crystal precursors (Makovicky *et al*., 2006). Sr contents are generally high, ranging from 781 to 3025 ppm in the matrix and from 1531 to 3583 ppm in the crystals. The highest values are typical of the former aragonitic nature of the crystals as already established by Peryt *et al*. (1990). REE + Y distribution patterns normalized to PAAS (Post-Archaean Australian Shales) are presented in Fig. 2, together with other Neoproterozoic cap dolostone and modern seawater patterns for comparison. Sambra carbonate patterns are evocative of seawater because of their positive La anomalies, negative Ce anomalies and slightly overchondritic Y/Ho values. However, they appear slightly MREE enriched, a possible diagenetic effect (Shields & Stille, 2001).

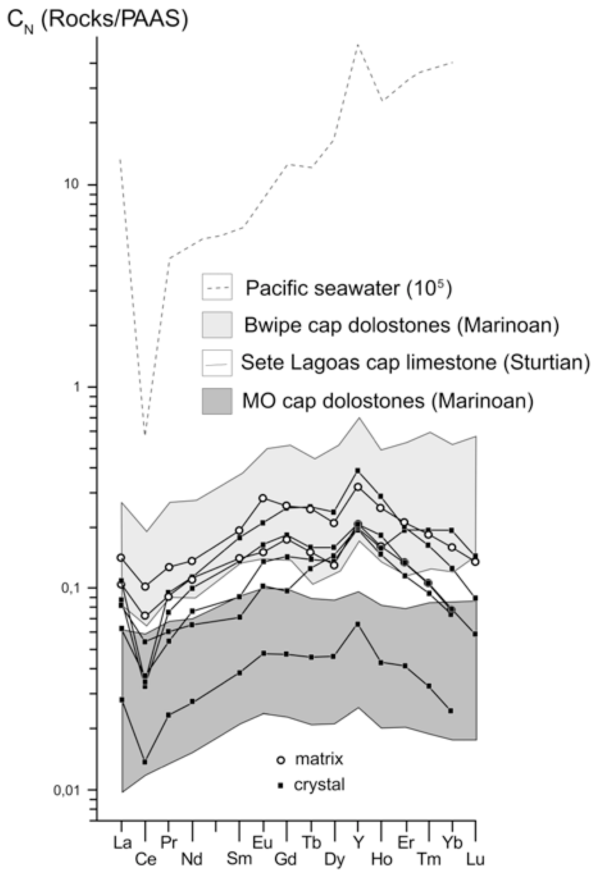

Fig. 2: **PAAS normalized REE + Y plots for Sete Lagoas compared to Pacific seawater (Elderfield & Greaves, 1982), Mirassol D'Oeste (MO) cap dolostones (Font *et al*., 2006) and Bwipe cap dolostones (Nédélec *et al*., 2007), both of post-Marinoan age.**

De Choudens-Sánchez & González (2009) identified that the main controls on the calcite vs aragonite precipitation are temperature, Mg/Ca ratios and carbonate species reaction kinetics. In our case aragonite and calcite appear to have co-precipitated, therefore only the last parameter will be investigated. We assume that some supersaturation in the carbonate species was responsible for the crystal formation. The control of the supersaturation is obtained through equilibrium of seawater with atmospheric pCO_2 followed by seawater concentration due to evaporation. The Neoproterozoic seawater composition is not known, so we use the composition of present-day seawater (Nordstrom *et al*., 1979). The pH is adjusted to various values after partial pressure of carbon dioxide (pCO2) comprised between 3 and 270 PAL (Present Atmospheric Level). Such high pCO_2 values may have been reached in the Snowball Earth aftermath (Pierrehumbert, 2004; Le Hir *et al*., 2009).

The reactive pathway in our model is as follows: the presumed "Neoproterozoic seawater" is submitted to different evaporation rates in order to reach the supersaturation of calcite and aragonite under different pCO_2. In each case, the saturation ratios for calcite and aragonite are calculated and then their respective induction times at the end of the evaporation period. The *induction time* is an experimental concept: it is the time required to produce N particles with sufficient size to make an observable change in the system (Westin & Rasmuson, 2005). The carbonate with the shortest induction time begins to precipitate alone. At the end of the simulations, the precipitated mole numbers of each carbonate species are calculated.

First, we examine the case for 20% evaporation. When pCO_2 is higher than 3 PAL, the induction time of calcite becomes shorter than the induction time of aragonite, whereas aragonite nucleates first for lower pCO_2 values (see Fig. 3). For these last conditions i.e., before the beginning of calcite crystallization, aragonite grows very fast and ca 50% of the final weight of aragonite precipitates. In the case of 40% evaporation, aragonite nucleation rate is greater than calcite nucleation rate, whatever pCO_2. In all cases, if pCO_2 increases, the number of moles of carbonates finally precipitated also increases.

The numerical model results imply that evaporation rate must not be higher than 20% for aragonite to nucleate first if $pCO_2 \leq 3$ PAL. We consider that such pCO_2 values are too low for the Neoproterozoic post-glacial conditions. Therefore, we retain a high evaporation rate (40%), that will induce aragonite first in any case. Besides, as the volume of precipitated carbonate increases with increasing pCO_2, the sizes and volumes of the Neoproterozoic aragonite crystals also suggest that pCO_2 was rather high.

The association of crystal fans with the three different facies indicates that they formed in a range of environmental conditions, from calm waters dominated by micrite settling to moderate energy tide- and wave-influenced environments, although the first setting is much more favorable than the others. In a

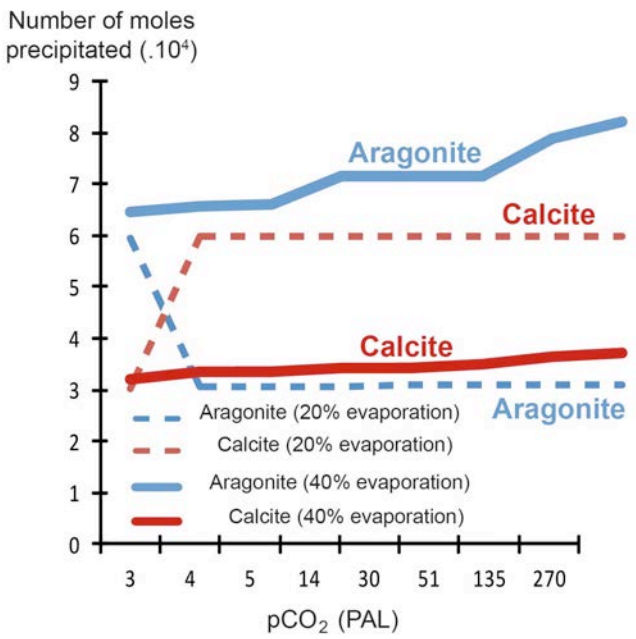

Fig. 3: **Number of precipitated moles of carbonates per liter of seawater vs pCO$_2$**

context of relatively high atmospheric pCO$_2$, calcium carbonate oversaturation was caused by intense evaporation in a shallow restricted area (Fig. 4). The cyclic aragonite crystal growth observed in the cap

limestones pleads for a seasonal/climatic rhythm corresponding to an intense evaporation during the dry season, conducting to an important precipitation of aragonite followed by calcite.

Descriptions of cap carbonate sections in SW Brazil, NW Canada, NW Namibia and Central Australia show that crystal fans occur systematically atop cap dolostones, but are limited to the breakslope sector of these platforms. Taken together, these observations are consistent with a localized setting with protected conditions. We suggest that crystal fans grew in relation with a post-glacial topography (morainic ridges) favouring the development of short-life restricted areas during the postglacial transgression.

Aragonite precipitates seem to be more common in much older times, such as the Palaeoproterozoic and the Neoarchaean (Sumner & Grotzinger, 2000). This is consistent with aragonite crystal formation triggered by a combination of high atmospheric pCO$_2$ and intense evaporation. Examples of aragonite crystal fans and cements observed in Phanerozoic successions are mainly of Triassic age (Assereto & Folk, 1980; Woods *et al*., 1999; Baud *et al*., 2005), namely they were formed during globally extensive evaporation settings on the Pangea supercontinent. In more recent times, the formation of aragonite crystal fans becomes unlikely.

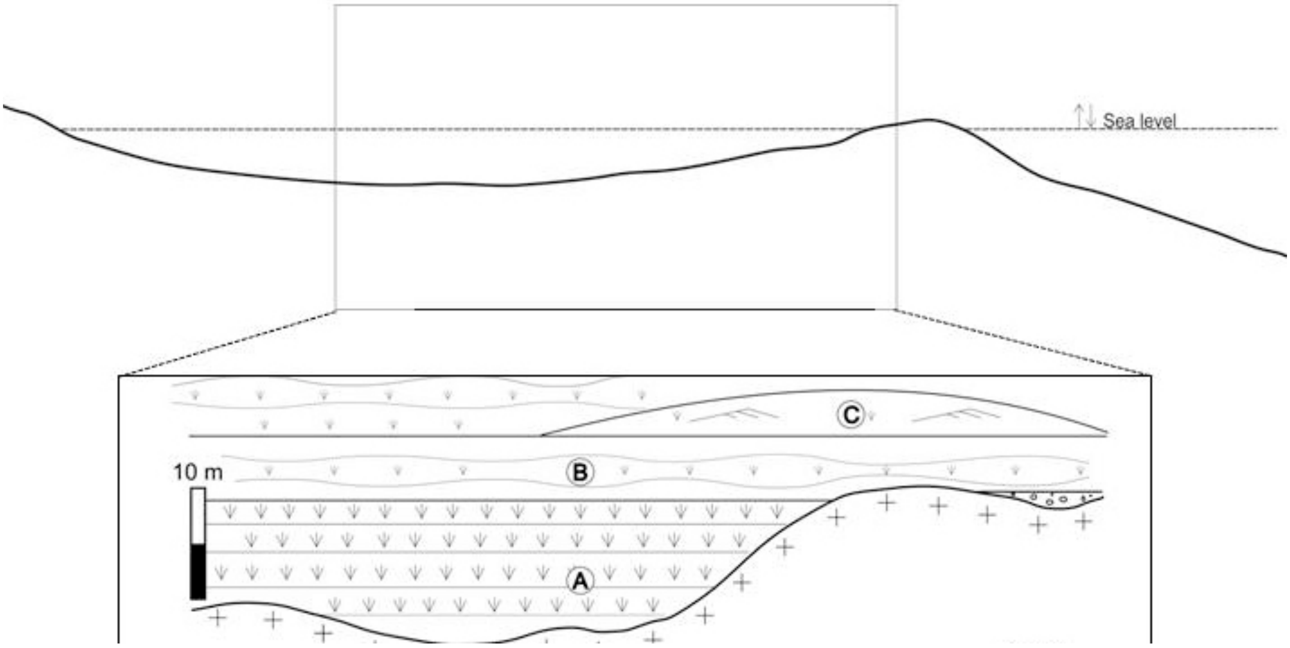

Fig. 4: **Paleoenvironmental reconstruction of aragonite crystal-fans precipitation in Sete Lagoas Formation. A limited marine connection allowed deposition of the three different facies: A) micritesettling facies, B) wave-influenced facies and C) tide-influenced facies.**

References

Assereto R. & Folk R.L. (1980). Diagenetic fabrics of aragonite, calcite and dolomite in an ancient peritidal –spelean environment: Triassic Calcare Rosso, Lombardia, Italy. *Journal of Sedimentary Petrology*, 50: 371-394.

Babinski M., Vieira L.C. & Trindade R.I.F. (2007). Direct dating of the Sete Lagoas cap carbonate (Bambuí Group, Brazil) and implications for the Neoproterozoic glacial events. *Terra Nova*, 19: 401-406.

Baud A., Richoz S. & Marcoux J. (2005). Calcimicrobial cap rocks from the basal Triassic units: western Taurus occurrences (SW Turkey). *Comptes Rendus Palevol*, 4: 569-582.

Corsetti F. A., Lorentz N.J. & Pruss S. B. (2004). Formerly-aragonite seafloor fans, Death Valley and Southeastern Idaho, United States: implications for "cap carbonate" formation and Snowball Earth. In: Jenkins G., McMenamin M. & Sohl L. (Eds), *The Extreme Proterozoic: Geology, Geochemistry, and Climate*. AGU Geophysical Monograph Series, 146: 33-44.

De Choudens-Sánchez V. & González L.A. (2009). Calcite and aragonite precipitation under controlled instanataneous supersaturation: elucidating the role of $CaCO_3$ saturation state and Mg/Ca ratio on calcium carbonate polymorphism. *Journal of Sedimentary Research*, 1979: 363-376.

Elderfield H. & Greaves M.J. (1982). The rare earth elements in seawater. *Nature*, 296: 214-219.

Font E., Nedelec A., Trindade R.I.F., Macouin M. & Charriere A. (2006). Chemostratigraphy of the Neoproterozoic Mirassol d'Oeste cap dolostones (Mato Grosso, Brazil): an alternative model for Marinoan cap dolostone formation. *Earth and Planetary Science Letters*, 250: 89-103.

Hoffman P.F., Halverson G.P., Domack E.W., Husson J.M., Higgins J.A. & Schrag D.P. (2007). Are basal Ediacaran (635 Ma) post-glacial "cap dolostones" diachronous? *Earth and Planetary Science Letters*, 258: 114-131.

Hoppe A., Karfunkel J. & Noce C.M. (2002). Inhaúma Site, State of Minas Gerais. Precambrian aragonitic layers, In: Schobbenhaus C., Campos D.A., Queiroz E.T., Winge M. & Berbert-Born M.L.C. (Eds), *Sítios Geológicos e Paleontológicos do Brasil.* Comissão Brasileira de Sítios Geológicos e Paleobiológicos (SIGEP), Brasília, 554pp.

James N.P., Narbonne G.M. & Kyser T.K. (2001). Late Neoproterozoic cap carbonates: Mackenzie Mountains, northwestern Canada: precipitation and global glacial meltdown. *Canadian Journal of Earth Sciences*, 38: 1229-1262.

Le Hir G., Donnadieu Y., Goddéris Y., Pierrehumbert R.T., Halverson G.P., Macouin M., Nédélec A. & Ramstein G. (2009). The Snowball Earth aftermath: exploring the limits of continental weathering processes. *Earth and Planetary Science Letters*, 277: 453-463.

Makovicky E., Karup-Møller S. & Li J. (2006). Mineralogy of the chrysanthemum stone. *Neues Jahrbuch für Mineralogie. Abhandlungen*, 182: 241-251.

Nédélec A., Affaton P., France-Lanord C., Charrière A. & Alvaro J. (2007). Sedimentology and chemostratigraphy of the Bwipe Neoproterozoic cap dolostones (Ghana, Volta Basin): A record of microbial activity in a peritidal environment. *Comptes Rendus Geoscience*, 339: 223-239.

Peryt T.M., Hoppe A., Bechstadt T., Koster J., Pierre C. J. & Richter D.K. (1990). Late proterozoic aragonitic cement crusts, Bambui Group, Minas Gerais, Brazil. *Sedimentology*, 37: 279-286.

Pierrehumbert R.T. (2004). High levels of atmospheric carbon dioxyde necessary for the termination of global glaciation. *Nature*, 429: 646-649.

Pruss S.B., Corsetti F.A. & Fischer W.W. (2008). Sea-floor precipitated carbonate fans in the Neoproterozoic Rainstorm Member, Johnie Formation, Death Valley region, USA. *Sedimentary Geology*, 207: 34-40.

Shields G.A. & Stille P. (2001). Diagenetic constraints on the use of cerium anomalies as palaeoseawater redox proxies: an isotopic and REE study of Cambrian phosphorites. *Chemical Geology*, 175: 29-48.

Sumner D.Y. & Grotzinger J.P. (2000). *Late Archean precipitation: petrography, fácies associations, and environmental significance.* SEPM Special publication, 67: 123-159.

Vieira L.C., Trindade R.I.F., Nogueira A.C.R. & Ader M. (2007). Identification of a Sturtian cap carbonate in the Neoproterozoic Sete Lagoas carbonate platform, Bambuí Group, Brazil. *Comptes Rendus Geoscience*, 339: 240-258.

Westin K.J., & Rasmuson A.C. (2005). Nucleation of calcium carbonate in presence of citric acid, DTPA, EDTA and pyromellitic acid. *Journal of colloid and interface science*, 282: 370-379.

Woods A.D., Bottjer D.J., Mutti M. & Morrison J. (1999). Lower Triassic large sea-floor carbonate cements: their origin and a mechanism for the prolonged biotic recovery from the end-Permian mass extinction. *Geology*, 27: 645-648.

Palaeoenvironmental changes at the Middle–Late Jurassic transition: deciphering local and global variations

Hubert Wierzbowski

Institute of Geological Sciences, Polish Academy of Sciences, ul. Twarda 51/55, 00-818 Warszawa, Poland; E-Mail: hwierzbo@twarda.pan.pl

Prominent tectonic and oceanographic changes took place on Earth during the Middle–Late Jurassic transition (Late Callovian–Early Oxfordian). They include the culmination of a period of the enhanced oceanic crust spreading, a global sea-level rise, opening of seaways, starvation of sedimentary basins and a decline of carbonate platforms (Norris & Hallam, 1995; Jacquin *et al*., 1998; Morettini *et al*., 2002; Dromart *et al*., 2003; Cecca *et al*., 2005; Wierzbowski *et al*., 2009). The enhanced oceanic crust spreading during the Middle–Late Jurassic transition was likely a source of a deepest in the Phanerozoic minimum of the seawater $^{87}Sr/^{86}Sr$ ratio (Jones *et al*., 1994; Wierzbowski *et al*., 2012). The global sea-level rise resulted in the intensification of sea currents and the starvation of sedimentary basins, both of which are manifested by the presence of abundant condensations or omission surfaces in the lithological record of Tethyan and peri-Tethyan sections (Norris & Hallam, 1995; Rais *et al*., 2007). Despite the decline of low latitude carbonate platforms, marly sedimentation persisted in many subtropical areas (cf. Matyja, 1977; Norris & Hallam, 1995; Giraud, 2009). Boreal and Subboreal basins were characterized by a continuous siliciclastic sedimentations at the Middle–Late Jurassic transition. Clastic deposits of the Middle–Late Jurassic boundary of the Russian Platform are additionally reported to be carbonate and organic-rich (Sazanova & Sazanov, 1967). It is postulated that the opening of seaway during the Middle–Late Jurassic transition allowed multi-directional migrations of ammonites and planktonic foraminifers in the northern hemisphere as well as the unification of dinocyst assemblages (Brassier & Geleta, 1993; Matyja & Wierzbowski, 1995; Marchand & Thierry, 1997; Riding *et al*., 1999; 2011; Oxford *et al*., 2002; Hudson *et al*., 2005). Isotope and micropalaeontologic records of Western Europe show a cooling episode in the Late Callovian–Early Oxfordian (Abbink *et al*., 2001; Dromart *et al*., 2003; Nunn *et al*., 2009). The data, along with sedimentologic and faunistic proxies, were used for building-up theories of severe cooling and glaciation at the Middle–Late Jurassic transition and subsequent warming in the Middle Oxfordian (Dromart *et al*., 2003; Donnadieu *et al*., 2011). The presence of a prolonged period of cooling comprising the entire Oxfordian calculated from the large isotope dataset of West European fish teeth (Lécuyer *et al*., 2003; Fig. 1) and a cooling in the Middle and earliest Late Oxfordian in the Kachchh Basin of India (Alberti *et al*., 2012) raises however doubts about the existence of the short-lived global cooling at the Callovian–Oxfordian transition. A prolonged (Late Callovian–Middle Oxfordian) period of the presence of cold bottom waters in the Middle Russian Sea has recently been documented with belemnite isotope record (Wierzbowski & Rogov, 2010, 2011; and unpublished data; Fig. 1). The occurrence of cold bottom waters in the epicontinental Middle Russian Sea is interpreted as a result of establishing of wide marine connections with the Boreal basin during the sea-level highstand. The period of the presence of the cold bottom waters coincides with the invasions of Tethyan ammonite and belemnite fauna into the Russian Platform (Wierzbowski & Rogov, 2010, 2011; and unpublished data). Available geologic data point to the presence of warm climate near the South Pole at the Middle–Late Jurassic transition (Jenkyns *et al*., 2012). A warming of the Arctic climate is postulated for the latest Callovian based on the disappearance of glendonites from North Siberia sections (Kaplan, 1978; Rogov & Zakharov, 2010; Wierzbowski & Rogov, 2011) and the diversification of Arctic bivalve assemblage (Kaplan *et al*., 1979). Occurrences of organodetritic and oolite limestones in the uppermost Callovian of the North Siberia are also interpreted as a result of the warming of the Boreal basin (Kaplan *et al*., 1979).

The deepening of sedimentary basins that occurred during the global sea-level highstand at the Middle–Late Jurassic transition may have enabled the outflow of cold waters from the Boreal Sea. The Boreal waters might have sunk forming cold bottom currents. Such process might have enabled the inflow of warmer superficial currents to the Boreal Sea. It is consistent with reported warming of this basin during the Late Callovian. Boreal currents may have induced local cooling in adjacent basins at the Middle–Late Jurassic transition. They may also have contributed to the spread of Boreal cephalopod fauna in this time-period, although the spread is associated with northern migration of Tethyan cephalopods (cf. Matyja & Wierzbowski, 1995; Wierzbowski & Rogov, 2011). The deceleration of carbonate productivity in the oceans during the Late Callovian–Early Oxfordian was suggested to have resulted in a build-up of oceanic alkalinity and a decrease in atmospheric CO_2 concentration (Donnadieu *et al*., 2011). A subtle to moderate global climate cooling induced by the decrease in atmospheric CO_2 content might have occurred in the Early Oxfordian, although there is no evidence for a frigid climate or the formation of continental ice in circum-polar regions in this time (cf. Donnadieu *et al*., 2011). Further studies are needed to precisely document polar and global climate variations during the Middle–Late Jurassic transition. Available geochemical, sedimentologic and faunistic data show however a major effect of changes in seawater circulation and bathymetry on the observed temperature record of investigated marine basins during the Middle–Late Jurassic transition. A noticeable global climate warming is inferred for the Early Kimmeridgian (in Boreal zonation) only based on isotope and palynological records of many areas (cf. Abbink *et al*., 2001; Wierzbowski, 2002, 2004; Lécuyer *et al*., 2003; Wierzbowski *et al*., 2006; Nunn *et al*., 2009). The presence of positive $\delta^{13}C$ excursion(s) noted in the Upper Callovian–Middle Oxfordian records of marine carbonates and terrestrial organic carbon is linked to the sea-level rise and the reduced rate of the weathering carbon input to the oceans as there is no evidence for the widespread of organic rich sediments (cf. Bartolini *et al*., 1996; Morettini *et al*., 2002; Wierzbowski, 2002; Nunn *et al*., 2009; Wierzbowski *et al*., 2009). The recovery of carbonate platforms observed after the Middle–Late Jurassic transition in tropical and subtropical zones may be regarded as a result of the increased weathering calcium flux to the oceans (triggered by the sea-level fall) under the warm Late Jurassic climate. The spread and diversification of carbonate platforms and bioherms during the Late Jurassic changed the environment of epicontinental and shelf seas and resulted in the deposition of thick sequences of Upper Jurassic carbonate rocks (cf. Dromart *et al*., 2003; Cecca *et al*., 2005).

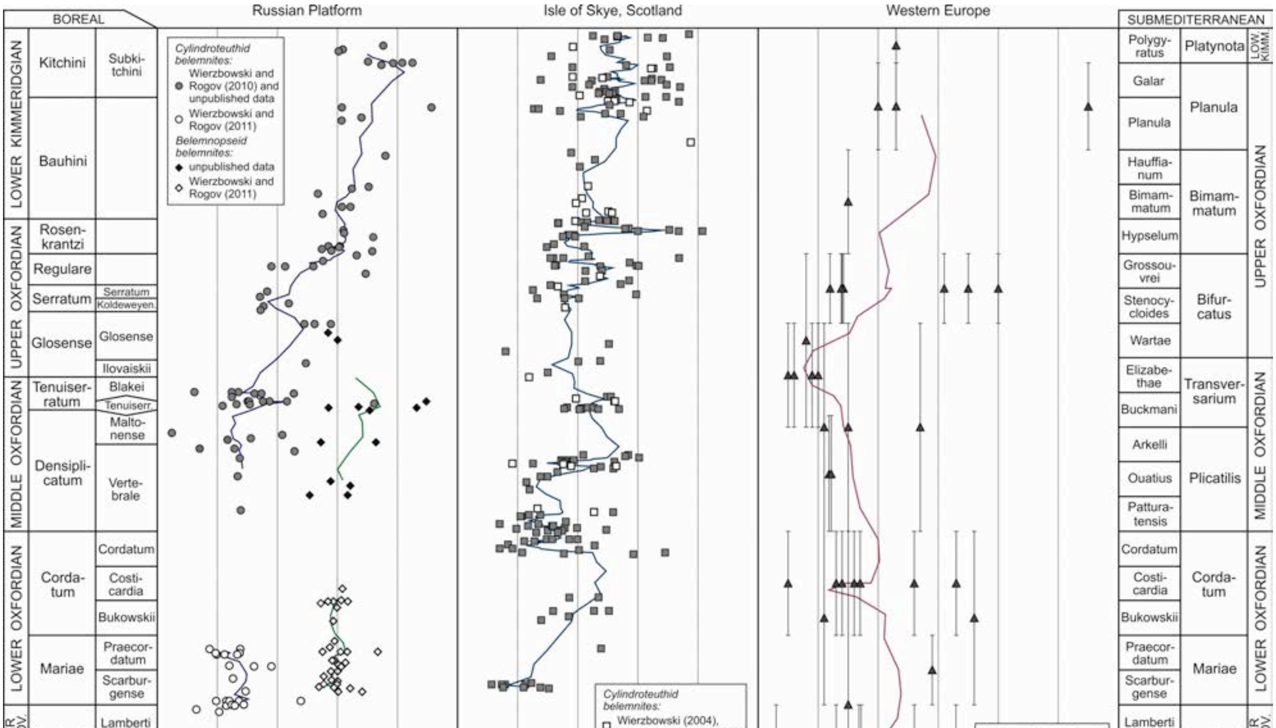

Fig. 1.: **Upper Callovian–Lower Kimmeridgian stratigraphy and δ18O values of well-preserved belemnite rostra and vertebrate teeth from the Russian Platform, Scotland and Western Europe. Curves represent 5-point running averages.**

References

Abbink O., Targarona J., Brinkhuis H. & Visscher H. (2001). Late Jurassic to earliest Cretaceous palaeoclimatic evolution of southern North Sea. *Global and Planetary Change*, 30: 231–256.

Alberti M., Fürsich F.T. & Pandey D.K. (2012). The Oxfordian stable isotope record $\delta^{18}O$, $\delta^{13}C$) of belemnites, brachiopods, and oysters from the Kachchh Basin (western India) and its potential for palaeoecologic, palaeoclimatic, and palaeogeographic reconstructions. *Palaeogeography, Palaeoclimatology, Palaeoecology*, 344-345: 49–68.

Bartolini A., Baumgartner P.O. & Hunziker J. (1996). Middle and Late Jurassic carbon stable-isotope stratigraphy and radiolarite sedimentation of the Umbria-Marche Basin (Central Italy). *Eclogae Geologica Helvetica*, 89: 811–844.

Brassier M. & Geleta S. (1993). A planktonic marker and Callovian–Oxfordian fragmentation of Gondwana: Data from Ogaden Basin, Ethiopia. *Palaeogeography, Palaeoclimatology, Palaeoecology*, 104: 177–184.

Cecca F., Martin Garin B., Marchand D., Lathuiliere B. & Bartolini A. (2005). Paleoclimatic control of biogeography and sedimentary events in Tethyan and peri-Tethyan areas during the Oxfordian (Late Jurassic). *Palaeogeography, Palaeoclimatology, Palaeoecology*, 222: 10–32.

Donnadieu Y., Dromart G., Godderis Y., Puceat E., Brigaud B., Dera G., Dumas C. & Oliver N. (2011). A mechanism for brief glacial episodes in the Mesozoic greenhouse. *Paleoceanography*, 26: PA3212.

Dromart G., Garcia J.-P., Gaumet F., Picard S., Rousseau M., Atrops F., Lecuyer C. & Sheppard S.M.F. (2003). Perturbation of the carbon cycle at the Middle/Late Jurassic transition: geological and geochemical evidence. *American Journal of Science*, 303: 667–707.

Giraud F. (2009). Calcareous nannofossil productivity and carbonate production across the Middle-Late Jurassic transition in French Subalpine Basin. *Geobios*, 42: 699–714.

Hudson W., Hart M.B., Sidorczuk M. & Wierzbowski A. (2005). Jurassic planktonic foraminifera from Pieniny Klippen Belt and their taxonomic and phylogenetic importance (Carpathians, southern Poland). *Volumina Jurassica*, 3: 1–10.

Jacquin T., Dardeau G., Durlet C., De Graciansky P.-C. & Hantzpergue P. (1998). The North Sea cycle: an overview of 2nd order transgressive/regressive facies cycles. In: de Graciansky P.-C., Hardenbol J., Jacquin T. & Vail P.R. (Eds), *Western Europe, in Mesozoic and Cenozoic Sequence Stratigraphy of European Basins.* SEPM Special Publication, 60: 445–466.

Jenkyns H.C., Schouten-Huibers L., Schouten S. & Sinninghe Damsté J.S. (2012). Warm Middle Jurassic–Early Cretaceous high-latitude sea-surface temperatures from the Southern Ocean. *Climate of the Past*, 8: 215–226.

Jones C. E., Jenkyns H.C., Coe A.L. & Hesselbo S.P. (1994). Strontium isotopic variations in Jurassic and Cretaceous seawater. *Geochimica Cosmochimica Acta*, 58: 3061–3074.

Kaplan M.E. (1978). Calcite pseudomorphoses from the Jurassic and Lower Cretaceous deposits of Northern East Siberia. *Geol. Geofiz.*: 19, 62–70 [in Russian].

Kaplan M.E., Meledina S.V. & Shurygin B.N. (1979). Kelloveyskie Morya Severnoy Sibiri. Usloviya Osadkonakopleniya i Sushchestvovaniya Fauny. *Izdatelstvo Nauka, Sibirskoye Otdeleniye*, Novosibirsk.

Lécuyer C., Picard S., Garcia J.P., Sheppard S.M.F., Grandjean P. & Dromart G. (2003). Thermal evolution of Tethyan surface waters during the Middle–Late Jurassic: evidence from δ_{18}O values of marine fish teeth. *Paleoceanography*, 18: 1076.

Marchand D. & Thierry J. (1997). Enregistrement des variations morphologiques et de la composition des peuplements d'ammonites durant le cycle régressif/transgressif de 2_e ordre Bathonian inférieur-Oxfordian inférieur en Europe occidentale. *Bulletin de la Société Géologique de France*, 168, 121–132.

Matyja B.A. (1977). The Oxfordian in the south-western margin of the Holy Cross Mts. *Acta Geologica Polonica* 27: 41–64.

Matyja B.A. & Wierzbowski A. (1995). Biogeographic differentiation of the Oxfordian and Early Kimmeridgian ammonite faunas of Europe, and its stratigraphic consequences. *Acta Geologica Polonica*, 45: 1–8.

Morettini E., Santantonio M., Bartolini A., Cecca F., Baumgartner P.O. & Hunziker J.C. (2002). Carbon isotope stratigraphy and carbonate production during the Early–Middle Jurassic: examples from the Umbria–Marche–Sabina Apennines (central Italy). *Palaeogeography, Palaeoclimatology, Palaeoecology*, 184: 251–273.

Norris M.S. & Hallam A. (1995). Facies variations across the Middle–Upper Jurassic boundary in Western Europe and the relationship to sea-level changes. *Palaeogeography, Palaeoclimatology, Palaeoecology*, 116: 189–245.

Nunn E.V., Price G.D., Hart M.B., Page K.N. & Leng M.J. (2009). Isotopic signals from Callovian–Kimmeridgian (Middle–Upper Jurassic) belemnites and bulk organic carbon, Staffin Bay, Isle of Skye, Scotland. *Journal of the Geological Society, London*, 166: 633–641.

Oxford M.J., Gregory F.J., Hart M.B., Henderson A.S., Simmons M.D. & Watkinson M.P. (2002). Jurassic planktonic foraminifera from the United Kingdom, *Terra Nova*, 14: 205–209.

Rais P., Louis-Schmid B., Bernasconi S.M. & Weissert H. (2007). Palaeoceanographic and palaeoclimatic reorganization around the Middle–Late Jurassic transition. *Palaeogeography, Palaeoclimatology, Palaeoecology*, 251: 527–546.

Riding J.B., Fedorova V.A. & Ilyina V.I. (1999). Jurassic and lowermost Cretaceous dinoflagellate cyst biostratigraphy of the Russian Platform and northern Siberia, Russia. *AASP Contributions Series*, 36: 1–179.

Riding J.B., Quattroocchio M.E. & Martínez M.A. (2011). Mid Jurassic (Late Callovian) dinoflagellate cysts from the Lotena Formation of the Neuquén Basin, Argentina and their palaeogeographical significance. *Review of Palaeobotany and Palynology*, 163: 227–236.

Rogov M.A. & Zakharov V.A. (2010). Jurassic and Lower Cretaceous glendonite occurrences and their implications for Arctic paleoclimate reconstructions and stratigraphy. *Earth Science Frontiers*, 17: 345–347.

Sazonova I.G. & Sazonov N.T. (1967). Paleogeografiya Russkoy Platformy v Yurskoe i Rannemelovoe Vremya. *Izdatelstvo „Nedra",* Leningrad.

Wierzbowski A., Coe A.L., Hounslow M.W., Matyja B.A., Ogg J.G., Page K.N., Wierzbowski H. & Wright J.K. (2006). A potential stratotype for the Oxfordian/Kimmeridgian boundary: Staffin Bay, Isle of Skye, UK. *Volumina Jurassica*, 4, 17–33.

Wierzbowski H. (2002). Detailed oxygen and carbon isotope stratigraphy of the Oxfordian in Central Poland. *International Journal of Earth Sciences (Geol. Rundsch.)*, 91: 304–314.

Wierzbowski H. (2004). Carbon and oxygen isotope composition of Oxfordian–Early Kimmeridgian belemnite rostra: palaeoenvironmental implications for Late Jurassic seas. *Palaeogeography, Palaeoclimatology, Palaeoecology*, 203: 153–168.

Wierzbowski H. & Rogov M. (2010). Carbon and oxygen isotope composition of Upper Callovian-Lower Kimmeridgian (Middle-Upper Jurassic) cephalopod shells from the Russian Platform: a proxy for a global climate change? *Earth Science Frontiers*, 17: 336–337.

Wierzbowski H. & Rogov M.A. (2011). Reconstructing the palaeoenvironment of the Middle Russian Sea during the Middle–Late Jurassic transition using stable isotope ratios of cephalopod shells and variations in faunal assemblages. *Palaeogeography, Palaeoclimatology, Palaeoecology*, 299: 250–264.

Wierzbowski H., Anczkiewicz R., Bazarnik J. & Pawlak J. (2012). Strontium isotope variations in Middle Jurassic (Late Bajocian–Callovian) seawater: Implications for Earth's tectonic activity and marine environments. *Chemical Geology*, 334: 171–181.

Wierzbowski H., Dembicz K. & Praszkier T. (2009). Oxygen and carbon isotope composition of Callovian–Lower Oxfordian (Middle–Upper Jurassic) belemnite rostra from central Poland: a record of a Late Callovian global sea-level rise? *Palaeogeography, Palaeoclimatology, Palaeoecology*, 283, 182–194.

Authors

P

R

S

T

V

W

Y

STRATA

Actes du Laboratoire de Géologie Sédimentaire et Paléontologie De l'Université Paul-Sabatier Toulouse (1984 – 2005),
puis Travaux de Géologie sédimentaire, Stratigraphie et Paléontologie (de 2006 à 2009).

Les ouvrages marqués avec un « * » sont seuls disponibles.
Toute commande doit être adressée à STRATA
strata.mp@free.fr
Tarifs et disponibilité à vérifier sur http://strata.mp.free.fr

Série 2 : Mémoires

Vol. 1 – 1984*	**BILOTTE M.** (1985) – Le Crétacé supérieur des plates-formes est-pyrénéennes, Atlas.
Vol. 2 – 1985*	**CANEROT J., GOY A. et coll.** - Le Jurassique des Ibérides orientales, Espagne. Livret-guide d'excursion. 182 p., 49 fig., 10 pl.
Vol. 3 – 1985	**PAUTAL L. –** Populations fossiles, associations micropaléontologiques et paléoenvironnements des séries deltaïques ilerdiennes des Corbières (Aude – France).
Vol 4 – 1985	**LEPICARD B.** – Le Crétacé terminal et le Paléocène basal dans les Petites Pyrénées et les dômes annexes. Biostratigraphie – Sédimentologie. 288 p. 130 fig., 27 tab., 4 pl. ph., 2 pl. ht.
Vol. 5 – 1985*	**BILOTTE M. –** Le Crétacé supérieur des plates-formes est-pyrénéennes. 438 p., 121 fig. 53 tabl. (avec l'Atlas).
Vol. 6 – 1986	**CUBAYNES R.** – Le Lias du Quercy méridional : étude lithologique, biostratigraphique, paléoécologique et sédimentologique. 574 p., 201 fig., 36 pl.
Vol. 7 – 1987	**CUBAYNES R., FAURÉ Ph. et coll.** – Le Jurassique du Quercy. Généralités. Livret-Guide d'excursion. 159 p. 57 fig., 4 tab., 4 pl. ph.
Vol. 8 – 1987	**SOUHEL A.** – Dynamique sédimentaire des couches rouges intercalaires (Bathonien – Cénomanien) dans l'Atlas de Beni Mellal (Haut Atlas Central, Maroc. 173 p., 79 fig., 3 pl.
Vol. 9 – 1988*	**BOURGES Ph.** – Sédimentation alluviale et tectonique extensive dans le Permien du détroit de Rodez. 186 p., 54 fig., 20 pl.
Vol. 10 – 1988*	**CUGNY P. –** Analyse quantitative des faciès dans diverses formations crétacées des marges néotéthysiennes et atlantiques. Associations paléontologiques et paléoenvironement. 331 p., 199 fig.
Vol. 11 – 1989	**SANCHEZ-RIOS MA.** – Foraminifères planctoniques et nannoplancton calcaire de quelques sites du Crétacé supérieur mexicain et sud-pyrénéen. 255 p., 24 fig., 16 tab., 26 pl.
Vol. 12 – 1989	**SOUQUET P., FONDECAVE-WALLEZ M.J.** – Stratigraphie séquentielle dans l'avant fosse sud-pyrénéenne. Groupe d'Aren : Campanien, Maastrichtien, Danien. 71 p., 29 fig.
Vol. 13 – 1990	**BILOTTE M.** – Le Sénonien supérieur du bassin d'avant-pays Sous-pyrénéen de l'Ariège et de la Haute-Garonne. 96 p., 33 fig.
Vol. 14 – 1991	**ANDREU-BOUSSUT B.** – Les Ostracodes du Crétacé moyen (Barrémien à Turonien) le long d'une transversale Agadir-Nador (Maroc). 2 tomes. 765 p., 243 fig., 14 tab., 73 pl.
Vol. 15 – 1991	**ETTACHFINI M.** – Le Valanginien de l'Atlas Atlantique (Maroc). Stratigraphie et ammonitofaune. 177 p. , 34 fig., 6 tabl., 11 pl.
Vol. 16 – 1992	**TAJ-EDDINE K.** – Le Jurassique terminal et le Crétacé basal dans l'Atlas Atlantique (Maroc). Biostratigraphie, sédimentologie, stratigraphie séquentielle et géodynamique. 289 p., 132 fig., 9 pl., 4 annexes.
Vol. 17 – 1992	**FRECHENGUES, PEYBERNES B., LUCAS Cl. et SOUQUET P**. – Le Trias des Pyrénées centrale et orientales franco-espagnoles. Livret-guide de l'excursion Pyrénées 92 du Groupe Français du Trias.
Vol. 18 – 1993	**ETTACHFINI E.M.** – Le Vraconien, Cénomanien et Turonien du bassin d'Essaouira (Haut Atlas Occidental, Maroc). Analyse lithologioque, biostratigraphique et sédimentologique, stratigraphie séquentielle. 245 p, 87 fig., 10 tab.

Vol. 19 – 1993	**BEGOUEN V. –** Les kystes de Dinoflagellés du Crétacé supérieur de la zone Sous-pyrénéenne (France). Biostratigraphie, analyse des faciès et approche cladistique des Péridinales. 257 p., 79 fig., 5 tab. h.t.
Vol. 20 – 1993*	**CISZAK R. –** Évolution géodynamique de la Chaîne tellienne en Oranie pendant le Paléozoïque et le Mésozoïque. 513 p., 107 fig., 17 pl.
Vol. 21 – 1993	**PERRET M.F. –** Recherches micropaléontologiques et biostratigraphiques (conodontes-foraminifères) dans le Carbonifère pyrénéen. 597 p., 160 fig., 24 pl.
Vol. 22 – 1994	**QUAJOUN A. –** Le Toarcien du Quercy septentrional : Stratigraphie et micropaléontologie. 236 p., 70 fig., 15 pl.
Vol. 23 – 1994	**VAN DE POEL H.M. –** Messinian marginal-marine and continental faciès and their stratigraphy in the Eastern Almeria Province (S.E. Spain). 202 p. 47 fig., 5 tabl., 8 pl.
Vol. 24 – 1994	**CUBAYNES R. et REY J, coll. BRUNEL F., FAURE Ph., RUGET C et BONNET L. –** Corrélations stratigraphiques dans le Lias du Quercy. Généralités, livret-Guide d'excursion. 64 p., 19 fig., 5 pl., 1 pl. h. texte, 1 annexe.
Vol. 25 – 1994	**BOUCHOUATA A.** – La Ride de Talmest-Tazoult (Haut-Atlas Central, Maroc). Lithostratigraphie, biostratigraphie et relations tectonique – sédimentation au cours du Jurassique. 223 p., 45 fig., 14 pl.
Vol. 26 – 1995	**REY J. et coll. –** Du Lias nord-aquitain aux molasses miocènes. Généralités, livret-Guide d'excursion. 194 p., 84 fig., 1 tabl.
Vol. 27 – 1996*	**SOUHEL A. –** Le Mésozoîque dans le Haut-Atlas de Beni Mella au Maroc. Stratigraphie, sédimentologie et évolution géodynamique. 265 p., 125 fig., 5 tab., 6 pl.
Vol. 28 – 1997	**BRUNEL F.** – Stratigraphie séquentielle du Domérien du Quercy septentrional. 280 p., 55 fig., 20 tabl., 9 pl.
Vol. 29 – 1998*	**ALMERAS Y., ELMI S.** – Les Brachiopodes jurassiques moyens de la Bordure vivaro-cévenole (Bassin du Sud-Est, France). 145 p. 18 fig., 24 tabl., 9 pl.
Vol. 30 – 1998*	**WITAM O. –** Barrémien-Aptien de l'Atlas atlantique, Maroc. Lithographie, biostratigraphie, sédimentologie, stratigraphie séquentielle et géodynamique et paléontologie 421 p., 176 fig., 12 pl.
Vol. 31 – 1998	**JAMES V.** – La plate-forme carbonatée ouest-pyrénéenne au Jurassique moyen et supérieur. Stratigraphie séquentielle, stades d'évolution, relations avec la subsurface en Aquitaine méridionale. 351 p., 178 fig., 5 tabl., 11 pl.
Vol. 32 – 1998	**CHARCOSSET P.** – Reconstitution d'un segment de la marge ouest-téthysienne au Bathonien dans les Grands Causses et le Bas-Languedoc. Analyse séquentielle à divers ordres et dynamique de bassin. 351 p., 178 fig., 5 tabl., 11 pl.
Vol. 33 – 1999*	**BILOTTE M., KOESS L. et LE LOEUF J. –** Moins 96 millions d'années à moins 65 millions d'années autour de la vallée de l'Aude. 116 p. , 67 fig.
Vol. 34 – 2000	**LEZIN C., CISZAK R. avec coll. REY J. –** Le passage Lias – Dogger dans le Quercy et les Grands Causses. Généralités, livret-guide d'excursion. 106 p., 26 fig., 1 tabl.
Vol. 35 – 2000	**LEZIN C. –** Analyse des faciès et stratigraphie intégrée : application aux événements du passage Lias – Dogger sur la plate-forme du Quercy. 317 p, 138 fig., 9 pl.
Vol. 36 – 2000*	**ALMERAS Y. et FAURE Ph. –** Brachiopodes liasiques des Pyrénées. Paléontologie, biostratigraphie, paléobiographie et paléoenvironement. 55 text-fig., 70 tabl., 56 fig. h.t., 23 pl.
Vol. 37 – 2001	**CANEROT J., MAJESTE-MENJOULAS C. et TERNET Y.** – La Faille nord-pyrénéenne. Mythe ou réalité ? Excursion géologique AGSO, 2001.
Vol. 38 – 2002	**ROBERT E.** – La transgression albienne dans le Bassin andin (Pérou) : Biostratigraphie, Paléontologie (Ammonites) et stratigraphie séquentielle. 380 p., 91 fig., 38 pl.
Vol. 39 – 2002*	**FAURE. Ph.** – Le Lias des Pyrénées. Tome 1 - 365 p., 187 fig. ; Tome 2 - 396 p., 169 fig., 25 pl.
Vol. 40 – 2002	**GARDERE Ph. –** Les sables fauves. Dynamique sédimentaire et évolution morpho-structurale du Bassin d'Aquitaine au Miocène moyen. 217 p., 77 fig., 6 pl.
Vol. 41 – 2003	**LAURENT Y.** – Les faunes de vertébrés continentaux du Maastrichtien supérieur de l'Europe. Systématique et biodiversité. 81 p., 14 fig., 56 pl.
Vol. 42 – 2004	**CUBAYNES R. et coll. –** Les dépôts littoraux du Jurassique sur la bordure quercynoise (Aquitaine). Généralités. Livret-guide d'excursion. 85 p., 36 fig.
Vol. 43 – 2004	**ETTACHFINI M. –** Les ammonites du Néocomien dans l'Atlas atlantique, Maroc. Biostratigraphie, paléontologie, paléobiogéographie et paléoécologie. 225 p., 57 fig., 6 tab., 33 pl.
Vol. 44 – 2006*	**ROSSI A. –** Les Ostracodes du Crétacé inférieur (Berriasien et Barrémien de l'Atlas atlantique). Apport en paléoécologie, stratigraphie séquentielle et paléogéographique. 371 p., 127 fig., 18 tabl., 24 pl. ht.

Vol. 45 – 2008 **ETTACHFINI E.M.** – La transgression au passage du Cénomanien au Turonien sur le domaine atlasique marocain. Stratigraphie intégrée et relations avec l'événement océanique mondial. 299 p., 14 fig., 36, 36 pl. h.t.

Vol. 46 – 2009* **DEBROAS E.J.** – Géologie du bassin versant du Baget (zone nord-pyrénéenne, Ariège, France) : nouvelles observations et conséquences. 95 p., 15 fig., 19 annexes, 9 pl.

Série 1 : Communications

Vol. 1 – 1984 Marges européennes et africaines à l'articulation Atlantique – Téthys. 139 p.

Vol. 2 – 1985* Travaux du Laboratoire de Géologie Sédimentaire et Paléontologie de l'Université Paul-Sabatier. 8 communications, 121 p.

Vol. 3 – 1987* Travaux du Laboratoire de Géologie Sédimentaire et Paléontologie de l'Université Paul-Sabatier. 7 communications, 127 p.

Vol. 4 – 1988 Phylogénèse des Protistes et autres organismes microscopiques : rôle du milieu dans les phénomènes évolutifs. 171 p.

Vol. 5 – 1989 Stratigraphie séquentielle et corrélations eustatiques. Réunion spécialisée de la S.G.F. et du C.F.S., Toulouse, 1989. 155 p.

Vol. 6 – 1994* Acte du premier congrès français de stratigraphie, Toulouse 12, 13, 14 septembre 1994. 209 p.

Vol. 6 – 1995* Le Bassin Aquitain. Evolution, sédimentation et stratigraphie. Séance de la Société Géologique de France. 74 p.

Vol. 8 – 1996* PICG Participation au Bilan Perspective. Séance de la Société Géologique de France, Paris le 05/11/1996. 103 p.

Vol. 9 – 1998* La limite Paléocène Eocène en Europe. Evénements et corrélations. Séance de la Société Géologique de France, Paris le 19 et 20 janvier 1998. 134 p.

Vol. 10 – 2000* Les évènements du passage du Lias - Dogger. Séance de la Société Géologique de France, Toulouse. 140 p.

Vol. 11 – 2001 Two hundred years of Pterosaurs. A symposium on the anatomy, évolution, palaeobiology and environment of Mesozoic Flying Reptiles. Toulouse 2001. 103 p.

Vol. 12 – 2002 Eight international conodont symposium held in Europe – ECOS VIII, Toulouse/Albi, Juin 2002. 110 p.

Vol. 13 – 2006 30 millions d'années de biodiversité dynamique dans le paléokarst du Quercy. 283 p.

'Pre-Cenozoic climates' is a multidisciplinary workshop that broadly addresses the pre-Cenozoic climatic phenomena and processes. The purpose of the workshop is to extend our understanding of the natural variations that take place within the earth's climate system in deep times by bringing together specialists from diverse fields including sedimentology, paleontology, geochemistry (data-community) and numerical modeling (model-community).

Objectives

This workshop aims at exploring climate reconstructions and processes throughout the pre-Cenozoic time. In recent years, the number of available data has grown exponentially, including paleontological, sedimentological, isotopic, and geochemical data. Two questions arise : (1) is there a unified picture of the pre-Cenozoic climates and environmental evolution emerging from this large amount of data, and (2) how can we promote dialogue between numerical models, which deliver large amounts of climatic and environmental parameters, and geological observations? The workshop offers data- and model-workers an opportunity to discuss the strengths and weaknesses of the geological proxies and numerical models, to share their vision about the reconstruction of pre-Cenozoic climates, and to debate about emerging scientific questions.

Organized by

Yves GODDÉRIS, Bernard ANDREU, Markus ARETZ, Guillaume DERA, Yannick DONNADIEU, Vanessa LEBEDEL, Carine LÉZIN, Mélina MACOUIN, Elise NARDIN, Delphine ROUBY, Anne-Marie COUSIN and Valérie CECCAREL.

Géosciences Environnement Toulouse
Observatoire Midi-Pyrénées, CNRS, Université Paul Sabatier
14 avenue Edouard Belin
F-31400 Toulouse

http://pc2iw.sciencesconf.org/

Editeur : Association Strata. Muséum d'Histoire Naturelle de Gaillac, 81400, Gaillac

Dépôt légal 2ème trimestre 2013

2013 PRE-CENOZOIC CLIMATES - INTERNATIONAL WORKSHOP -When data and modeling meet STRATA Série 1 - Vol. 14